

**FILLER RETENTION IN PAPERMAKING BY POLYMERIC
AND MICROPARTICULATE RETENTION AID SYSTEMS**

by

Alois VANERЕК

Department of Chemistry

McGill University

Montréal, Québec

November 2004

© *Alois VANERЕК*



Library and
Archives Canada

Bibliothèque et
Archives Canada

Published Heritage
Branch

Direction du
Patrimoine de l'édition

395 Wellington Street
Ottawa ON K1A 0N4
Canada

395, rue Wellington
Ottawa ON K1A 0N4
Canada

Your file Votre référence

ISBN: 0-494-12960-3

Our file Notre référence

ISBN: 0-494-12960-3

NOTICE:

The author has granted a non-exclusive license allowing Library and Archives Canada to reproduce, publish, archive, preserve, conserve, communicate to the public by telecommunication or on the Internet, loan, distribute and sell theses worldwide, for commercial or non-commercial purposes, in microform, paper, electronic and/or any other formats.

The author retains copyright ownership and moral rights in this thesis. Neither the thesis nor substantial extracts from it may be printed or otherwise reproduced without the author's permission.

AVIS:

L'auteur a accordé une licence non exclusive permettant à la Bibliothèque et Archives Canada de reproduire, publier, archiver, sauvegarder, conserver, transmettre au public par télécommunication ou par l'Internet, prêter, distribuer et vendre des thèses partout dans le monde, à des fins commerciales ou autres, sur support microforme, papier, électronique et/ou autres formats.

L'auteur conserve la propriété du droit d'auteur et des droits moraux qui protègent cette thèse. Ni la thèse ni des extraits substantiels de celle-ci ne doivent être imprimés ou autrement reproduits sans son autorisation.

In compliance with the Canadian Privacy Act some supporting forms may have been removed from this thesis.

Conformément à la loi canadienne sur la protection de la vie privée, quelques formulaires secondaires ont été enlevés de cette thèse.

While these forms may be included in the document page count, their removal does not represent any loss of content from the thesis.

Bien que ces formulaires aient inclus dans la pagination, il n'y aura aucun contenu manquant.


Canada

"Sláb je ten, co ztratil v sebe víru
a malý ten, co zná jen malý cíl"

Svatopluk Čech

ABSTRACT

Mineral pigments are added to paper with the aim of improving its optical and printing properties. The colloidal behavior of calcium carbonate filler shows a dependence on the quality of water used in suspensions, presence of dissolved and colloidal substances and type of polymer used as a retention aid. The role of the retention aids is to attach colloidal particles, such as fines and mineral pigments, to pulp fibers before or during the paper is made. Two very different single-component retention aids were utilized in calcium carbonate fillers destabilization and deposition on fibers. Cationic polyethylenimine destabilized or facilitated deposition of the filler on fibers by a charge neutralization mechanism while cationic polyacrylamide flocculated or deposited the filler on fibers via a bridging mechanism.

In the presence of anionic dissolved and colloidal substances, the amount of cationic polyacrylamide had to be increased in order to achieve the same degree of pigment flocculation. The reason for the increase was due to the fact that the cationic polyacrylamide formed a polyelectrolyte complex with the anionic substances, namely sulfonated kraft lignin. The reaction between cationic polyacrylamide and lignin was found to be nearly stoichiometric. Low molecular weight cationic polyacrylamide formed mostly colloidal complexes while high molecular weight cationic polyacrylamide formed predominantly coacervate complexes; this was mainly due to differences in characteristic times of lignin association with the cationic polyacrylamide, clustering of polyacrylamide molecules and reformation of polymer chains.

The performance of two-component retention aid systems consisting of a cationic polyacrylamide and anionic microparticles were evaluated by deposition of calcium carbonate filler on pulp fibers. Kaolin clay and bentonite were used to heteroflocculate polyacrylamide-covered surfaces of the fibers and pigment. Due to their inability to delaminate, kaolin clay and acid-treated montmorillonite showed no effect of calcium carbonate filler deposition. After cation exchange with sodium-rich solutions, which caused the montmorillonite to delaminate, the montmorillonite flocculation efficiency considerably improved. Kaolin clay neither delaminated after the cation exchange nor improved calcium carbonate deposition. Bentonite was found to completely delaminate when using polyacrylamide-treated fibers. When added to a suspension of fibers, filler and cationic polyacrylamide, bentonite was found to be in a form of stacks containing on average four platelets.

An alternative way to paper filling with pigment was tested on stationary sheets and on slow and fast Fourdrinier pilot paper machines. Using a secondary headbox on the pilot paper machines, a high degree of loading (above 30%) could be achieved using positive clay or calcium carbonate fillers. However, the fillers lowered the paper strength as they interfered with the fiber-fiber bonding in a similar fashion found in conventionally filled papers.

RÉSUMÉ

Les pigments minéraux sont ajoutés au papier pour l'amélioration des propriétés optiques et d'impression. Les propriétés colloïdales du carbonate de calcium comme l'agent de remplissage démontrent une dépendance sur la qualité de l'eau utilisée dans la préparation des suspensions, la présence de substances colloïdales et dissoutes ainsi que le type de polymère utilisé comme aide à la rétention. Le rôle des aides à la rétention est d'attacher les particules colloïdales, tels que les pigments minéraux, aux fibres de pâtes lors de la fabrication du papier. Deux aides à la rétention uni-composantes très différentes furent utilisées dans la déstabilisation et le dépôt sur les fibres de l'agent de remplissage carbonate de calcium. Le polyéthylèneimine cationique a déstabilisé ou causé le dépôt de l'agent de remplissage sur les fibres par un mécanisme de neutralisation de charge alors que le polyacrylamide cationique a causé la flocculation ou le dépôt sur les fibres par un mécanisme de pontage.

Dans la présence de substances anioniques dissoutes et colloïdales, la quantité requise du polyacrylamide cationique a dû être augmentée pour arriver au même degré de flocculation de pigment. Cette augmentation fut attribuée à la formation d'un complexe polyélectrolyte entre le polyacrylamide cationique et des substances anioniques provenant de la lignine Kraft sulfonée. La réaction entre le polyacrylamide cationique et la lignine s'avérait presque stoichiométrique. Dû aux temps caractéristiques de l'association de la lignine avec le polyacrylamide cationique, le groupement des molécules de polyacrylamide et la reconformation des chaînes

polymériques, le polyacrylamide cationique de poids moléculaire bas forme principalement des complexes colloïdaux alors que le polyacrylamide cationique de haut poids moléculaire forme principalement des complexes de type “coacervate”.

La performance de systèmes d'aide à la rétention à deux composants comprenant le polyacrylamide cationique et des microparticules anioniques furent évalués par le dépôt de l'agent de remplissage carbonate de calcium sur des fibres de pâtes. L'argile kaolin et bentonite furent utilisées pour la flocculation “hetero” des surfaces de fibres et pigments recouvertes de polyacrylamide. Puisqu'ils ne manifestent pas la délamination, l'argile kaolin et le montmorillonite traité d'acide n'avaient pas d'effet sur le dépôt de carbonate de calcium. Suite à l'échange de cations avec des solutions fortes en sodium, ce qui causait la délamination du montmorillonite, l'efficacité de flocculation du montmorillonite a augmenté de façon importante. L'argile kaolin menait ni à la délamination après l'échange de cations, ni à une amélioration du dépôt de carbonate de calcium. Par contre le bentonite démontrait une délamination complète quand les fibres traitées de polyacrylamide furent utilisées. Le bentonite, quand ajouté à une suspension de fibres, charge et polyacrylamide cationique, existait sous forme de piles ayant en moyenne quatre plaques.

Une approche alternative au chargement du papier avec pigment fut évaluée sur des feuilles de papier stationnaires et sur des machines à papier pilote à basse et haute vitesses de type Fourdrineir. En utilisant une tête de machine secondaire sur la machine à papier pilote, un haut degré de chargement (supérieur à 30%) fut atteint en utilisant de l'argile positive ou les agents de remplissage carbonate de calcium.

Cependant, les agents de remplissage ont réduit la résistance mécanique du papier en interférant avec les liaisons fibre-fibre telles que souvent observé dans les papiers chargés de façon conventionnelle.

FOREWORD

The thesis was prepared in accordance with an article B2 of the Guidelines for Thesis Preparation of McGill University. The article B2 reads as follows:

As an alternative to the traditional thesis format, the dissertation can consist of a collection of papers of which the student is an author or co-author. These papers must have a cohesive, unitary character making them a report of a single program of research. The structure for the manuscript-based thesis must conform to the following:

1. Candidates have the option of including, as part of the thesis, the text of one or more papers submitted, or to be submitted, for publication, or the clearly-duplicated text (not the reprints) of one or more published papers. These texts must conform to the "Guidelines for Thesis Preparation" with respect to font size, line spacing and margin sizes and must be bound together as an integral part of the thesis. (Reprints of published papers can be included in the appendices at the end of the thesis.)
2. The thesis must be more than a collection of manuscripts. All components must be integrated into a cohesive unit with a logical progression from one chapter to the next. In order to ensure that the thesis has continuity, connecting texts that provide logical bridges preceeding and following each manuscript are mandatory.
3. The thesis must conform to all other requirements of the "Guidelines for Thesis Preparation" in addition to the manuscripts.

The thesis must include the following:

1. a table of contents;
2. a brief abstract in both English and French;
3. an introduction which clearly states the rational and objectives of the research;
4. a comprehensive review of the literature (in addition to that covered in the introduction to each paper);
5. a final conclusion and summary;
6. a thorough bibliography;
7. Appendix containing an ethics certificate in the case of research involving human or animal subjects, microorganisms, living cells, other biohazards and/or radioactive material.

4. As manuscripts for publication are frequently very concise documents, where appropriate, additional material must be provided (e.g., in appendices) in sufficient detail to allow a clear and precise judgement to be made of the importance and originality of the research reported in the thesis.

5. In general, when co-authored papers are included in a thesis the candidate must have made a substantial contribution to all papers included in the thesis. In addition, the candidate is required to make an explicit statement in the thesis as to who contributed to such work and to what extent. This statement should appear in a single section entitled "Contributions of Authors" as a preface to the thesis. The supervisor must attest to the accuracy of this statement at the doctoral oral defence. Since the task of the examiners is made more difficult in these cases, it is in the candidate's interest to clearly specify the responsibilities of all the authors of the co-authored papers.

6. When previously published copyright material is presented in a thesis, the candidate must include signed waivers from the publishers and submit these to the Graduate and Postdoctoral Studies Office with the final deposition, if not submitted previously. The candidate must also include signed waivers from any co-authors of unpublished manuscripts.

7. Irrespective of the internal and external examiners reports, if the oral defence committee feels that the thesis has major omissions with regard to the above guidelines, the candidate may be required to resubmit an amended version of the thesis. See the "Guidelines for Doctoral Oral Examinations," which can be obtained from the web (<http://www.mcgill.ca/fgsr>), Graduate Secretaries of departments or from the Graduate and Postdoctoral Studies Office, James Administration Building, Room 400, 398-3990, ext. 00711 or 094220.

8. In no case can a co-author of any component of such a thesis serve as an external examiner for that thesis.

This thesis comprises nine chapters. Chapter 1 introduces the field of research and provides an overview of research related to the subject of the thesis. Chapters 2, 3, 4, 5, 6, 7 and 8 present principal results of the conducted research. The Chapters 2-8 are written in a manuscript format. Chapter 9 summarizes the findings of the conducted research and also presents scientific contributions.

The following are the manuscripts written by the author or co-authored, which are used in the preparation of this thesis. Manuscripts 1, 2, 3, 4, 5, 6 and 7 are the base for Chapters 2, 3, 4, 5, 6, 7 and 8, respectively. The co-authors are the thesis supervisor and two of his colleagues (B. Alince in manuscripts 1, 2, 4, 5, 6 and G. Garnier in manuscript 7), who were involved in supervision.

1. Vanerek, A., Alince, B., and van de Ven, T.G.M., "Colloidal Behavior of Ground and Precipitated Calcium Carbonate Fillers: Effect of Cationic Polyelectrolytes and Water Quality". *Journal of Pulp and Paper Science* **26**(4), 135-139 (2000).
2. Vanerek, A., Alince, B., and van de Ven, T.G.M., "Interaction of Calcium Carbonate Fillers with Pulp Fibers: Effect of Surface Charge and Cationic Polyelectrolytes". *Journal of Pulp and Paper Science* **26**(9), 317-322 (2000).
3. Vanerek, A., and van de Ven, T.G.M., "Coacervate Complex Formation between Cationic Polyacrylamide and Anionic Sulfonated Kraft Lignin". For *Journal of Colloid and Interfaces Science* or *Langmuir* (to be submitted).
4. Vanerek, A., Alince, B., and van de Ven, T.G.M., "Delamination and Flocculation Efficiency of Sodium-Activated Kaolin and Montmorillonite". For *Colloids and Surfaces A: Physicochemical and Engineering Aspects* (to be submitted).

5. Vanerek, A., Alince, B., and van de Ven, T.G.M., "Bentonite Delamination Induced by Pulp Fibers Pretreated with Cationic Polyacrylamide". For *Colloids and Surfaces A: Physicochemical and Engineering Aspects* (to be submitted).
6. Alince, B., Vanerek, A., and van de Ven, T.G.M., "Clay Particle Deposition in a Fibre Web: An Alternative Way of Filling Paper?" *Journal of Pulp and Paper Science* **28**(9), 315-321 (2002).
7. van de Ven, T.G.M., Vanerek, A., and Garnier, G., "Filling Wet Paper with the Use of a Secondary Headbox". *Industrial and Engineering Chemistry Research* **43**, 2280-2286 (2004).

CONTRIBUTIONS OF AUTHORS

The co-authors in published articles 1, 2 and 6 (Chapters 2, 3 and 7) are Dr. B. Alince and Dr. T.G.M. van de Ven. They were involved in co-supervision of A. Vanerek who performed the principal research and wrote the manuscripts 1 and 2.. Dr. Alince was the first author in the article 6 (Chapter 7) because of the potential patent application.

The co-authors in a published article 7 (Chapter 8) are Dr. T.G.M. van de Ven and Dr. G. Garnier. They were involved in co-supervision of A. Vanerek who was involved in both mill trials. The testing and analysis for the second mill trial was done exclusively by A. Vanerek, who also wrote the section of the paper dealing with the second mill trial. Dr. T.G.M van de Ven was the first author because of the potential patent application.

The co-author in an unpublished manuscript 3 (Chapters 4) is Dr. T.G.M. van de Ven, the thesis supervisor. The principal research and writing of the manuscript were done by A. Vanerek.

The co-authors in unpublished manuscripts 4 and 5 (Chapters 5 and 6) are Dr. B. Alince and Dr. T.G.M. van de Ven. They were involved in co-supervision of A. Vanerek who performed the principal research and also wrote both manuscripts.

All the required signed waivers from publishers as well as from the co-authors of published and unpublished work were submitted with the final copy of this thesis.

ACKNOWLEDGEMENTS

I wish to thank:

My supervisor Dr. Theo van de Ven, for his guidance, support, inspiring discussions, contagious enthusiasm about science and willingness to share his knowledge.

Dr. Bob Alince, for giving me the chance to come to McGill, for his patience, mentorship, constant motivation and invaluable advice.

McGill, Paprican, Domtar, NSERC, Network of Centres of Excellence (NCE) for Mechanical-Wood Pulps for financial support.

All members of Pulp and Paper Research Centre, Dr. van de Ven's papermaking group and Beer Club. I would like to thank in particular to: Agatha, Alex, Boon, Byoung-Uk, Carol, Claudia, Cecile, Clare, Clements, Charles, Chris, Colleen, Craig, Danko, Daniela, David, Ežo, Françoise, Gabina, Hedieh, Jan Paul, Jindra, Jurek, Kamiti, Klara, Liz, Louis, Maher, Mehdi, Miro, Pat'a, Petra, Pierre, Rado, Renata, Roger, Robert, Sophie, Tom and Virginie.

My dear friends for being there for me when it mattered the most: Janna, Mehdi, Nuna and Shaune.

My parents, my sisters and my nephews.

And finally, to Monica, my dearest, without whom this all would not be possible.

TABLE OF CONTENTS

ABSTRACT	III
RÉSUMÉ	V
FOREWORD	VIII
CONTRIBUTIONS OF AUTHORS	XII
ACKNOWLEDGEMENTS	XIII
TABLE OF CONTENTS	XIV
LIST OF FIGURES	XX
LIST OF TABLES	XXIX

CHAPTER 1

INTRODUCTION	2
1.1. BACKGROUND	3
1.2. PULP FIBERS AND FINES	4
1.3. FILLING OF PAPER WITH MINERAL PIGMENTS	6
1.3. RETENTION AIDS	7
1.4. FLOCCULATION OF PARTICLES BY POLYELECTROLYTES	10
1.5. DISSOLVED AND COLLOIDAL SUBSTANCES (DCS)	12
1.6. EFFECT OF MINERAL PIGMENTS ON PAPER STRENGTH	13
1.7. SCOPE OF THE THESIS	14
1.8. REFERENCES	16

CHAPTER 2

COLLOIDAL BEHAVIOR OF GROUND AND PRECIPITATED CALCIUM CARBONATE FILLERS: EFFECTS OF CATIONIC POLYELECTROLYTES AND WATER QUALITY	24
---	----

2.1. ABSTRACT	25
2.2. INTRODUCTION.....	25
2.3. EXPERIMENTAL.....	27
2.3.1. <i>Materials</i>	27
2.3.2. <i>Experimental techniques</i>	27
2.4. RESULTS AND DISCUSSION	28
2.4.1. <i>Surface charge of CaCO₃.....</i>	28
2.4.2. <i>Colloidal stability of CaCO₃.....</i>	31
2.4.3. <i>Effects of cationic polyelectrolytes.....</i>	33
2.4.4. <i>Effect of anionic contaminants.....</i>	40
2.5. CONCLUDING REMARKS.....	43
2.6. ACKNOWLEDGEMENT	44
2.7. REFERENCES	44

CHAPTER 3

INTERACTION OF CALCIUM CARBONATE FILLERS WITH PULP FIBERS: EFFECT OF SURFACE CHARGE AND CATIONIC POLYELECTROLYTES	47
--	-----------

3.1. ABSTRACT	48
3.2. INTRODUCTION.....	48
3.3. EXPERIMENTAL.....	50
3.3.1. <i>Materials</i>	50
3.3.2. <i>Methods.....</i>	50
3.4. RESULTS AND DISCUSSION.....	51
3.4.1. <i>Rate of deposition in the absence of polyelectrolytes.....</i>	51
3.4.2. <i>Effect of surface charge</i>	56
3.4.3. <i>Effect of polyethylenimine.....</i>	60
3.4.4. <i>Effect of polyacrylamide</i>	65

3.4.5. Retention in Handsheets.....	70
3.5. CONCLUDING REMARKS	72
3.6. ACKNOWLEDGEMENT	73
3.7. REFERENCES	73

CHAPTER 4

COACERVATE COMPLEX FORMATION BETWEEN CATIONIC POLYACRYLAMIDE AND ANIONIC SULFONATED KRAFT LIGNIN 77

4.1. ABSTRACT	78
4.2. INTRODUCTION.....	78
4.3. EXPERIMENTAL	81
4.3.1. Materials	81
4.3.2. Polyelectrolyte complex formation procedure	84
4.3.3. Determination of SKL in the supernatant	86
4.4. RESULTS AND DISCUSSION.....	87
4.4.1. Reaction stoichiometry between cPAM and SKL.....	87
4.4.2. Effect of Mw on coacervate complex formation.....	91
4.4.3. Effect of DS on coacervate complex formation.....	96
4.4.4. Mechanism of colloidal and coacervate complex formation.....	98
4.5. CONCLUSIONS	104
4.6. ACKNOWLEDGEMENTS	105
4.7. REFERENCES	105

CHAPTER 5

DELAMINATION AND FLOCCULATION EFFICIENCY OF SODIUM- ACTIVATED KAOLIN AND MONTMORILLONITE 110

5.1. ABSTRACT	111
5.2. INTRODUCTION.....	111

5.3. EXPERIMENTAL	114
5.3.1. <i>Materials</i>	114
5.3.2. <i>Deposition experiments</i>	116
5.3.3. <i>Cation exchange procedure</i>	117
5.3.4. <i>Particle size measurements</i>	119
5.4. RESULTS AND DISCUSSION	119
5.4.1. <i>PCC deposition on fibers using various microparticle systems</i>	119
5.4.2. <i>pH of microparticle suspensions</i>	121
5.4.3. <i>Cation exchange treatment of microparticle suspensions</i>	123
5.4.4. <i>Microparticle delamination during cation exchange</i>	129
5.4.5. <i>Effect of shear on microparticle delamination</i>	134
5.4.6. <i>Acid treatment of bentonite</i>	137
5.4.7. <i>Elemental analysis</i>	141
5.5. CONCLUSIONS	143
5.6. ACKNOWLEDGEMENTS	144
5.7. REFERENCES	144

CHAPTER 6

BENTONITE DELAMINATION BY PULP FIBERS MEASURED BY CALCIUM CARBONATE DEPOSITION	150
6.1. ABSTRACT	151
6.2. INTRODUCTION	151
6.3. EXPERIMENTAL	154
6.3.1. <i>Materials</i>	154
6.3.2. <i>Deposition of PCC on fibers</i>	156
6.3.3. <i>Deposition of PCC on fibers pretreated with cPAM and bentonite</i>	158
6.4. RESULTS AND DISCUSSION	159
6.4.1. <i>Deposition of PCC on fibers</i>	159

6.4.2. PCC deposition on fibers using fractionated bentonite	159
6.4.3. PCC deposition on fibers pretreated with cPAM and HSA bentonite.....	163
6.4.4. Delamination of HSA bentonite induced by fibers pretreated with cPAM.....	166
6.4.5. Delamination of HSA bentonite during PCC deposition.....	173
6.5. CONCLUSIONS	176
6.6. ACKNOWLEDGMENTS	177
6.7. REFERENCES	177

CHAPTER 7

CLAY PARTICLE DEPOSITION IN A FIBER WEB: AN ALTERNATIVE WAY OF FILLING PAPER? 182

7.1. ABSTRACT	183
7.2. INTRODUCTION.....	183
7.3. PROCEDURE.....	187
7.4. RESULTS	191
7.5. CONCLUSIONS	204
7.6. ACKNOWLEDGEMENTS	205
7.7. REFERENCES	205

CHAPTER 8

FILLING WET PAPER WITH THE USE OF A SEONDARY HEADBOX 208

8.1. ABSTRACT	209
8.2. INTRODUCTION.....	209
8.3. FILLING WET PAPER USING A SECONDARY HEADBOX	211
8.4. MATERIALS	214
8.4.1. Slow Fourdrinier machine	214
8.4.2. Fast Fourdrinier machine.....	215

8.5. PILOT PAPER MACHINES	216
8.6. RESULTS	220
<i>8.6.1. Slow Fourdrinier machine</i>	<i>220</i>
<i>8.6.2. Fast Fourdrinier machine</i>	<i>224</i>
8.7. CONCLUDING REMARKS	236
8.8. ACKNOWLEDGMENT	236
8.9. REFERENCES	237

CHAPTER 9

CONCLUSIONS	240
9.1. OVERVIEW.....	241
9.2. ORIGINAL CONTRIBUTIONS.....	244

LIST OF FIGURES

CHAPTER 2

Figure 2.1: Electrophoretic mobility as a function of CaCO_3 concentration measured in distilled water, tap water and white water from a fine paper mill. (a) PCC, (b) GCC.

Figure 2.2: Relative size of CaCO_3 aggregates in distilled (a) and tap (b) water as a function of shear realized by increasing the flow rate of the suspensions (1000 ppm) in a tube. At a flow rate of 300 mL/min, the shear rate is around 10^3 s^{-1} .

Figure 2.3: Electrophoretic mobility of CaCO_3 dispersed in distilled (top) and tap (bottom) water (500 ppm) as a function of PEI addition.

Figure 2.4: Stability ratio W of CaCO_3 dispersion in distilled water (1000 ppm) as a function of cationic polyelectrolyte addition. In the presence of polyethylenimine, the originally aggregating PCC and GCC become stable ($W = \infty$). With polyacrylamide the rate of flocculation becomes faster ($W < 1$).

Figure 2.5: Relative particle size of CaCO_3 (1000 ppm) upon addition of cationic polyacrylamide (\circ). Reformation of size after subjecting the original flocs to sonication (\bullet).

Figure 2.6: Schematics of cationic polyelectrolyte action. (a) PEI adsorbs on pigment particles thus enhancing charge and repulsion. (b) cPAM adsorbs on pigment particles and forms a bridge, thus causing flocculation. (c) Flocs formed by cPAM after break-up do not reform if the surface coverage of the pigment particles by polymer is high.

Figure 2.7: Stability ratio W of CaCO_3 dispersed in tap water (1000 ppm) as a function of polyethylenimine addition. Due to its negative charge in tap water (Fig. 2.1), CaCO_3 aggregates instead of becoming stable, as in distilled water, shown by the broken line.

Figure 2.8: Effect of anionic contaminant SKL (sulfonated kraft lignin) on the flocculating ability of cationic polyacrylamide. The originally aggregating CaCO_3 becomes stable in the presence of 5 mg SKL per gram CaCO_3 . With increasing content of SKL more cationic polymer is needed to cause flocculation. CaCO_3 conc. 400 ppm.

CHAPTER 3

Figure 3.1: Deposition of CaCO_3 on fibers suspended in distilled water as a function of time. CaCO_3 dispersed in distilled water and added in the amount of 125, 500 and 1000 mg/g fibers in 500 cm^3 water. The curves are the calculated best fit through the experimental points. PCC (top), GCC (bottom).

Figure 3.2: Reciprocal amount of CaCO_3 deposited onto fibers versus reciprocal amount remaining in suspension at steady state.

Figure 3.3: Deposition of CaCO_3 on fibers suspended in tap water as a function of time. CaCO_3 dispersed in distilled water and added in the amount of 125, 500 and 1000 mg/g fibers in 500 cm^3 water.

Figure 3.4: Deposition of CaCO_3 on fibers suspended in tap water as a function of time. CaCO_3 dispersed in tap water and added in the amount of 100, 250 and 500 mg/g fibers in 500 cm^3 water.

Figure 3.5: Deposition of CaCO_3 on fibers suspended in distilled water as a function of time in the presence of PEI. 125, 500 and 1000 mg CaCO_3 dispersed in distilled water added to 1 g fibers in 500 cm^3 followed by PEI addition: (a) 0.1 mg; (b) 1.0 mg; and (c) 10 mg.

Figure 3.6: Deposition of CaCO_3 on fibers suspended in distilled water as a function of time in the presence of cPAM. 125, 500 and 1000 mg CaCO_3 dispersed in distilled water added to one gram fibers in 500 cm^3 followed by cPAM addition: (a) 0.1 mg; (b) 1.0 mg; and (c) 10 mg.

Figure 3.7: Energy of interaction between a fiber and a pigment both fully coated by polymer (schematic).

CHAPTER 4

Figure 4.1: Hydrolysis of cPAM at $\text{pH} \geq 7$ resulting in a negatively charged polyacrylamide.

Figure 4.2: An example of polyelectrolyte complex formation: (A) Formation of a thread-like precipitate that forms a large-scale network (coacervate complex) after cPAM was added to SKL and the solution was gently stirred for about 10 s; (B) The same PEC after 1 min agitation, the network shrank with time, expelling solvent and eventually becoming a single aggregate. The diameter of the aggregate is around 1 cm. The presence of much smaller colloidal complexes is also evident. For better visualization, the concentration of SKL was lowered to 0.5 g/L, cPAM addition was 5 mg and the total volume was 100 cm^3 .

Figure 4.3: The amount of SKL in insoluble PEC (i.e. colloidal and coacervate complexes combined) as a function of DS of added cPAM determined by light adsorption of supernatants containing unreacted SKL. Each point on the plot represents an average value for cPAM additions of 3, 5, 10, 20 and 40 mg introduced to 100 mg SKL. The total volume was 100 cm^3 . Experimental errors were within 5%. For DS = 25%, three cPAM's with Mw of 3, 5, and 6 MDa were used. The points are almost superimposed. A nonionic PAM (DS = 0%) was also used as a reference.

Figure 4.4: The formation of the coacervate complex as a function of cPAM with DS = 25%. Three molecular weights (3, 5, and 6 MDa) were used. The concentration of SKL was 1 g/L and the total volume was 100 cm^3 .

Figure 4.5: The ratio between the formation of colloidal and coacervate complexes. Three cPAM's with the same DS (25%), but three different Mw (3, 5 and 6 MDa) were used. The white portion of the bar represents the formation of the coacervate complex and the black portion represents the colloidal complex. The bar height represents the total amount of insoluble complex formed per mg cPAM added.

Figure 4.6: The formation of the coacervate complex as a function of a molecular weight and charge densities of cPAM. Each point on the plot represents an average value for cPAM additions of 3, 5, 10, 20 and 40 mg introduced to 100 mg SKL. The total volume was 100 cm^3 . A nonionic PAM was also used as a reference (\circ).

Figure 4.7: Schematic drawing of reconfiguration of cPAM after association with SKL. After the charge neutralization reaction of cPAM with SKL, the polyelectrolyte complex has an overall net zero charge, and the system tends to reconfom due to the interaction between the anionic and cationic sites.

Figure 4.8: Schematic drawing of the effect of molecular weight of cPAM on the formation of colloidal and coacervate complexes. Low molar mass cPAM forms predominantly colloidal complexes while high molar mass cPAM forms mostly coacervate complexes with SKL.

CHAPTER 5

Figure 5.1: Summary of the experimental procedure. A suspension consisting of 1 g fiber in 500 cm³ of tap water was stirred at 1500 rpm. At given intervals 200 mg PCC and 2 mg cPAM were added and supernatant samples collected. The speed of stirring was increased to 5000 rpm and microparticles were added followed by a supernatant sampling 5 s after the addition.

Figure 5.2: PCC deposition on fibers using various microparticle systems: Bnt (A), Clay (B), Mnt 20 (C) and Mnt 200 (D). The final PCC deposition is determined 5 s after the microparticle addition. The pH of the suspensions was around 8.

Figure 5.3: Final PCC deposition on fibers as a function of Mnt 200 addition. (S) refers to ion exchange with 1 M NaCl and 1 M Na₂CO₃; (S+H) to ion exchange with 1 M NaCl, 1 M Na₂CO₃ and 0.5 M NaOH; and (H) to ion exchange with 0.5 M NaOH.

Figure 5.4: Final PCC deposition on fibers as a function of Mnt 20 addition. (S) refers to ion exchange with 1 M NaCl and 1 M Na₂CO₃; (S+H) to ion exchange with 1 M NaCl, 1 M Na₂CO₃ and 0.5 M NaOH; and (H) to ion exchange with 0.5 M NaOH.

Figure 5.5: Final PCC deposition on fibers as a function of Clay addition. (S+H) refers to ion exchange with 1 M NaCl, 1 M Na₂CO₃ and 0.5 M NaOH; and (H) to ion exchange with 0.5 M NaOH.

Figure 5.6: Final PCC deposition on fibers as a function of Mnt 20 addition. Mnt 20 was treated with 1 M NaCl, 1 M Na₂CO₃ and 0.5 M NaOH and then subjected to a high shear before its addition to the suspension of fibers, PCC and cPAM.

Figure 5.7: Final PCC deposition as a function of addition of untreated Bnt and Bnt treated with 0.5 M HCl. The pH of the treated Bnt suspensions is indicated in parentheses.

CHAPTER 6

Figure 6.1: Summary of the experimental procedure. A suspension of 1 g of fibers dispersed in 500 cm³ of tap water was stirred at 1500 rpm. At given intervals 200 mg of PCC, 2 mg of cPAM were added and supernatant samples were collected. The speed of stirring was increased to 5000 rpm followed by bentonite addition and supernatant sampling 5 s after the bentonite addition.

Figure 6.2: PCC deposition on fibers using a microparticle retention aid system comprising cPAM and bentonite. The graph shows the final PCC deposition, i.e. 5 s after bentonite addition.

Figure 6.3: Final PCC deposition on fibers (i.e. 5 s after bentonite addition) using high surface area (HSA) and low surface area (LSA) bentonite fractions. The cPAM concentration was 2 mg/g fiber.

Figure 6.4: Kinetics of PCC deposition on fibers pretreated with cPAM and various amounts of HSA bentonite. The speeds of stirring during both fiber pretreatment with bentonite and PCC deposition were 100 rpm.

Figure 6.5: Bentonite blocks the surface of cPAM-treated fibers, and hence, prevents PCC deposition.

Figure 6.6: Kinetics of PCC deposition on fibers pretreated with cPAM and various amounts of HSA bentonite. The speeds of stirring during fiber pretreatment with bentonite and during PCC deposition were 5000 rpm and 100 rpm, respectively.

Figure 6.7: Maximum PCC deposition on fibers pretreated with cPAM and HSA bentonite. After bentonite was added, fibers coated with cPAM were subjected to either a low shear (100 rpm) or a high shear (5000 rpm). The arrow indicates monolayer coverage of bentonite on cPAM-treated fibers (~2.5 mg/g fiber).

Figure 6.8: Maximum PCC deposition on pretreated fibers with cPAM and HSA bentonite. During fiber pretreatment, the addition of bentonite and the stirring speed were kept constant at 2.5 mg/g fibers and 100 rpm, respectively.

Figure 6.9: Final PCC deposition on fibers using HSA bentonite at 1500 rpm and 5000 rpm.

CHAPTER 7

Figure 7.1: Electrophoretic mobility (EM) as a function of pH of pulp fibers (measured on fines derived from and believed to represent the fibers), untreated clay and clay treated with PEI.

Figure 7.2: PEI adsorption and electrophoretic mobility of fibers and clay.

Figure 7.3: Clay content of sheets after passing 1% and 10% clay suspensions adjusted to pH 6, 8 and 10 before (open bars) and after (full bars) washing with pure water (adjusted to pH 6, 8 and 10). Fiber negative, clay negative.

Figure 7.4: SEM at X900 and X14 500 magnification of top (A) and bottom (B) of sheets after washing. Fiber negative, clay negative.

Figure 7.5: Clay content of sheets after passing 1% and 10% clay suspensions at pH 6, 8 and 10 before (open bars) and after (full bars) washing with pure water. Fiber positive, clay positive.

Figure 7.6: Clay content of sheets. Fiber positive, clay negative.

Figure 7.7: SEM at X900 and X14 500 magnification of top (A) and bottom (B) of sheets after passing 10% clay suspensions and washing with pure water at pH 6. Fiber positive, clay negative.

Figure 7.8: Schematic representation of the kinetics of clay particles depositing on fibers in a wet sheet for 1% and 10% clay dispersion. t_f is the time at the end of the experiment.

Figure 7.9: SEM at X900 and X14 500 magnification of the top (A) and bottom (B) of sheets after passing 1% clay suspension and washing with pure water. Fiber positive, clay negative.

Figure 7.10: Clay content of sheet. Clay positive, fiber negative.

Figure 7.11: SEM at X900 and X14 500 magnification of top (A) and bottom (B) of sheets after passing 10% of clay suspensions and washing with pure water at pH 10. Fiber negative, clay positive.

CHAPTER 8

Figure 8.1: Schematic drawing of water replacement in a wet sheet with a filler suspension.

Figure 8.2: Schematic drawing of filling wet paper on a Fourdrinier machine equipped with a secondary headbox. On the slow machine, the filler suspension was pumped directly to the headbox using the fan pump only. On the fast machine, the filler suspension was pumped (dashed pump) into a waterline (dashed) that fed the secondary headbox.

Figure 8.3: Photographs of a filler suspension flowing out of the secondary headbox onto wet paper on a slow Fourdrinier machine (top) and a fast Fourdrinier machine (bottom). The locations of the two drylines are consistent with the predictions of Eq. 3.

Figure 8.4: ISO brightness and ISO opacity for papers filled with clay from the secondary headbox.

Figure 8.5: Total energy absorption (TEA) of wet-filled sheets as a function of clay content.

Figure 8.6: Retention of PCC in paper (black bars). The total bar height corresponds to the amount of PCC added. The parentheses refer to PCC treatments with polymers. The different bars are for various runs with different secondary headbox concentrations (proportional to the addition levels shown in the figure).

Figure 8.7: Relation between retained and added PCC for positive and negative PCC's. The parentheses refer to PCC treatments with polymers; a-stabilizer and c-starch represent anionic stabilizer and cationic starch, respectively.

Figure 8.8: ISO brightness of top sides of sheets as a function of PCC content. The parentheses refer to PCC treatments with polymers; a-stabilizer and c-starch represent anionic stabilizer and cationic starch, respectively.

Figure 8.9: Comparison of brightness on top and bottom sides of sheets filled with various amounts of PCC, treated in various ways. The parentheses refer to PCC treatments with polymers.

Figure 8.10: Concentration of starch-treated PCC throughout the sheet. The sheet was divided in 12 layers by peeling. Layer 1 is the top layer; layer 12 is the bottom layer.

Figure 8.11: Breaking length of PCC-filled sheets as function of PCC content, in both the machine and cross directions. The parentheses refer to PCC treatments with polymers; a-stabilizer and c-starch represent anionic stabilizer and cationic starch, respectively.

Figure 8.12: SEM images of top and bottom sides (left and right images, respectively) of sheet filled with anionic PCC. The PCC content is 8.4%.

Figure 8.13: SEM images of top and bottom sides (left and right images, respectively) of sheet filled with PEI-treated PCC. The PCC content is 14.4%.

LIST OF TABLES

CHAPTER 2

Table 2.1: Conductivity (C), electrophoretic mobility (EM) and pH of a CaCO_3 suspension.

CHAPTER 3

Table 3.1: Electrophoretic mobility of CaCO_3 .

Table 3.2: PEI adsorption, charge and relative size of PCC as a function of PEI addition at pH 9.5.

Table 3.3: PEI adsorption and charge of fibers as a function of PEI addition at pH 9.5.

CHAPTER 4

Table 4.1: Summary of used polyacrylamides and their description in terms of degree of substitution (DS) and molecular weight (Mw).

Table 4.2: Reaction stoichiometry of PEC formation between cPAM and SKL.

Table 4.3: Theoretical prediction of characteristic times of association τ_a and clustering τ_c .

CHAPTER 5

Table 5.1: An overview of the microparticle systems.

Table 5.2: pH of microparticle systems at a concentration of 10 g/L.

Table 5.3: The cation exchange treatment of Mnt 200 and pH profiles. Each wash consisted of centrifugation, decanting and redispersion of the microparticles in ultra pure water.

Table 5.4: The number of platelets, n , in montmorillonite stacks as a function of Mnt 200 cation exchange treatment. The radius of montmorillonite, a_d , is assumed to be 300 nm.

Table 5.5: The number of platelets, n , in montmorillonite and bentonite stacks as a function of shearing time. Both, Mnt 20 and Clay were treated with 1 M NaCl, 1 M Na₂CO₃ and 0.5 M NaOH. The shaded rows represent untreated Mnt 20 and Clay and Mnt 20 and Clay treated with 0.5 M NaOH, respectively. The radii of the montmorillonite and clay, a_d , are assumed to be 300 nm and 100 nm, respectively.

Table 5.6: The number of platelets, n , for untreated Bnt and Bnt treated with 0.5 M HCl. The pH of the treated Bnt suspensions is indicated in parentheses. The radius of bentonite, a_d , is assumed to be 300 nm.

Table 5.7: The sodium content in untreated Mnt 200; Mnt 200 treated with 1 M NaCl and 1 M Na₂CO₃; Mnt 200 treated with 1 M NaCl, 1 M Na₂CO₃ and 0.5 M NaOH; and Mnt 200 treated with 0.5 M NaOH.

Chapter 1

INTRODUCTION

1.1. Background

The name paper is derived from *papyrus*, a reedy plant, used by the ancient Egyptians as the first writing material over 2000 B.C. [1]. Paper was made by beating and pressing the papyrus stems together. However, the first true paper was made from *bamboo* in China in 300 B.C. [2]. Manufacturing this type of paper involved basic processes, which are used in today's papermaking. The plants were converted to pulp by defibering the stems with the use of chemical and mechanical actions. The pulp suspension was then diluted and paper was formed by immersing screens into pulp suspensions and lifting them up to allow water to escape. The use of paper spread throughout Asia to Europe in the Middle Ages.

The first paper mills appeared in Italy, France, Germany and Spain in the 15th century. The first paper mill in North America was established near Philadelphia in 1690. Paper production was revolutionized with the invention of the continuous papermaking machine in France in 1798 [3]. In recent times, papermaking has evolved into a complex process consisting of a variety of operations aimed to improve paper properties and, at the same time, to accommodate the need to produce paper on very fast paper machines. For these reasons, many additives, such as mineral pigments, internal sizing agents, dry-strength and wet-strength agents, retention aids, etc., are commonly added to a suspension of pulp before the paper is made. Paper is formed on a paper machine where diluted pulp suspensions, typically at 0.2-1.0% consistency, are applied from a headbox on a forming wire which can travel at velocities of around 1000 m/min [2]. The paper is formed by dewatering the suspensions down to about 15%, at which point the paper is removed from the

forming wire and enters the press section of the paper machine. Processes utilized in between preparation of pulp suspensions (i.e. including also additions of various additives) and paper formation on paper machines are referred to as the *wet end* of papermaking.

1.2. Pulp fibers and fines

The main component in paper is pulp fibers. Fibers can be divided into two categories depending on the fiber origin: (i) softwood from coniferous trees and (ii) hardwood from deciduous trees. While softwood consists of long, uniform cells called *tracheids*, hardwood is more complex as it contains long, narrow cells called *libriform* fibers along with short, wide cells called *vessels*. Besides the libriform fibers and vessels, hardwoods also contain a large number of parenchyma cells.

Another difference is in the fiber dimensions. Softwood fibers are around 3-5 mm in length and 30 μm in diameter while hardwood fibers are around 2 mm long and about 20 μm thick. The chemical composition of softwood and hardwood fibers is similar in many aspects. Softwood fibers contain around 42% *cellulose* (cellulose is the main building block of fiber cells) and 28% *lignin* (lignin is intercellular material, which cements the fibers together). Hardwoods contain around 45% cellulose and 20% lignin.

There are many developed technologies to extract pulp fibers from trees, some of which utilize elevated temperatures followed by mechanical action. The pulp fibers obtained by these processes are called *thermo-mechanical pulps* (TMP). Trees are cut into woodchips, and these are first softened by the use of steam and then defibrillated

using large refiners. The fibers are separated from one another by the mechanical action between two refiner plates. This process also generates a large portion of fine material, such as fiber fragments and fibrils, which are generally called *fines*. The fines content in TMP is usually between 30-40%.

Other typical pulping processes utilize heat and chemical action, and the obtained pulps are referred to as *chemical pulps*. Unlike in thermo-mechanical pulping where lignin is preserved, lignin is dissolved by the action of chemicals in chemical pulping. In *kraft* pulping, which is one of the most common chemical pulping processes, lignin is dissolved by sodium hydroxide along with sodium sulfide. This process makes the separation of individual pulp fibers relatively easy. In addition, this type of pulping produces a relatively low amount of fines. In the kraft pulp, the fines content is around 4% and 10% for softwood and hardwood, respectively.

In general, fines in chemical pulps improve the final strength of paper while fines in thermo-mechanical pulps improve both strength and optical properties [4], making the fines indispensable in papermaking. However, due to their small size, not all fines are retained in a paper sheet. The un-retained fines pass through a wire of the paper machine, and are returned back and mixed with a fresh pulp slurry leading to a gradual increase of fines content in the system. This may cause many problems, mainly breaks of the sheet of paper. Another negative effect which is related to high fines content in process waters is in the increased surface area. Cellulose fibers are considered to have an external surface area around $1 \text{ m}^2/\text{g}$ [5, 6] while the external surface area of fines is around $10 \text{ m}^2/\text{g}$ [6-8]. Many additives are introduced to the

pulp furnish during papermaking and the majority of additives adsorbs on cellulosic surfaces. Due to increasing volume fraction of fines in the pulp suspensions, most of the additives will end up on fines rather than fibers. This may have several consequences: (i) more fines concentrated in the system usually means larger amounts of additives are required; (ii) most additives are expensive and increase the cost of paper; and (iii) in the case of poor retention, fines treated additives are recirculated and may cause overfloculation, poor drainage, inferior formation and paper strength and problems with paper machine runnability.

1.3. Filling of paper with mineral pigments

Mineral pigments, such as clay, calcium carbonate, titanium dioxide, etc., are commonly used in papermaking. These mineral fillers are added to paper in order to improve optical and printing properties. In addition, most fillers are cheaper than the fibers, which helps to lower the cost of paper.

Since the late 1980s, precipitated calcium carbonate (PCC) has become one of the most frequently used pigments in the pulp and paper industry [9]. The shift to precipitated calcium carbonate was a result of a new technology first realized by Pfizer Inc., which enabled PCC to be manufactured on-site. This method is based on passing flue gases, which come from a lime kiln and contain kiln dust, through kiln dust separators. The removed kiln dust, which contains calcium oxide, is then mixed with water forming calcium hydroxide. The saturated solutions of calcium hydroxide are allowed to react with carbon dioxide gas, which produces high purity precipitated calcium carbonate [10-12]. The size and morphology of PCC particles can be

controlled by changing conditions such as temperature, time of reaction and rate of mixing. Calcite with a scalenohedral shape has become one of the most frequently used PCC fillers in papermaking because of its superior optical properties [9].

Results regarding surface charge of calcium carbonates were often a subject of controversy. Some results indicated that calcium carbonate pigments are negatively charged [13], while others suggested the opposite [14]. This ambiguity arises partly from the fact that some calcium carbonate pigments (usually ground calcium carbonate) are treated with anionic dispersants. The anionic dispersant provides calcium carbonate with a strong negative charge, and ensuing electrostatic repulsion renders the pigment colloidally stable. It was also reported that the surface charge changes as a function of calcium carbonate concentration [15]. At high PCC concentrations the surface charge is positive, but reverses to negative at lower concentrations. It was shown that untreated calcium carbonate suspended in pure water is positively charged due to partial calcium carbonate dissolution and readsorption of calcium ions on the pigment surfaces [16]. However, it is still unclear why the surface charge changes as a function of calcium carbonate concentration, although some suggestions were made that electrolytes or impurities might be the reason.

1.3. Retention aids

Fibers suspended in water acquire a negative charge due to dissociation of functional groups on the fiber surfaces. The formation and concentration of individual functional groups may vary depending on the pulping process. One of the most

important groups determining the fiber charge are the carboxyl groups. The carboxyl groups are negatively charged under common papermaking conditions [17]. Most of the common mineral fillers used in papermaking are also negative, and consequently, pigment particles will not deposit on fibers due to electrostatic repulsion. During paper formation, most of the filler with a diameter smaller than the wire openings, would naturally escape from the forming sheet and only large pigments would be retained due to filtration. In order to incorporate the maximum amount of the pigment, so-called retention aids must be used. In general, the retention aids are cationic polyelectrolytes whose role is to eliminate electrostatic repulsion between fibers and pigment by the means of modifying or reversing the negative charge. However, the salt concentration in most mills is sufficiently high to screen electrostatic charges and without the use of proper retention aids the bonds are weak.

Retention of fine particles using one-component systems (cationic polyelectrolytes only) is usually inadequate. This led to a development of multi-component retention aids. The most common two-component retention aid systems are: (i) dual retention aid system consisting of a highly charged, low molecular weight cationic polymer and a high molecular weight anionic polymer; (ii) microparticulate retention aid system comprising anionic microparticles and a low charge density, high molecular weight cationic polymer; and (iii) a nonionic polymer in combination with phenolic-based resins.

One of the most widely used two-component retention aid systems is the microparticulate retention aid system which utilizes bentonite and a cationic polyacrylamide [18]. The cationic polyelectrolyte is first added to a suspension

consisting of fibers, fines and mineral pigment. The system flocculates, but is consequently redispersed by shear generated by fan pumps and/or pressure screens before the headbox of a paper machine. Bentonite is added at this point, which causes the system to reflocculate where bentonite particles act as a bridge between polymer-coated surfaces. The microparticulate retention aid systems considerably improve the retention of fine particles, yet at the same time improve drainage [19]. This phenomenon is in contrast with a general trend where retention of fine material in the fiber mat causes slower drainage of the sheet.

The exact mechanism by which microparticulate systems operate is still elusive. The general consensus is that after polymer addition, the polymer adsorbs on fibers and pigment causing flocculation by a bridging mechanism [20-22]. The system is then redispersed by high shear, which causes the flocs to break up. During the floc breakup, the following can happen to the polymer: (i) polymer transfer from one particle to another particle [23]; and/or (ii) actual breakage of polymer chains [24, 25]. The effect of both phenomena results in a suspension which contains particles covered with cationic polymer. Subsequent addition of bentonite to suspensions containing such polymer-coated particles causes the system to reflocculate where bentonite acts as a bridge between two polymer-coated surfaces. It has been shown that the flocculation by microparticles is superior to flocculation by polymer only [26-28]. Also the bond strength of the flocs increases considerably [29].

Many questions have been raised as to how bentonite platelets with a thickness of $\sim 1\text{nm}$ and a width of $\sim 200\text{ nm}$ can flocculate fibers which have a high

degree of roughness. Other points raised pertain to bentonite delamination, namely whether complete bentonite delamination is necessary for successful flocculation.

1.4. Flocculation of particles by polyelectrolytes

In papermaking, fibers, fines and mineral particles flocculate as a result of interaction with adsorbing polymers. In general, two mechanisms can be distinguished: (i) charge neutralization [30, 31] (also called patch or mosaic mechanisms); and (ii) polymer bridging [20-22] .

Flocculation by charge neutralization is based on modification of a surface charge by the adsorbing polymer, which is oppositely charged. Since most colloids in papermaking are negatively charged, cationic polyelectrolytes have to be utilized. The colloidal particles are initially stable due to a strong negative charge. The adsorbing cationic polymer interacts with the negative charges diminishing electrostatic repulsion between colloidal particles and inadvertently causing flocculation. The maximum flocculation occurs when colloidal particles are overall electroneutral, i.e. negative charges balances positive charges. With increasing polymer additions, more of the polymer starts to adsorb and, as a consequence, colloidal particles start to become more positive thus leading to a lower degree of flocculation. Ultimately, if too much of polymer is added, the colloidal particles will become positive and reestablish strong electrostatic repulsion, which will prevent particles from aggregating. An example of particle destabilization by charge neutralization is a system involving cationic polyethylenimine [32-34].

Flocculation by a bridging mechanism occurs when one part of a polymer chain adsorbs on one colloidal particle and another portion of the polymer chains adsorbs on a second colloidal particle *bridging* these two particles together, hence the name bridging mechanism. Besides the ability of the polymer to adsorb, another requirement is in the chain length of the polymer. Based on classical DLVO theory [35, 36], the charge of colloidal particles is compensated by counterions present, in the case of papermaking, in water. The concentration of counterions is highest at the particle surface, but decreases over distance until it reaches the bulk concentration. This distance over which the counterion concentration decays is called *electrostatic double layer*. As two particles approach, the counterion shells around the particles start to overlap, which results in electrostatic repulsion. To circumvent this phenomenon, polymers flocculating by the bridging mechanism must have a polymer chain longer than the two electrostatic double layer thicknesses. The maximum flocculation by the bridging mechanism occurs when half of the surface is bare and half is covered with the polymer. If an excess of polymer is added, this will lead to stabilization of the colloidal particles by so-called steric repulsion [37]. An example of particle destabilization by the bridging mechanism is a system involving cationic polyacrylamide [37, 38].

In papermaking, interactions among colliding colloidal particles are complex. Depending on flow and particle size, particle collisions can be either induced by shear (*orthokinetic*) or diffusion (*perikinetic*). Due to turbulent flow, collision rates among colloidal particles are orthokinetic, except for extremely small particles ($<0.1\mu\text{m}$). Smoluchowski was the first to estimate the collision rate constants between two

spherical particles for both orthokinetic and perikinetic processes [39]. Smoluchowski's theory was later modified for spherical particles and long rods by Petlicki and van de Ven [40]. However, not all collisions lead to deposition or flocculation, and therefore, a new parameter called collision efficiency was introduced by van de Ven [41] to compensate for collisions not leading to a particle capture. Adsorption of polymers and deposition of colloidal particles on fibers was found to be analogous to gas molecule adsorption, and hence could be described by modified Langmuir kinetics [17, 42]. An excellent summary of possible colloidal particle interactions in pulp suspensions based on Langmuir-Smoluchowski kinetics is presented by van de Ven [43].

1.5. Dissolved and colloidal substances (DCS)

The flocculation efficiency of retention aids is decreased in contaminated systems [44-46]. Due to water system closure and very often due to poor washing efficiency during pulping, dissolved and colloidal substances (also known as anionic trash) are carried over to papermaking. The dissolved and colloidal substances include around a hundred different contaminants, of which the most common are fines, mineral particles, dissolved lignin and hemicelluloses, resins, wood extractives, etc. [47-52]. These contaminants are negatively charged and will compete with the fibers and pigment for the cationic retention aids.

The general consensus is that cationic polymers added to a suspension of fibers, fines and pigment will, in the presence of DSC, interact with the anionic contaminants first. This leads to a poor flocculation and consequently to a poor

retention of the fine particles in paper. To compensate for the loss of the retention aids in the reaction with DCS, high additions of the cationic polymer are required. It is believed that from the increased polymer addition, a certain portion of the polymer has to first neutralize the excess of negative charge generated by DCS, and the remaining polymer will then flocculate the fibers and fine material.

However, some retention aids performed well in highly contaminated systems. This indicates that some cationic retention aids operate by a different mechanism than that which is based on neutralization of DCS.

1.6. Effect of mineral pigments on paper strength

Optical properties, such as brightness, opacity, light scattering coefficient, etc., of papers filled with mineral pigments are considerably enhanced due to increased reflectivity [53]. However, inclusion of the mineral pigment in the paper has an unfavorable effect on paper strength [54]. The reason for the decrease in tensile strength of paper is caused by deposition of colloidal particles on fiber surfaces. In un-filled papers during drying, water is evaporated and due to capillary forces, the fiber surfaces are brought closely together, which results in a development of fiber-fiber bonds. The fiber-fiber bonding is believed to originate from formation of hydrogen bonds between fiber surfaces [55]. In filled papers with mineral pigments, colloidal particles deposit on fiber surfaces and inadvertently prevent fiber-fiber bonding. As a consequence, the strength of paper decreases.

1.7. Scope of the thesis

The objectives of this thesis are the following:

1. To explain colloidal behavior of ground and precipitated calcium carbonate fillers in the presence of cationic polyelectrolytes and to compare the effect of water quality on the filler and polyelectrolytes.
2. To elucidate the mechanism by which cationic polyelectrolytes operate in the presence of dissolved and colloidal substances.
3. To determine the extent of microparticle delamination in suspensions containing fibers and mineral pigment and the effect of delamination on flocculation efficiency.
4. To design an alternative way to paper filling by passing concentrated filler suspensions through a wet sheet.

In Chapter 2, the change in surface charge of ground and precipitated calcium carbonate pigments with respect to water quality and concentration of the pigments is explained. The effect of dissolved and colloidal substances on calcium carbonate flocculation is also presented.

In Chapter 3, interactions of ground and precipitated calcium carbonate pigments with pulp fibers are explained in terms of Langmuir-Smoluchowski kinetics. Variables of interest are water quality, type of cationic polyelectrolyte and polyelectrolyte concentration.

In Chapter 4, a mechanism by which cationic polyacrylamide operates in the presence of dissolved and colloidal substance is established. The cationic polymer

and the anionic substances form polyelectrolyte complexes. The effect of polymer charge and molecular weight on the formation of polyelectrolyte complexes is studied.

In Chapter 5, a relationship between delamination of microparticles and flocculation efficiency between fibers and precipitated calcium carbonate is established. The role of cations in delamination of hydrogenated montmorillonite is presented.

In Chapter 6, the extent of bentonite delamination in pulp suspensions is quantified. The role of fibers coated with cationic polyacrylamide on bentonite delamination is defined.

In Chapter 7, the feasibility of filling of paper by passing concentrated filler suspensions through a wet sheet of paper, which is stationary, is determined.

In Chapter 8, an alternative method to paper filling from Chapter 7 was successfully tested on slow and fast pilot paper machines.

In Chapter 9, the findings provided in this thesis are summarized and original contributions are also provided.

1.8. References

- [1] Koops, M., "Historical Account of the Substances Which Have Been Used to Describe Events, and to Convey Ideas, from the Earliest Date to the Invention of Paper", T. Burton, London, (1800).
- [2] Smook, G.A., "Handbook for Pulp & Paper Technology", Angus Wilde Publications, Vancouver, (1992).
- [3] Clapperton, R.H., "The Papermaking Machine. Its Invention, Evolution and Development", Pergamon Press, (1967).
- [4] Retulainen, E. and Nieminen, K., "Fibre Properties as a Control Variables in Papermaking? Part 2. Strengthening Interfibre Bonds and Reducing Grammage". *Paperi Ja Puu - Paper and Timber* **78**(8), 305-312 (1996).
- [5] Stamm, A.J., "Wood and Cellulose Science", Ronald Press, New York, (1964).
- [6] Marton, J., "Surface Chemical Role of Fines in Papermaking Furnish". *Ind. Eng. Chem. Prod. Res. Dev.* **21**, 146-150 (1982).
- [7] Wood, J.R. and Karnis, A., "Determination of Specific Surface Area of Mechanical Pulp Fines from Turbidity Measurements". *Paperi Ja Puu - Paper and Timber* **78**(4), 181-186 (1996).
- [8] Wood, J.R., Groding, M. and Karnis, A., "Characterization of Mechanical Pulp Fines with a Small Hydrocyclone. Part I. The Principle and Nature of Separation". *J. Pulp Pap. Sci.* **17**(1), J1-J5 (1991).

- [9] Gill, R.A., "The Behavior of on-Site Synthesized Precipitated Calcium Carbonates and Other Calcium Carbonate Fillers on Paper Properties". *Nordic Pulp Pap. Res. J.* **2**, 120-127 (1989).
- [10] Silenius, P. and Leskelä, M., "Filler for Use in Paper Manufacture and Procedure for Producing a Filler", PCT International Patent Application, WO 97/01670 (1997).
- [11] Huege, F.R., "Method of Manufacturing High Purity Calcium Carbonate", PCT International Patent Application, WO 97/11030 (1997).
- [12] Fortier, S.M., Jackson, W.B., O'Rourke, P.B., Perez, R. and Bryan, D.P., "Precipitated Calcium Carbonate and Its Production and Use", PCT International Patent Application, WO 99/51691 (1999).
- [13] Douglas, H.W. and Walker, R.A., "The Electrokinetic Behaviour of Iceland Spar against Aqueous Electrolyte Solutions". *Trans. Faraday Soc.* **46**, 559-568 (1950).
- [14] Ney, P., "Potentiale Und Flotierbarkeit Von Mineralen", Springer-Verlag, Wien, New York, (1973).
- [15] Siffert, B. and Fimbel, P., "Parameters Affecting the Sign and the Magnitude of the Electrokinetic Potential of Calcite". *Colloids Surf.* **11**, 377-389 (1984).
- [16] Huang, Y.C., Fowkes, F.M., Lloyd, T.B. and Sanders, N.D., "Adsorption of Calcium Ions from Calcium Chloride Solutions onto Calcium Carbonate Particles". *Langmuir* **7**, 1742-1748 (1991).

- [17] Alince, B., Petlicki, J. and van de Ven, T.G.M., "Kinetics of Colloidal Particle Deposition on Pulp Fibers 1. Deposition of Clay on Fibers of Opposite Charge". *Colloids Surf.* **59**, 265-277 (1991).
- [18] Langley, J.G. and Litchfield, E., "Dewatering Aids for Paper Applications", Tappi Press, Tappi Papermakers Conference Proceedings, Atlanta, (1986).
- [19] Covarrubias, R.M., Paracki, J. and Mirza, S., "New Advances in Microparticle Retention Technologies". *Appita J.* **55**(4), 272 (2002).
- [20] Dickinson, E. and Eriksson, L., "Particle Flocculation by Adsorbing Polymers". *Adv. Colloid Interface Sci.* **34**, 1 (1991).
- [21] van de Ven, T.G.M., "Kinetic Aspects of Polymer and Polyelectrolyte Adsorption on Surfaces". *Adv. Colloid Interface Sci.* **48**, 121 (1994).
- [22] Swerin, A., Ödberg, L. and Wågberg, L., "An Extended Model for the Estimation of Flocculation Efficiency Factors in Multicomponent Flocculant Systems". *Colloids Surf. A* **113**, 25 (1996).
- [23] Asselman, T. and Garnier, G., "Mechanism of Polyelectrolyte Transfer During Heteroflocculation". *Langmuir* **16**(11), 4871-4876 (2000).
- [24] Tanaka, H., Swerin, A. and Ödberg, L., "Cleavage of Polymer Chains During Transfer of Cationic Polyacrylamide from Cellulose Fibers to Polystyrene Latex". *J. Colloid Interface Sci.* **153**(1), 13-22 (1992).
- [25] Tanaka, H., Swerin, A. and Ödberg, L., "Transfer of Cationic Retention Aid from Fibers to Fine Particles and Cleavage of Polymer Chains under Wet-End Papermaking Conditions". *Tappi J.* **76**(5), 157-163 (1993).

- [26] Swerin, A., Sjödin, U. and Ödberg, L., "Flocculation of Cellulosic Fibre Suspensions by Model Microparticulate Retention Aid Systems". *Nordic Pulp Pap. Res. J.* **4**, 398 (1993).
- [27] Swerin, A., Risinger, G. and Ödberg, L., "Flocculation in Suspensions of Microcrystalline Cellulose by Microparticle Retention Aid Systems". *J. Pulp Pap. Sci.* **23**(8), J374 (1997).
- [28] Swerin, A. and Ödberg, L., "Flocculation of Cellulosic Fibre Suspensions by a Microparticulate Retention Aid System Consisting of Cationic Polyacrylamide and Anionic Montmorillonite". *Nordic Pulp Pap. Res. J.* **1**, 22 (1996).
- [29] Swerin, A., Risinger, G. and Ödberg, L., "Shear Strength in Papermaking Suspensions Flocculated by Retention Aid Systems". *Nordic Pulp Pap. Res. J.* **1**, 30 (1996).
- [30] Gregory, J., "Rates of Flocculation of Latex Particles by Cationic Polymers". *J. Colloid Interface Sci.* **42**(2), 448-456 (1973).
- [31] Runkanaa, V., Somasundaran, P. and Kapurb, P.C., "Mathematical Modeling of Polymer-Induced Flocculation by Charge Neutralization". *J. Colloid Interface Sci.* **270**(2), 347-358 (2004).
- [32] Porubská, J., Alince, B. and van de Ven, T.G.M., "Homo- and Heteroflocculation of Papermaking Fines and Fillers". *Colloids Surf. A* **210**, 223-230 (2002).
- [33] Alince, B. and van de Ven, T.G.M., "Stability of Clay Suspensions - Effect of pH and Polyethylenimine". *J. Colloid Interface Sci.* **155**, 465-470 (1993).

- [34] Suty, S., Alince, B. and van de Ven, T.G.M., "Stability of Ground and Precipitated CaCO_3 Suspensions in the Presence of Polyethylenimine and Salt". *J. Pulp Pap. Sci.* **22**(9), J321-J326 (1996).
- [35] Derjaguin, B.V. and Landau, L., *Acta Physicochim. U.S.S.R.* **14**, 633 (1941).
- [36] Verwey, E.J.W. and Overbeek, J.T.G., "Theory of the Stability of Lyophobic Colloids", Elsevier, Amsterdam, (1948).
- [37] Alince, B. and Bednar, F., "Role of Cationic Polyacrylamide in Fiber- CaCO_3 Pigment Interactions". *J. Appl. Polymer Sci.* **88**(10), 2409-2415 (2003).
- [38] Alince, B., Bednar, F. and van de Ven, T.G.M., "Deposition of Calcium Carbonate Particles on Fiber Surfaces Induced by Cationic Polyelectrolyte and Bentonite". *Colloids Surf. A* **190**, 71-80 (2001).
- [39] Smoluchowski, M., "Versuch Einer Mathematischen Theorie Der Koagulationskinetik Kolloider Lösungen". *Z. Phys. Chem.* **92**(29), 129 (1917).
- [40] Petlicki, J. and van de Ven, T.G.M., "Shear-Induced Deposition of Colloidal Particles on Spheroids". *J. Colloid Interface Sci.* **148**(1), 14-22 (1992).
- [41] van de Ven, T.G.M., "Fundamentals of Papermaking", *Physicochemical and hydrodynamic aspects of fines and filler retention. 9th Fundamental research symposium*, Eng. Publ. Ltd., London, Cambridge, Sept. 1989, (1989).
- [42] Petlicki, J. and van de Ven, T.G.M., "Adsorption of Polyethylenimine onto Cellulose Fibers". *Colloids Surf. A* **83**(1), 9-23 (1994).
- [43] van de Ven, T.G.M., "Particle Deposition on Pulp Fibers. The Influence of Added Chemicals". *Nordic Pulp Pap. Res. J.* **8**(1), 130-134 (1993).

- [44] Sundberg, A., Ekman, R., Holmbom, B. and Grönfors, H., "Interactions of Cationic Polymers with Components in Thermomechanical Pulp Suspensions". *Paperi Ja Puu - Paper and Timber* **76**(9), 593-598 (1994).
- [45] Alince, B., "Effect of Contaminants on Filler Retention in Mechanical Pulp". *Paperi Ja Puu - Paper and Timber* **69**(3), 230-233 (1987).
- [46] Alince, B., "Contaminants, Clay Retention and Polyethylenimine". *Paper Technology* **6**, 27-30 (1991).
- [47] Holmbom, B., "Dissolved and Colloidal Substances in Papermaking", *Nordisk Forskarkurs i Papperskemi*, Rönninge, Sweden, (1995).
- [48] Nylund, J., Lagus, O. and Rosenholm, J.B., "Dissolved and Colloidal Substances from Mechanical Pulp Suspensions - Stability and Flocculation Behaviour". *Colloids Surf. A* **104**, 137-146 (1995).
- [49] Nylund, J., Lagus, O. and Eckerman, C., "Character and Stability of Colloidal Substances in a Mechanical Pulp Suspension". *Colloids Surf. A* **85**, 81-87 (1994).
- [50] Thornton, J., Ekman, R., Holmbom, B. and Örså, F., "Polysaccharides Dissolved from Norway Spruce in Thermomechanical Pulping and Peroxide Bleaching". *J. Wood Chem. Tech.* **14**(2), 159-175 (1994).
- [51] Kleen, M. and Lindström, K., "Polysaccharides and Lignins in Newsprint Process Waters Studied by Pyrolysis-Gas Chromatography/Mass Spectrometry". *Nordic Pulp Pap. Res. J.* **2**, 111-118 (1994).

- [52] Ekman, R. and Holmbom, B., "The Wood Extractives in Alkaline Peroxide Bleaching of Groundwood from Norway Spruce". *Nordic Pulp Pap. Res. J.* **3**, 188-191 (1989).
- [53] Kubelka, P. and Munk, F., "Ein Beitrag Zur Optik Der Farbanstriche". *Zeit. Für Tekn. Physik* **12**, 593-601 (1931).
- [54] Aaltio, J., "The Effect of Fillers on the Strength of Paper". *Paperi ja Puu* **38**, 589-602 (1956).
- [55] Nissan, A.H., "An Interpretation of the Beating Process of Paper Based on the Hydrogen-Bond Theory of the Mechanical Properties of Cellulose Sheets". *Tappi J.* **41**, 131-134 (1958).

Chapter 2

Mineral pigments dispersed in water become charged due to dissociation of functional groups. The surface charge of mineral pigments can either be positive or negative depending on many factors such as type of a mineral structure, pH, and presence of impurities in water. This will consequently affect the pigment interaction with polyelectrolytes.

2.1. Abstract

Untreated calcium carbonate pigments, both precipitated (PCC) and ground (GCC), behave similarly when dispersed in water. Their charge, either positive or negative, depends on the CaCO_3 concentration and the purity of the water. However, in neither case is the charge strong enough to prevent aggregation of pigment particles. They aggregate at a similar rate and their surface charge is very sensitive to impurities in water. In the presence of cationic polyelectrolytes their behavior depends on the type of adsorbed polymers. Highly charged polyethylenimine (PEI) stabilizes both PCC and GCC due to increased electrostatic repulsion. Polyacrylamide (cPAM), on the other hand, flocculates both by a bridging mechanism. Low dosages of cPAM cause flocculation of CaCO_3 even in the presence of large excess of dissolved anionics such as sulfonated kraft lignin.

2.2. Introduction

Calcium carbonate pigments, used as fillers in papermaking, come in two forms, either precipitated or ground. These two forms are referred to as PCC and GCC, respectively. Commercial GCC is usually treated with a dispersant (e.g. polyacrylate) which provides the particles with a negative charge. The electrostatic repulsion is strong enough to prevent aggregation of the particles, and thus commercial GCC suspensions are reasonably colloidally stable. Because of their negative charge, GCC particles do not deposit on negatively charged pulp fibers and, therefore, the use of retention aids is necessary to incorporate them into paper. On the other hand, PCC is usually not treated and, in pure form (in distilled water), could have a positive charge which promotes deposition of PCC particles on fibers. The charge, however, is not strong enough to provide sufficient repulsion between the

particles to stabilize the system and, consequently, when dispersed in water, PCC particles aggregate.

The fact that PCC and GCC have different surface characteristics results in different behavior of PCC and GCC in the presence of cationic polyethylenimine (PEI). It was found that PEI adsorption on stable GCC causes it to coagulate, because of the neutralization of the negative charges of GCC by PEI. PEI adsorption on PCC increases the positive charge of the particles and the aggregating PCC suspension becomes stable. The behavior of PEI-coated GCC and PCC particles can be explained satisfactorily on the basis of the classical DLVO-theory of colloid stability [1].

In this paper we describe experiments on GCC not treated with dispersants. As we will see, such untreated GCC behaves similarly to PCC and is very different from commercial GCC, showing that the difference between commercial GCC and PCC is mainly due to the different surface charge. It will also be shown that when untreated GCC and PCC are suspended in a solution containing anionic trash (anionic colloidal and dissolved substances), these can adsorb onto the GCC or PCC and make the pigments behave much like commercial GCC.

Here the main interest is in the behavior of CaCO_3 in the presence of cationic polyelectrolytes which are used as retention aids in order to incorporate pigments into paper. All the retention aids adsorb on pigments but, depending on the type of polymer, they affect the stability of colloidal particles in different ways. We used (i) a highly charged polyethylenimine, which is believed to modify the charge of pigment particles and acts via an electrostatic mechanism, and (ii) a low-charge density cationic polyacrylamide, which is presumed to act via a bridging mechanism.

2.3. Experimental

2.3.1. Materials

- PCC (Albacar HO) and a non-commercial untreated GCC were provided by Specialty Minerals. The mean particle size as determined by a disk centrifuge was 1.35 μm and 0.93 μm , respectively.
- Polyethylenimine (Polymin P), a branched polyelectrolyte with primary, secondary and tertiary amino groups in the ratio 1:2:1, was obtained from BASF. The mass average molecular weight $M_w \approx 6 \cdot 10^5$ [2] (PEI).
- Cationic polyacrylamide (Percol 292), obtained from Allied Colloids, $M_w \approx 3 \cdot 10^6$ (cPAM).
- Sulfonated kraft lignin (Reax 85A), obtained from Westvaco (SKL).

2.3.2. Experimental techniques

PCC and GCC suspensions were characterized by microelectrophoresis (Rank Brothers Mark II, Cambridge, England) for charge determination and by a photometric dispersion analyzer (PDA) (also Rank Brothers) for stability evaluation. With the PDA, fluctuations in turbidity of suspensions flowing through a tube are measured which, together with the average turbidity, provides information about particle size and number. Pigment flocculation leads to a change in the number and sizes of particles and causes changes in turbidity [3]. More details can be found in Ref. [1]. The resistance of flocs to shear was evaluated by changing the flow rate of the suspensions in the tube.

2.4. Results and discussion

2.4.1. Surface charge of CaCO_3

It has been reported that the surface charge of PCC depends on its concentration, varying from negative at low concentrations to positive at higher concentrations [4]. We have confirmed this observation for both PCC and untreated GCC dispersed in distilled water, as shown in Fig. 2.1. Several explanations of this observation, offered by number of authors, are covered in Ref. [4]. Although our work is not concerned with a better understanding of this phenomenon, the effect of water quality on electrophoretic mobility shown in Fig. 2.1 and Table 2.1 leads to the following speculation. The positive charge is believed to originate from the fact that CaCO_3 is partially soluble in water and the Ca^{2+} ions tend to readsorb preferentially on the crystal surface. The obvious question then is: why is the charge negative at low concentrations, even when the water is saturated with the dissolved Ca^{2+} ? (The conductivity of the water is the same at low and high CaCO_3 concentrations, as shown in Table 2.1.) Experiments performed with water of different degrees of purity (deionized, distilled, doubly distilled) have shown that the concentration where PCC has a zero charge is lower, the higher the purity of the water, implying that even distilled water contains some impurities affecting the charge. Assuming, since the surface charge of CaCO_3 is low, that at the point of zero charge about 10% of the surface is covered by an anionic impurity of molecular weight around 100, then the concentration of impurities is about 10^{-7} mol/L, which is below the detection limit of conductivity measurements. These impurities can adsorb on PCC, but when the PCC concentration is large, the total surface area of PCC is large as well and small amounts of impurities per particle affect the charge very little. When the concentration and the total surface area are low, the amount of impurities per particle is much larger and thus these impurities significantly affect the surface charge.

Table 2.1: Conductivity (C), electrophoretic mobility (EM) and pH of a CaCO₃ suspension.

Sample	Distilled Water			Tap Water		
	C ¹	EM ²	pH	C ¹	EM ²	pH
Water	0.8	-	6.6	263	-	7.7
PCC 30 ppm	45	-0.9	9.7	264	-2.0	7.1
PCC 1000 ppm	46	+1.0	9.7	265	-1.5	8.0
GCC 30 ppm	40	-0.8	9.3	272	-2.1	7.6
GCC 1000 ppm	43	+1.2	9.4	265	-2.0	7.6

1. $\mu\Omega \text{ cm}^{-1}$

2. $10^{-8} \text{ m}^2 \text{ s}^{-1} \text{ V}^{-1}$

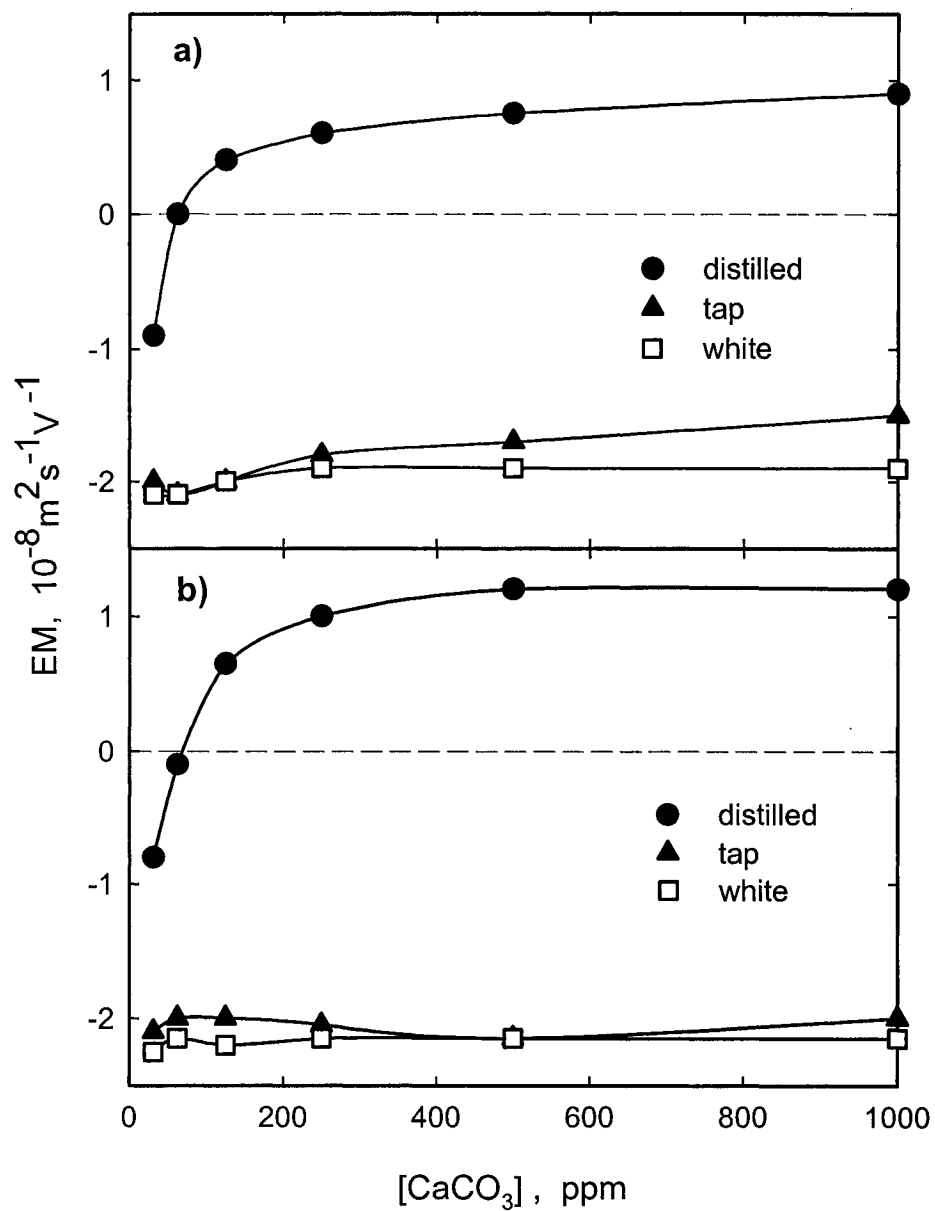


Fig. 2.1: Electrophoretic mobility as a function of CaCO_3 concentration measured in distilled water, tap water and white water from a fine paper mill. (a) PCC, (b) GCC.

As shown in Fig. 2.1, tap water contains sufficient impurities that can adsorb on CaCO_3 and reverse the charge to negative. The electrophoretic mobilities of CaCO_3 measured in white water from a fine paper mill are similar to those in tap water. Thus, when PCC is used in papermaking and added to process water which contains dissolved anionic substances, it will quickly change its charge from positive to negative. One can conclude that when positively charged PCC is required in papermaking in order to promote its deposition on negatively charged fibers, it must be dispersed in clean water and added as late as possible to the papermaking suspension to minimize the adsorption of anionic substances.

The untreated GCC behaves exactly the same as PCC and thus one can conclude that untreated GCC and PCC have almost identical surface characteristics. Data in Table 2.1, which show that PCC and GCC suspensions have nearly identical conductivities, pH's and electrophoretic mobilities, confirm this conclusion.

2.4.2. Colloidal stability of CaCO_3

When CaCO_3 pigments are dispersed in either distilled or tap water, both PCC and untreated GCC particles aggregate, i.e. the system is unstable. This implies that the surface charge is not sufficiently large to prevent the van der Waals attraction force from coagulating the particles. The aggregates are rather weak and can be broken up by shear. This is shown in Fig. 2.2, where the relative size of the aggregates is measured by the PDA as a function of shear rate. Both PCC and GCC aggregates are broken down in a similar fashion. Extrapolating to papermaking conditions, where the shear can be as high as 10^4 s^{-1} [5], one can conclude that untreated CaCO_3 pigments will be present in the form of single particles or small aggregates.

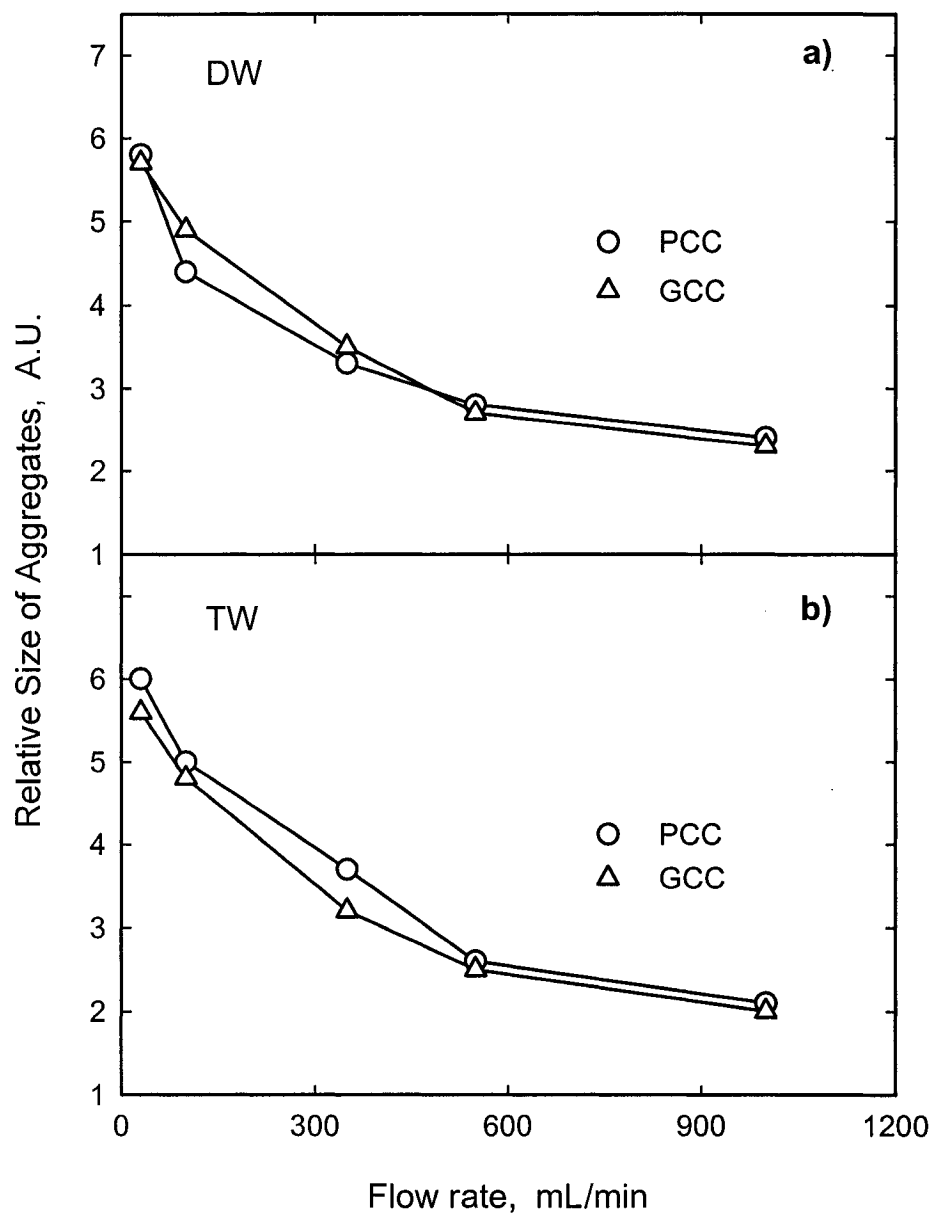


Fig. 2.2: Relative size of CaCO_3 aggregates in distilled (a) and tap (b) water as a function of shear realized by increasing the flow rate of the suspensions (1000 ppm) in a tube. At a flow rate of 300 mL/min, the shear rate is around 10^3 s^{-1} .

2.4.3. Effects of cationic polyelectrolytes

Common retention aids are water soluble polymers carrying a positive charge which is supplied by amino groups built into their chemical structure. They come in a variety of types, differing in molar mass, charge density and degree of branching. They all adsorb on CaCO_3 pigments but, depending on their type, they can affect the behavior of CaCO_3 differently. Most cationic polymers are expected to have a low affinity for positive PCC or untreated GCC because of electrostatic repulsion, which counteracts the thermodynamic driving force for adsorption. Polyethylenimine (PEI) has been shown to adsorb on PCC and the adsorption isotherm is of the low affinity type [1], implying a dynamic equilibrium between PEI adsorption and desorption. Cationic polyacrylamide (cPAM) has a low affinity even for some negatively charged fillers [6,7], and therefore is also expected to adsorb weakly on PCC.

Figure 2.3 shows how PEI affects the surface charge of PCC and GCC in both distilled and tap water. Positive PCC and GCC in distilled water become more positive on PEI addition, while with negative PCC and GCC in tap water (negative due to adsorbed impurities), the charge is reversed from negative to positive. Electrophoretic mobility experiments with cPAM addition are difficult, since cationic cPAM hydrolyzes at high pH and becomes negative [8,9]. Therefore, cPAM-coated CaCO_3 pigments are initially positively charged, but become negatively charged with time.

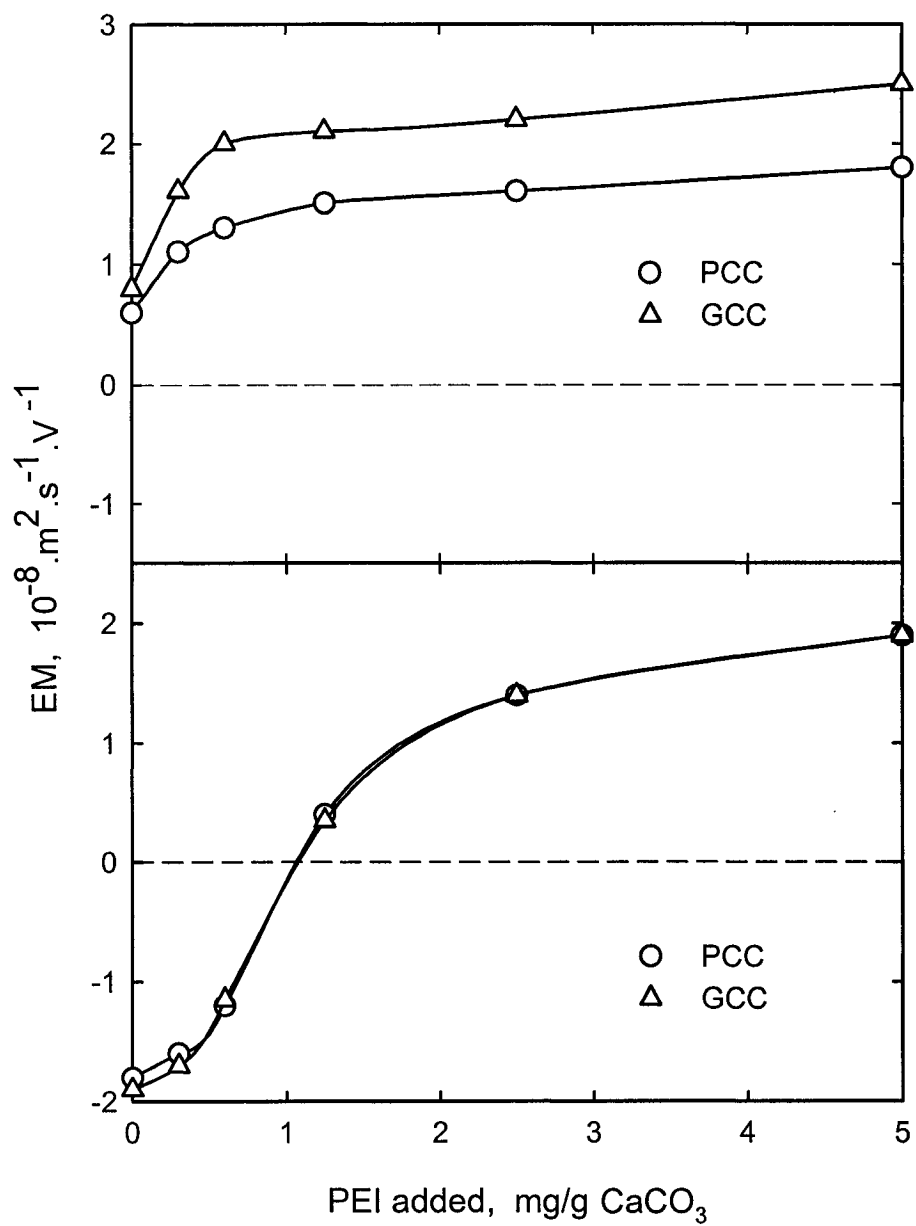


Fig. 2.3: Electrophoretic mobility of CaCO₃ dispersed in distilled (top) and tap (bottom) water (500 ppm) as a function of PEI addition.

The stability of CaCO_3 suspensions upon polyelectrolyte addition can be followed by turbidity measurements [1]. Results are usually expressed in terms of the stability ratio W , obtained by comparing the maximum destabilization rate to the rate of destabilization at given conditions. Thus the value $W = 1$ ($\log W = 0$) means that the system flocculates rapidly, while for $W = \infty$ the system is stable. In our experiments with PCC or GCC we have defined $W = 1$ for the flocculation rate in the absence of polymers. This rate was determined on samples subjected to sonication prior to measurement in order to disperse the aggregates. If destabilization with polymer is faster than without, then $W < 1$.

Results shown in Fig. 2.4 confirm the different action of the two polymers. The highly charged PEI adsorbs on CaCO_3 particles and, by enhancing their charge, the system becomes stable. PEI therefore acts like a dispersant. On the other hand, cPAM forms a bridge between the particles and causes flocculation, the rate of which is faster than that of the original sample. The existence of the bridge can be confirmed by observing the behavior of the system following a break-up of the flocs by, e.g. sonication. Results are shown in Fig. 2.5. At low polymer concentrations (up to 0.8 mg/g), the particles reflocculate after sonication to the same extent as before. At larger cPAM concentrations (over 1 mg/g), the non-sonicated system is flocculated, but after sonication the system does not reflocculate to the same extent. The reason that the non-sonicated system flocculates at high cPAM concentrations could be due to the competition between polymer adsorption and particle flocculation. If particles flocculate at a faster rate than polymer adsorption, aggregates form before cPAM has

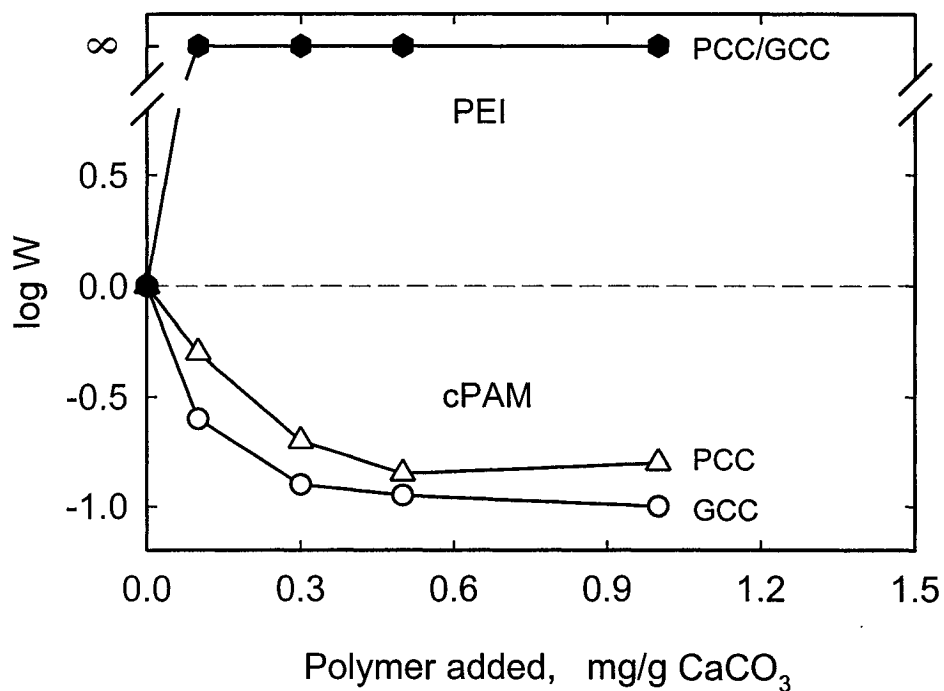


Fig. 2.4: Stability ratio W of CaCO_3 dispersion in distilled water (1000 ppm) as a function of cationic polyelectrolyte addition. In the presence of polyethylenimine, the originally aggregating PCC and GCC become stable ($W = \infty$). With polyacrylamide the rate of flocculation becomes faster ($W < 1$).

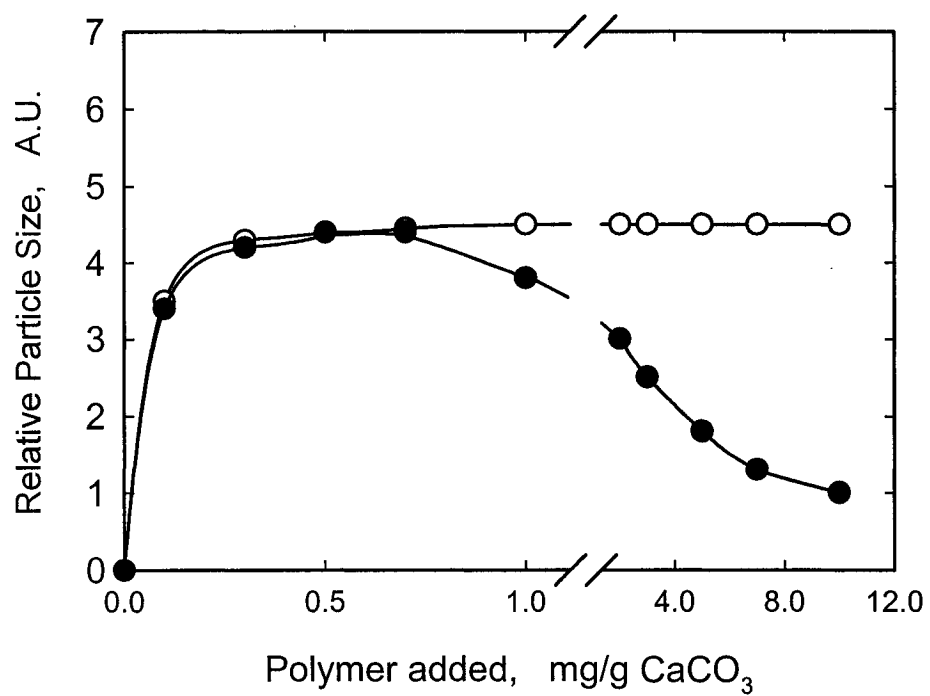


Fig. 2.5: Relative particle size of CaCO₃ (1000 ppm) upon addition of cationic polyacrylamide (○). Reformation of size after subjecting the original flocs to sonication (●).

a chance to stabilize the particles. On the basis of the classical Smoluchowski kinetics [10], one would expect polymer adsorption to be faster than particle flocculation, except when the adsorption efficiency is low. This suggests that cPAM adsorbs on CaCO_3 at a slow rate, implying a low affinity of cPAM for PCC or untreated GCC. After break-up of the flocs and stopping the sonication, the bridges can be reinstated provided that only a fraction of the particle surface is covered by polymers. If, on the other hand, the surface is fully covered by polymers, then after break-up the probability of reforming bridges is minimized. The cPAM dosage, where a transition occurs from complete reflocculation to a partial reflocculation, is about 0.8 mg/g CaCO_3 . This transition is expected to occur when about half the surface of the particles is coated by cPAM.

The interaction of PEI and cPAM with PCC or GCC is shown schematically in Fig. 2.6. Adsorbing PEI molecules increase the charge and stabilize the CaCO_3 pigments due to electrostatic repulsion (a), while cPAM can bridge and destabilize CaCO_3 particles (b). The particles do not experience an electrostatic repulsion when bridging occurs since the bridge is much longer than the distance over which electrostatic repulsion is acting. Upon breaking the bridges, they can be formed again depending on the extent of surface covered by polymer. Figure 2.6c shows that, when flocculated particles, fully coated with cPAM, are subjected to sonication, break-up of aggregates is not followed by bridge reinstatement.

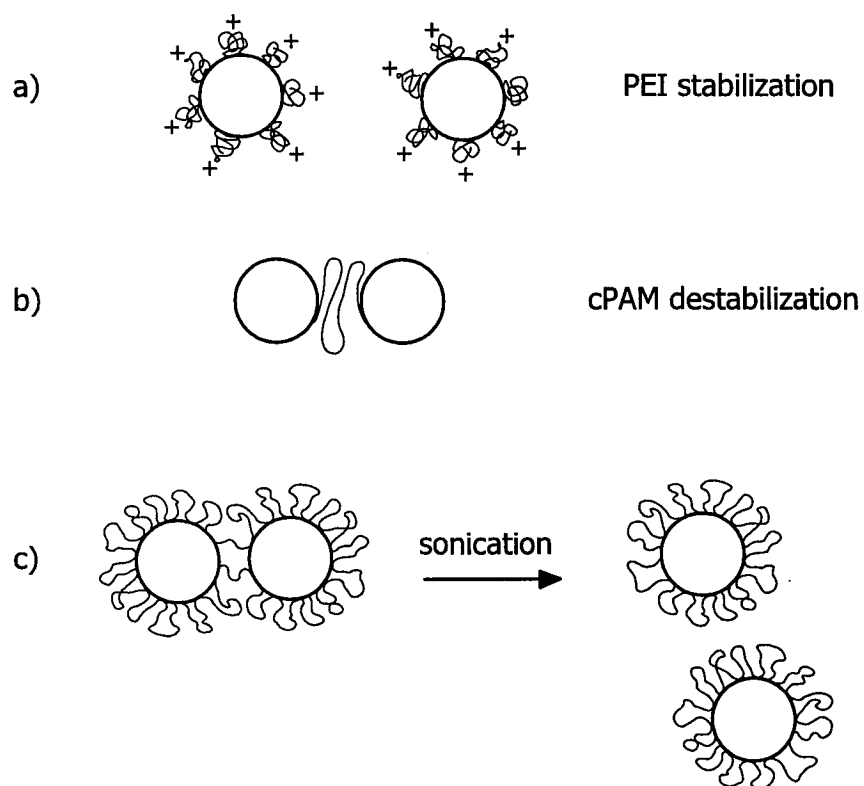


Fig. 2.6: Schematics of cationic polyelectrolyte action. (a) PEI adsorbs on pigment particles thus enhancing charge and repulsion. (b) cPAM adsorbs on pigment particles and forms a bridge, thus causing flocculation. (c) Flocs formed by cPAM after break-up do not reform if the surface coverage of the pigment particles by polymer is high.

In tap or white water, the CaCO_3 particles acquire a negative charge as seen in Fig. 2.1, which will affect the response of the particles to the presence of cationic polyelectrolyte. As shown in Fig. 2.7, the addition of PEI causes destabilization instead of stabilization, as was the case in distilled water (shown for comparison as a broken line). This is quite understandable because the polymer, by neutralizing the negative charge acquired by CaCO_3 in tap water as shown in Fig. 2.3, brings the system to an isoelectric point at which attractive van der Waals forces dominate. When more PEI is introduced and makes all the particles positively charged the system stabilizes. The action of cPAM, which is not governed by electrostatic interaction, is the same in both distilled and tap water.

2.4.4. Effect of anionic contaminants

The cationic retention aids are known to be less effective in systems contaminated by anionic substances present in the furnish. These are soluble and colloidal substances originating from fibers, additives, broke and other sources. Known as “anionic trash” or DCS (dissolved and colloidal substances) they are usually thought to form “inactive” complexes with the cationic polyelectrolytes [11] which then must be added in excess in order to perform their role. The effect of anionics, shown in Fig. 2.8, suggests that this explanation is incorrect. A sulfonated kraft lignin (SKL) was added in increasing amounts to the CaCO_3 suspension prior to the addition of cPAM. Even a small addition of 5 mg SKL per gram CaCO_3 is sufficient to stabilize the system by adsorbing on the pigment particles. As a result,

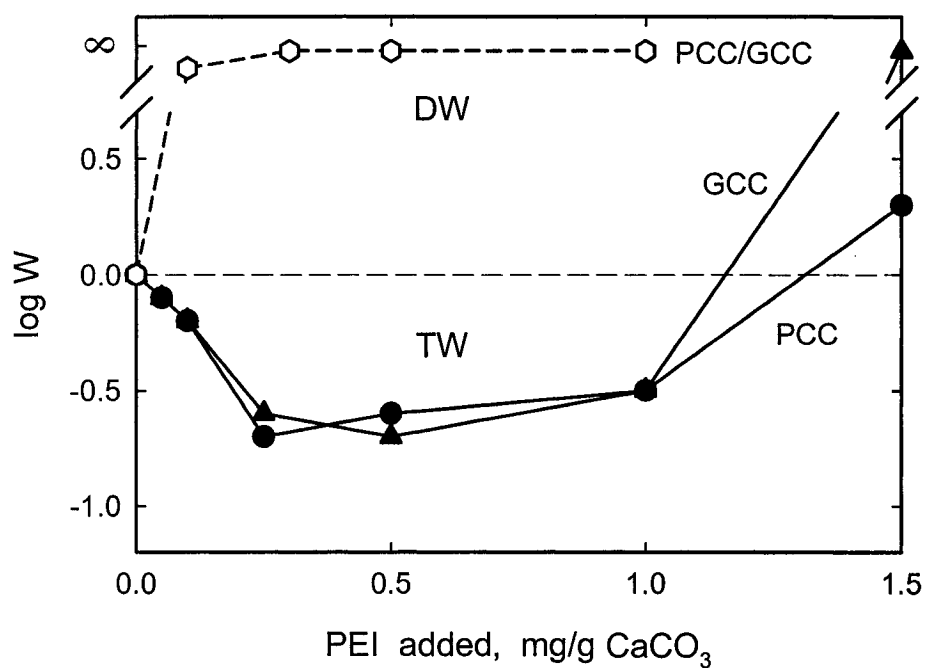


Fig. 2.7: Stability ratio W of CaCO_3 dispersed in tap water (1000 ppm) as a function of polyethylenimine addition. Due to its negative charge in tap water (Fig. 2.1), CaCO_3 aggregates instead of becoming stable, as in distilled water, shown by the broken line.

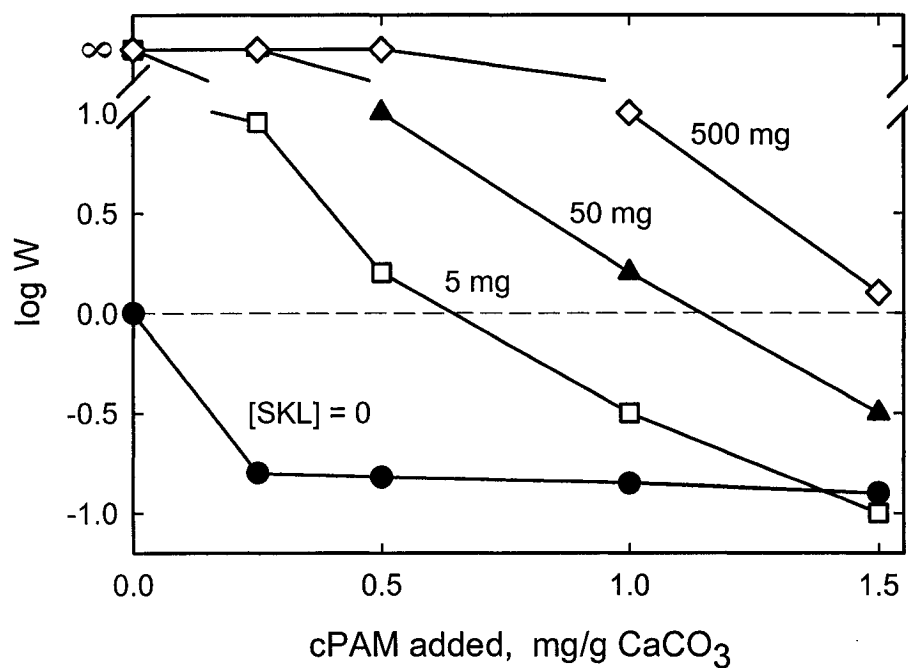


Fig. 2.8: Effect of anionic contaminant SKL (sulfonated kraft lignin) on the flocculating ability of cationic polyacrylamide. The originally aggregating CaCO_3 becomes stable in the presence of 5 mg SKL per gram CaCO_3 . With increasing content of SKL more cationic polymer is needed to cause flocculation. CaCO_3 conc. 400 ppm.

the SKL coated CaCO_3 particles behave similarly to commercial GCC treated with a dispersant [1]. In order to flocculate such stabilized particles more cPAM is required. However, it can be seen that even at very high SKL concentrations, cPAM can still flocculate CaCO_3 . It is unlikely that 1-2 mg cPAM can neutralize 500 mg SKL and that excess cPAM flocculates CaCO_3 . It is more likely that cPAM forms a complex with SKL which adsorbs and thus forms a bridge between CaCO_3 particles. The bridging takes place even in the presence of an excess of SKL which, by itself, adsorbs on the particles and stabilizes them. The affinity of the cPAM/SKL complex for CaCO_3 is expected to decrease with increasing SKL, resulting in a reduced flocculation efficiency. Therefore, more cPAM has to be introduced in order to cause efficient flocculation, but there is no need to completely eliminate the SKL. In practice, the detrimental effect of anionics on the performance of retention aids is dealt with by first adding a strongly charged cationic polyelectrolyte as a scavenger, the role of which is to interact with the anionics prior to the introduction of the retention aid.

2.5. Concluding remarks

We have shown that PCC and untreated GCC particles behave nearly identically. Their charge is affected by distilled, tap or white water in a similar way, as is their flocculation behavior in the presence of cationic polyelectrolytes. SKL-coated GCC or PCC, or pigments with adsorbed impurities behave similarly to GCC treated with an anionic dispersant. PEI and cPAM affect the behavior of CaCO_3 in different ways. PEI stabilizes PCC and GCC in distilled water, but flocculates both in

contaminated water. Cationic polyacrylamide flocculates the pigments independent of the quality of the water. An excess of anionic substances in solution decreases the flocculating ability of cPAM, most likely because of a complex formation between cPAM and the anionics.

2.6. Acknowledgement

The work was financially supported by a Domtar-NSERC IOR grant.

2.7. References

1. Suty, S., Alince, B., and van de Ven, T.G.M., "Stability of Ground and Precipitated CaCO_3 Suspensions in the Presence of Polyethylenimine and Salt". *J. Pulp Pap. Sci.* **22**(9), J321-J326 (1996).
2. Horn, D., in "Polymeric Amines and Ammonium Salts," (E.J. Goethals, Ed.), p.333, Pergamon, New York 1980.
3. Gregory, J., "Turbidity Fluctuation in Flowing Suspensions". *J. Colloid Interface Sci.* **105**, 357 -371 (1985).
4. Siffert, B., and Fimbel, P., "Parameters Affecting the Sign and Magnitude of the Electrokinetic Potential of Calcite". *Colloids Surf. A* **11**(3/4), 377-389 (1984).
5. Tam Doo, P.A., Kerekes, R.J., and Pelton, R.H., "Estimates of Maximum Hydrodynamic Shear Stresses on Fiber Surfaces in Paper Machine Wet End Flows and in Laboratory Drainage Testers". *J. Pulp Pap. Sci.* **10**(4), J80-J88 (1984).

6. Alince, B., "Mechanism of TiO₂ Pigment Retention on Pulp Fibers with Polyelectrolytes". *J. Colloid Interface Sci.* **105**, 357-371 (1985).
7. Boluk, M.Y., and van de Ven, T.G.M., "Effects of Polyelectrolytes on Flow-Induced Deposition of Titanium Dioxide Particles onto a Cellophane Surface". *Colloids Surf. A* **46**, 157-176 (1990).
8. Aksberg, R., and Wågberg, L., "Hydrolysis of Cationic Polyacrylamide". *J. Appl. Polymer Sci.* **38**, 297-304 (1989).
9. Kamiti, M., and van de Ven, T.G.M., "Impinging Jet Studies of the Kinetics of Deposition and Dissolution of Calcium Carbonate Particles". *Colloids Surf. A* **100**, 117-129 (1995).
10. van de Ven, T.G.M., "Particle Deposition on Pulp Fibers. The Influence of Added Chemicals". *Nord. Pulp Pap. Res. J.* **8**(1), 130-134 (1993).
11. Pelton, R.H., Allen, L.H., and Nugent, H.M. "Factors Affecting the Effectiveness of Some Retention Aids in Newsprint Pulp". *Svensk Papperstidning* **83**(9), 251-258 (1980).

Chapter 3

In Chapter 2, it was shown that mineral pigments dispersed in water become charged due to adsorption of potential determining ions or due to isomorphous substitution. The surface charge of mineral pigments was found to be either positive or negative depending on many factors such as type of a mineral structure, pH, and presence of impurities in water. In Chapter 3, the interaction of mineral pigments and cationic polyelectrolytes was extended to more complicated systems, which also contained pulp fibers. In the absence of cationic polyelectrolytes, the interaction of mineral pigments with pulp fibers is driven by electrostatic forces. Positively charged pigments deposit on negatively charged fibers following Langmuir-Smucowski kinetics, while negatively charged pigments and pulp fibers repel each other. In the presence of cationic polyelectrolytes, pigment deposition depends on the type of the cationic polyelectrolyte.

3.1. Abstract

In an aqueous suspension of negatively charged pulp fibers, dispersant-free CaCO_3 pigments deposit on the fibers provided that they are positively charged. This happens in distilled water. In water contaminated with anionic substances, the CaCO_3 acquires a negative charge and does not deposit without a retention aid. Introduction of cationic polyethylenimine (PEI) into the suspension promotes deposition driven by electrostatic interaction, provided the PEI concentration is not too large. With an excess of PEI, both the fiber and the pigment become positive and repel each other. Introduction of cationic polyacrylamide (cPAM) causes flocculation of the pigment and its deposition on fibers, regardless of the cPAM dosage, indicating that electrostatic interaction is not a dominant effect. However, the bridging mechanism alone is not satisfactory to explain the overall behavior.

3.2. Introduction

In a previous paper [1] we showed that aqueous suspensions of dispersant-free ground calcium carbonate (GCC), and precipitated calcium carbonate (PCC) behave nearly identically. Both are positively charged in distilled water and negatively charged in tap and white water. But in either case the charge is not strong enough to prevent aggregation of dispersed particles. Their response to the presence of cationic polyelectrolytes depends on the type of polymer. Strongly charged cationic polyethylenimine (PEI), by adsorbing on the pigment aggregates in pure water, enhances their positive charge and the system becomes colloidal stable because of increased electrostatic repulsion. In tap water, the PEI adsorbs on negatively charged

particles and promotes further aggregation due to elimination of electrostatic repulsion.

The cationic polyacrylamide (cPAM), representing the typical retention aid, acts by bridging mechanism. Its adsorption causes further flocculation of the pigment aggregates independent of the quality of water and at all dosages that were used.

Both PEI and cPAM are used to promote retention of fine particles in papermaking. Since they affect the colloidal behavior of CaCO_3 pigments differently, it is natural to ask whether or not they also affect the interaction of CaCO_3 fillers with pulp fibers in different ways.

Several studies have been reported on the interaction of CaCO_3 pigments with pulp fibers [2-6]. Regarding the action of retention aids, the general consensus is that highly charged cationic polyelectrolytes promote deposition of fillers on fibers via charge modification, while high molecular weight cationic polymers with a low charge density act by bridging the fillers to the pulp fibers. In this paper we will look in more detail at how polymer dosages and the state of pigment dispersion affect the deposition of CaCO_3 fillers on fibers and their retention in handsheets.

Of a particular interest is the different mechanism by which cationic polyelectrolytes promote retention of fine particles in the process of filling paper. A better understanding of the mechanism involved is a prerequisite for optimizing the performance of a given retention aid and for providing an explanation of its potential failure.

3.3. Experimental

3.3.1. Materials

Two types of calcium carbonate pigments were used: (1) Precipitated Albacar HO (Specialty Minerals) with an average particle size of 1.3 μm ; (2) Ground calcium carbonate not treated with dispersant (Specialty Minerals) with an average particle size of 0.9 μm . Fibers used were unbeaten, softwood, bleached kraft washed on an 80-mesh screen in order to remove the fines.

Two cationic polyelectrolytes were used: (1) polyethylenimine (PEI) POLYMIN P (BASF) of high charge density and molar mass $M_w \approx 6 \times 10^5$; (2) Polyacrylamide (cPAM) PERCOL 292 (Allied Colloids) of molar mass $M_w \approx 3 \times 10^6$.

3.3.2. Methods

One gram of fibers dispersed in 500 cm^3 water was kept suspended by slow paddle stirring (80 rpm). The appropriate amount of CaCO_3 dispersion was added, followed by the addition of a polymer solution if required. The deposition of CaCO_3 was determined by transmittance measurements of the supernatant at timed intervals starting at 15 sec. For this, a portion of the supernatant was withdrawn using a syringe equipped with a tip containing a screen to exclude the fibers. From the established calibration curve of light transmittance versus concentration, the amount of CaCO_3 in the supernatant was determined. The difference between what was added and what was left in the supernatant was considered as the amount of CaCO_3 deposited on the fibers.

The results will be unreliable if the state of the CaCO_3 dispersion changes, e.g. due to flocculation caused by polyelectrolyte addition. In such a case, the calibration curve established for a dispersed pigment is not valid. Therefore, the light transmittance of a CaCO_3 suspension was measured at varying additions of the polyelectrolytes. Prior to being measured, the samples were subjected to ultrasonic treatment. The resulting calibration curves, in both the absence and presence of polymer, were almost identical and, consequently, the results can be considered reliable.

3.4. Results and Discussion

3.4.1. Rate of deposition in the absence of polyelectrolytes

In distilled water, both PCC and untreated GCC are positively charged and deposit onto negatively charged pulp fibers. The deposition kinetics is shown in Fig. 3.1. Three levels of CaCO_3 addition were used (125, 500 and 1000 mg/g fiber). The pH in the systems was around 9.5 for all the cases investigated. It can be seen that the initial kinetics are linear (i.e. at short times the deposition increases linearly with time) and that a plateau is reached at long times. The deposition at the plateau is less than the amount added, implying that not all the added CaCO_3 ends up on the fibers. It follows from these results that the deposition process is a dynamic equilibrium between particle deposition and detachment, since the plateau values are increasing with increasing filler concentration.

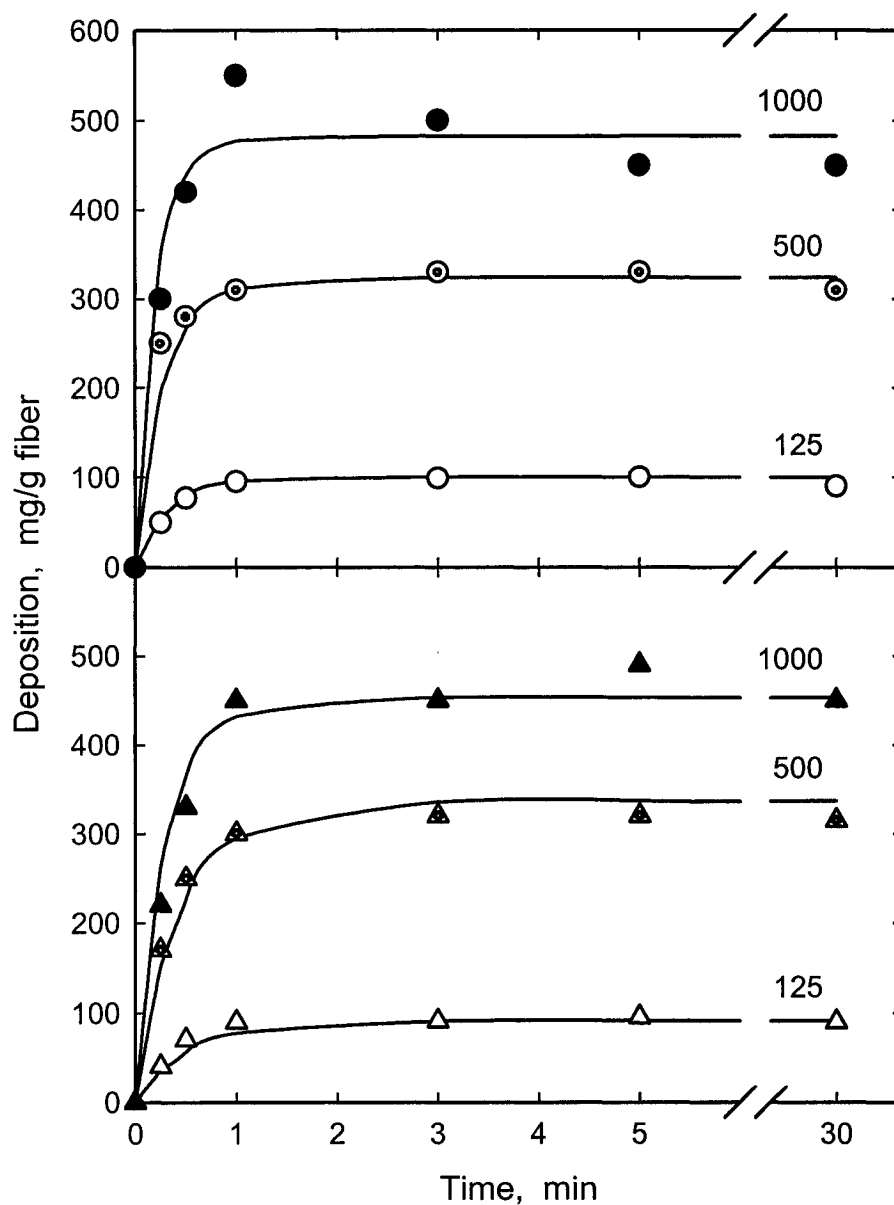


Fig. 3.1: Deposition of CaCO_3 on fibers suspended in distilled water as a function of time. CaCO_3 dispersed in distilled water and added in the amount of 125, 500 and 1000 mg/g fibers in 500 cm^3 water. The curves are the calculated best fit through the experimental points. PCC (top), GCC (bottom).

It has been shown that the deposition of fillers on fibers suspended in water closely follows Langmuir-Smoluchowski kinetics [7]:

$$\frac{d\theta}{dt} = k_1(n_o - \theta)(1 - \theta) - k_2\theta \quad (1)$$

where θ is the fractional coverage of the fibers by filler, i.e. $\theta = \Gamma/\Gamma_{max}$, Γ being the amount of filler deposited on the fibers and Γ_{max} the maximum amount that can deposit, t is the time, k_1 and k_2 are the deposition and detachment rate constants, respectively, and n_o is the initial concentration of filler normalized by the amount required for monolayer coverage. The rate constant k_1 can be expressed as [8]

$$k_1 = \alpha k_{sm} N_F \cong \frac{a}{\pi} G \phi_F \quad (2)$$

where k_{sm} is the Smoluchowski rate constant for collisions between fibers and small particles subjected to shear, given by $k_{sm} = GV_F/\pi$, G being the rate of shear and V_F the volume of a single fiber, N_F is the number of fibers per unit volume and ϕ_F the volume fraction of the fibers. The collision efficiency α is a strong function of the ratio a/R , a being the radius of the filler and R that of the fibers. When $a/R \ll 1$, $\alpha \ll 1$, but α increases steeply with increasing a/R ; α is also a function of shear and the colloidal forces operating between the fiber and the filler.

For calculating k_1 in our system composed of 1 g fiber in 500 cm³ water the volume fraction of unbeaten fibers, ϕ_F , can be obtained from the specific volume of swollen fibers. Depending on the type of fiber and the technique used the value is 2-3 cm³/g. Thus $\phi_F \approx 0.005$ and $k_1 \approx 1.6 \times 10^{-3} \alpha G$.

At steady state ($t = \infty$), Eq. (1) reduces to

$$\frac{I}{\Gamma_{\infty}} = \frac{K}{c_{\infty}} + \frac{I}{\Gamma_{max}} \quad (3)$$

K being the equilibrium (or steady-state) constant ($K = k_2/k_1$), and c_{∞} the concentration of filler in solution. In this notation, K is dimensionless and Γ and c_{∞} are expressed in units of g/g. Γ_{∞} is the amount of filler deposited on the fibers as $t \rightarrow \infty$.

The plateau values, Γ_{∞} , are plotted in a Langmuir plot (Eq. 3) in Fig. 3.2. From the intercept one obtains $\Gamma_{max} = 620$ mg/g and from the slope one finds that K 0.3 for both PCC and GCC. Although the sizes of PCC and GCC are slightly different (PCC = 1.3 μm , GCC = 0.9 μm), they deposit as small aggregates (see below), which apparently have a similar average size. From the value of Γ_{max} it follows that θ_{∞} ($\Gamma_{\infty}/\Gamma_{max}$) varies from about 0.15 for an addition of 125 mg CaCO_3 to about 0.7 for an addition of 1000 mg, while values of n_o (initial concentration/ Γ_{max}) range from 0.2 to 1.6. The initial deposition rate equals $k_1 n_o$ (cf. Eq. 1) and, from the initial rates shown in Fig. 3.1, one finds that $k_1 = 1 \text{ min}^{-1}$ and thus $k_2 = Kk_1 = 0.3 \text{ min}^{-1}$, implying that a CaCO_3 filler particle resides on average 3 minutes on the fiber before detachment. These results are consistent with previous findings [3] and confirm the reversible deposition of CaCO_3 on fibers. Since in the absence of stabilizers CaCO_3 particles are unstable, filler deposition and filler coagulation proceed simultaneously. Thus it is expected that, under conditions prevailing in Fig. 3.1, deposition of small aggregates occurs on the fibers. The calculated value of $k_1 = 1.6 \times 10^{-3} \alpha G$ at estimated shear rate at slow stirring $G \approx 1 \text{ s}^{-1}$ (60 min^{-1}) is $k_1 = 0.1 \text{ min}^{-1}$. From comparison with the

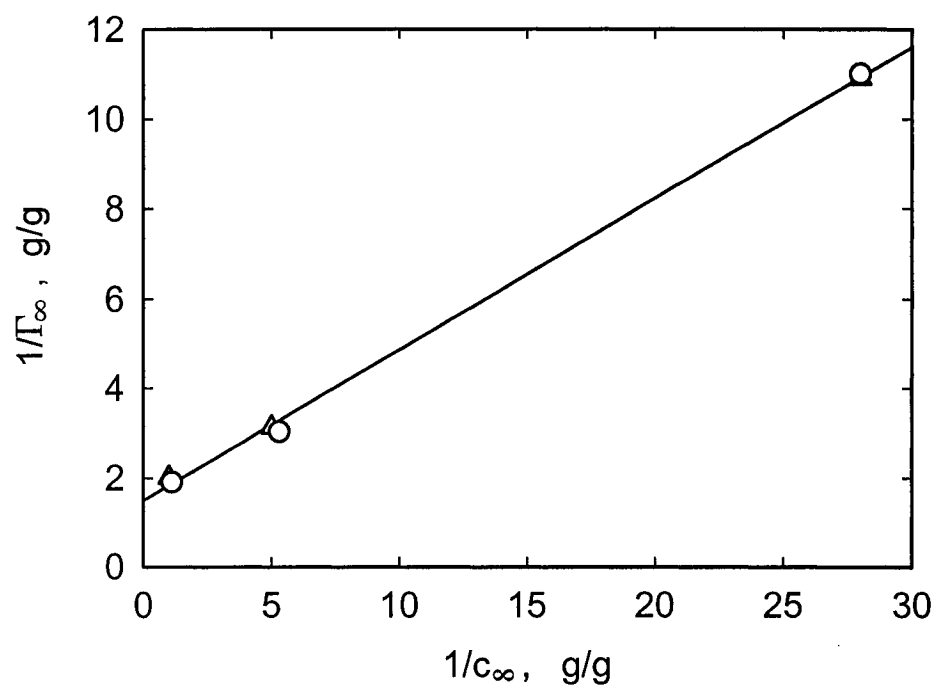


Fig. 3.2: Reciprocal amount of CaCO_3 deposited onto fibers versus reciprocal amount remaining in suspension at steady state.

observed rate $k_I \approx 1\text{min}^{-1}$ the efficiency factor $\alpha \approx 0.1$, a value typical of fast deposition in the absence of an energy barrier [8].

3.4.2. Effect of surface charge

The driving force for deposition is apparently the electrostatic interaction between positively charged CaCO_3 particles [1] and negatively charged fibers, which is expected to occur only when distilled water is used. With tap water the situation is different because the CaCO_3 acquires a negative charge [1]. In Table 3.1 are electrophoretic mobilities of PCC and GCC dispersed in distilled water, tap water and white water measured at concentration 200 mg CaCO_3/L .

As shown in Fig. 3.3, when the filler is dispersed in distilled water and added to fibers suspended in tap water, the deposition is lower and, with time, practically all the particles leave the fibers. This means that the initially positive particles deposit on fibers but with time acquire a negative charge and electrostatic repulsion causes their departure. Since the time scale of particle detachment is on the order of minutes, the adsorption of impurities on CaCO_3 must occur on a similar time scale. In papermaking, however, the shear can be 10^3 or 10^4 times as high and therefore the adsorption and the effect of impurities are expected to occur within a fraction of a second. To verify the argument that charge reversal is responsible for detachment, CaCO_3 was dispersed in tap water to reverse the charge before being added to the fibers. In such a case, (almost) no deposition takes place, as shown in Fig. 3.4. Therefore, it is not realistic to expect any deposition in process waters which contain enough anionic material to make CaCO_3 negative [1]. Consequently, in practice,

Table 3.1: Electrophoretic mobility of CaCO_3 *.

Water	PCC	GCC
Distilled	+0.7	+0.8
Tap	-1.7	-2.1
White	-1.9	-2.1

* $[\text{CaCO}_3]$ 200 mg/L, units in $10^{-8} \text{m}^2 \text{s}^{-1} \text{V}^{-1}$

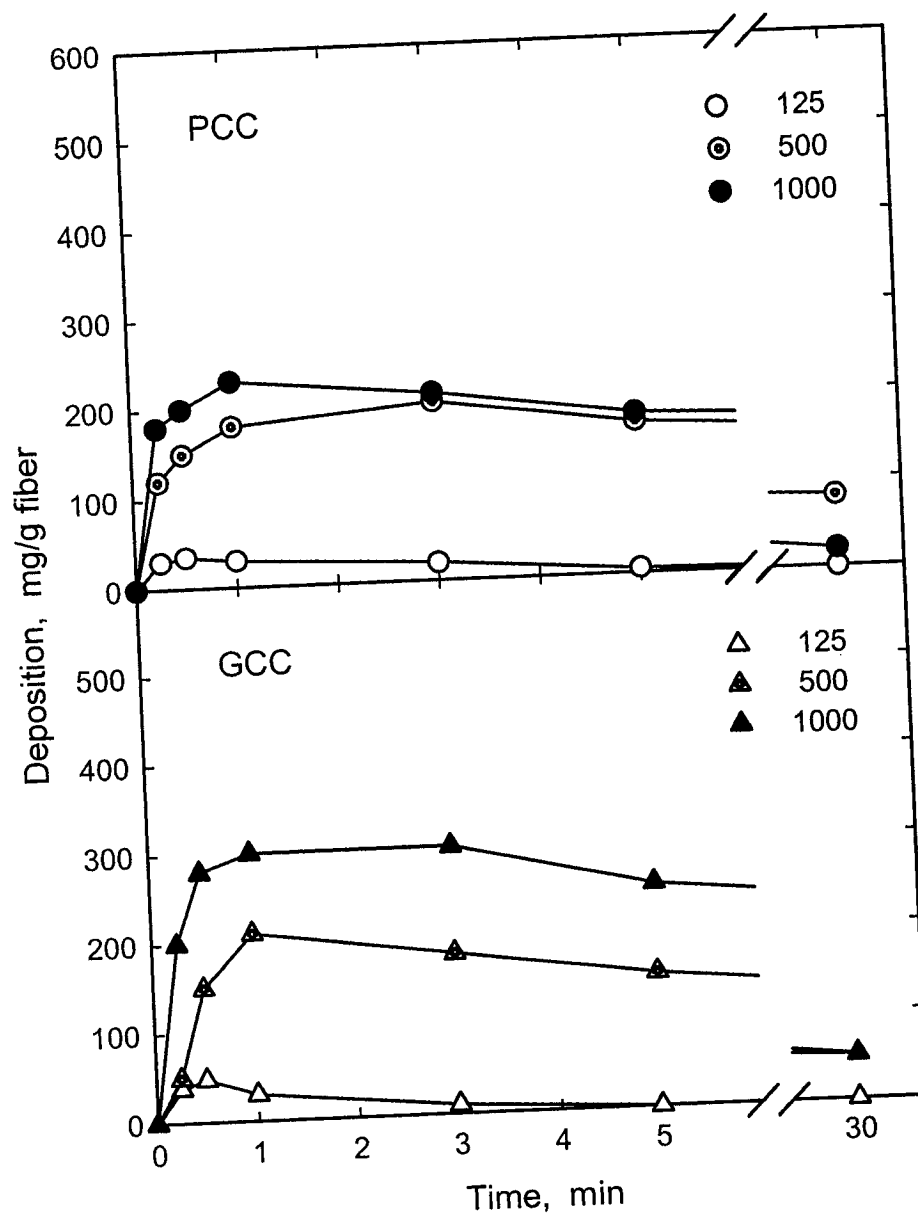


Fig. 3.3: Deposition of CaCO_3 on fibers suspended in tap water as a function of time. CaCO_3 dispersed in distilled water and added in the amount of 125, 500 and 1000 mg/g fibers in 500 cm^3 water.

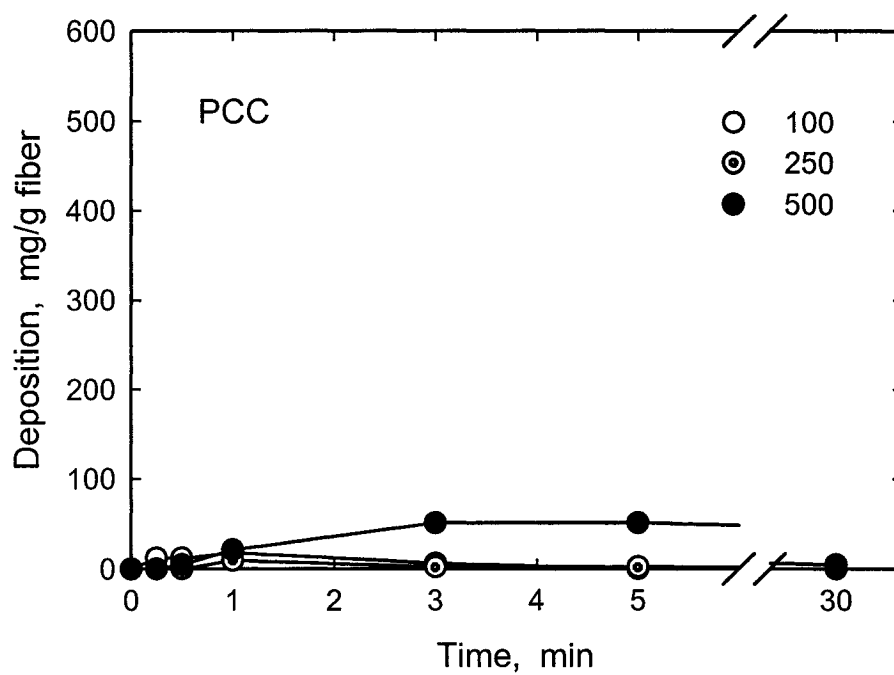


Fig. 3.4: Deposition of CaCO_3 on fibers suspended in tap water as a function of time. CaCO_3 dispersed in tap water and added in the amount of 100, 250 and 500 mg/g fibers in 500 cm^3 water.

retention aids are necessary to introduce CaCO_3 fillers into paper. The effects of two types of cationic polyelectrolytes are examined.

3.4.3. Effect of polyethylenimine

Before discussing these results, it is worthwhile to recall some facts about PEI adsorption on pulp fibers and CaCO_3 : (i) PEI adsorbs irreversibly on pulp fibers [9]; (ii) PEI adsorbs with a low affinity (reversibly) on CaCO_3 filler [10]; (iii) under low shear conditions (which apply to the present experiments) PEI, when added to a mixture of fibers and filler, adsorbs faster onto the filler than onto the fibers [11]; (iv) PEI stabilizes CaCO_3 ; and (v) non-coated CaCO_3 particles deposit on PEI-coated fibers with a low efficiency [3].

The data concerning PEI absorption and its effect on CaCO_3 charge and state of dispersion are shown in Table 3.2 [10], whereas data for fibers are presented in Table 3.3 [11]. The increase in relative size in Table 3.2 indicates aggregation of pigment particles.

When PEI is added to a mixture of fibers and CaCO_3 filler, one expects that PEI adsorbs (at low shear) on the filler preferentially. Therefore, if PEI is added in a sufficient amount, the CaCO_3 becomes stable and the positively charged single CaCO_3 particles deposit on still negatively charged fibers. The charge of fibers may reverse after enough PEI becomes adsorbed on them, due to adsorption of excess PEI or due to PEI transfer from CaCO_3 to fibers.

Table 3.2: PEI adsorption, charge and relative size of PCC as a function of PEI addition at pH 9.5.

PEI addition, mg/g	0	0.1	1	10
PEI adsorption, mg/g	0	—	0.2	3
E. mobility, $10^{-8}\text{m}^2\text{s}^{-1}\text{V}^{-1}$	+0.7	+0.8	+1.5	+2.0
Relative size, A.U.	5	5	1	1

Table 3.3: PEI adsorption and charge of fibers as a function of PEI addition at pH 9.5.

PEI addition, mg/g	0	0.1	1	10
PEI adsorption, mg/g	0	0.1	1	6
E. mobility, $10^{-8}\text{m}^2\text{s}^{-1}\text{V}^{-1}$	-1.3	-1.1	+1.0	+2.0

Figure 3.5 shows the deposition of CaCO_3 in the presence of various PEI additions. Since the data are similar for both the GCC and PCC, only one curve is presented. At the low PEI addition (0.1 mg) the deposition of CaCO_3 , added in the amount of 1000 mg, is similar to that in the absence of PEI (cf. Fig. 3.1). When 500 mg is added the deposition is lower than that without PEI, and when 125 mg is added the deposited CaCO_3 starts to leave the fiber at longer times. For the interpretation of this behavior it is important to realize that, with increasing level of CaCO_3 addition, the proportion of PEI per CaCO_3 decreases. Thus, when 0.1 mg PEI is introduced into the mixture of 1 g fibers and 1 g CaCO_3 , there is not enough PEI to reverse the charge of fiber or to stabilize the CaCO_3 (cf. Tables 3.2 and 3.3). Therefore, the deposition of small positively charged CaCO_3 aggregates on negatively charged fiber is driven by electrostatic attraction and the situation is similar to that in the absence of PEI (cf. Fig. 3.1). When the same amount of PEI (0.1 mg) is introduced into the mixture of 1 g fibers and 500 mg CaCO_3 (i.e. 0.2 mg PEI/g CaCO_3), there is apparently enough PEI to stabilize the CaCO_3 [1], which then deposits as positively charged individual particles instead of aggregates. Therefore, the rate as well as the extent of deposition decreases (cf. Fig. 3.1). In the case of 125 mg CaCO_3 addition (i.e. 0.8 mg PEI/g CaCO_3), the positively charged CaCO_3 initially deposits on the still negative fibers. However, with prolonged mixing the deposition decreases. A possible explanation is that polymer adsorption on fiber is slower than on CaCO_3 and also slower than CaCO_3 deposition [1]. Therefore the PEI, which has not been consumed by CaCO_3 , adsorbs on fiber causing electrostatic repulsion between the deposited CaCO_3 and fiber.

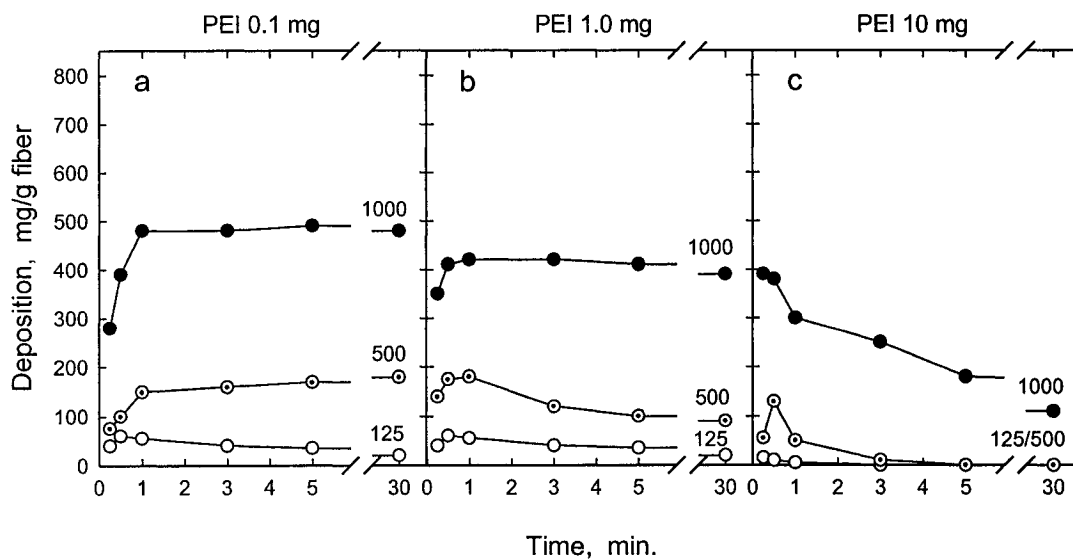


Fig. 3.5: Deposition of CaCO_3 on fibers suspended in distilled water as a function of time in the presence of PEI. 125, 500 and 1000 mg CaCO_3 dispersed in distilled water added to 1 g fibers in 500 cm³ followed by PEI addition: (a) 0.1 mg; (b) 1.0 mg; and (c) 10 mg.

This scenario is supported by the behavior at higher PEI additions as shown in Fig. 3.5b,c. The addition of 1mg/g fiber (i.e. 1, 2 and 8 mg/g CaCO_3) is sufficient to reverse the charge of fiber (cf. Table 3.3) but, before this happens, the CaCO_3 has already deposited. Therefore, after reaching a maximum, the particles start to leave the fiber because of electrostatic repulsion caused by charge reversal of fibers due to PEI adsorption. The process is quite pronounced at the highest level of PEI addition 10 mg/g fiber shown in Fig. 3.5c. With an increased number of PEI molecules, their rate of adsorption on fiber increases, and therefore the rate of CaCO_3 departure also increases. These results show that no deposition occurs when fibers and CaCO_3 fillers become fully coated by PEI. Although the presented data were obtained in distilled water, a similar trend was observed in tap water. The interpretation is inevitably simplified but it appears adequate to describe the process and the mechanisms involved.

Also it has to be realized that the process of particle deposition and polymer adsorption in a real system will be much faster than under the experimental conditions presented here. Because of much higher hydrodynamic shear in papermaking, what happens in the scale of minutes here will take place within a fraction of second.

3.4.4. Effect of polyacrylamide

When cPAM is used as a retention aid, the deposition behavior of CaCO_3 filler is very different than with PEI. This is shown in Fig. 3.6. The kinetics, as well

as the extent of deposition, are similar for all cPAM dosages. In comparison with PEI, the initial rate of deposition is faster and the extent of deposition is also higher (cf. Fig. 3.5). That the deposition is little affected by the amount of cPAM introduced is similar to the flocculation behavior of CaCO_3 by cationic cPAM [1], which is also insensitive to the dosage of cPAM. And, because the cPAM flocculates CaCO_3 , the deposition rate is faster than that of CaCO_3 stabilized with PEI. By analogy with the cPAM flocculation mechanism of CaCO_3 , which is believed to be due to polymer bridge formation between CaCO_3 particles [1], CaCO_3 attachment to the fiber appears to be mediated also by a polymeric bridge. This means that the electrostatic attraction, which is the driving force in promoting interaction between CaCO_3 particles and fibers in the case of PEI, is not dominant in the case of cPAM.

There is, however, a problem with the idea that the aggregates of CaCO_3 are attached to the fibers by a polymeric bridge. According to classical theory, for colloids flocculated by bridging there is an optimum surface coverage by polymer for maximum efficiency. Beyond this optimum coverage, the probability of bridge formation decreases with increasing surface coverage by the polymer and, at full coverage, the particles become dispersed because of steric repulsion. Therefore one would expect that at high dosage of cPAM, both the fibers and the fillers, become coated with cPAM and consequently no deposition would take place. But, as seen in Fig. 3.6c, this is not the case even at 10 mg cPAM addition. Similarly the behavior of CaCO_3 alone also shows that, contrary to expectation, the CaCO_3 flocculates at cPAM addition of 10 mg/g CaCO_3 [1]. In order to explain this behavior several possibilities can be considered.

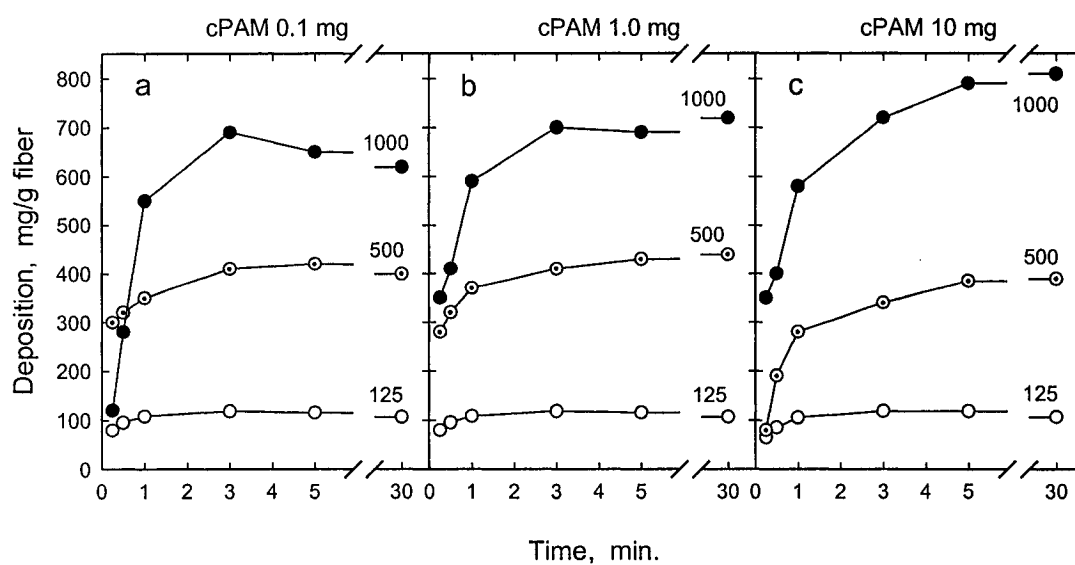


Fig. 3.6: Deposition of CaCO_3 on fibers suspended in distilled water as a function of time in the presence of cPAM. 125, 500 and 1000 mg CaCO_3 dispersed in distilled water added to one gram fibers in 500 cm^3 followed by cPAM addition: (a) 0.1 mg; (b) 1.0 mg; and (c) 10 mg.

One explanation is that the cPAM-coated pigments deposit before the excess of cPAM has time to coat the fibers, thus a bridge is formed and particles do not detach. However, one would expect that, with higher cPAM dosages, cPAM adsorption on fibers is faster and thus steric stability occurs earlier, resulting in less transient CaCO_3 deposition. This is not observed. A simple experiment also indicates that this mechanism is unlikely. When cPAM is added to fibers and allowed to adsorb before CaCO_3 is added, the deposition proceeds in a manner similar to that shown in Fig. 3.6.

The second possibility is that 10 mg cPAM is not sufficient to cover fully both the fibers and the CaCO_3 . It was reported that, at an addition of 10 mg cPAM to either 1 g fibers or CaCO_3 , the adsorption at pH 9 was 8 mg/g [12] and 5 mg/g, respectively. Since the adsorbed amounts will increase on both the fibers and the CaCO_3 with increased cPAM additions, this indicates only partial coverage. However, even at 50 mg cPAM addition (not shown) leads to similar deposition kinetics, making this possibility unlikely.

A third explanation is that the adsorbed polymer layer is not sufficiently thick to prevent deposition due to van der Waals attraction. The interaction energy between a fiber and a pigment, both fully coated with polymer, is shown schematically in Fig. 3.7. It consists of an attractive van der Waals energy and a repulsive energy due to overlapping polymer layers (steric repulsion). If the adsorbed cPAM layer is not thick enough to prevent flocculation into the energy minimum, as shown in Fig. 3.7, the pigment does not establish direct contact with the fiber, but remains attracted to the

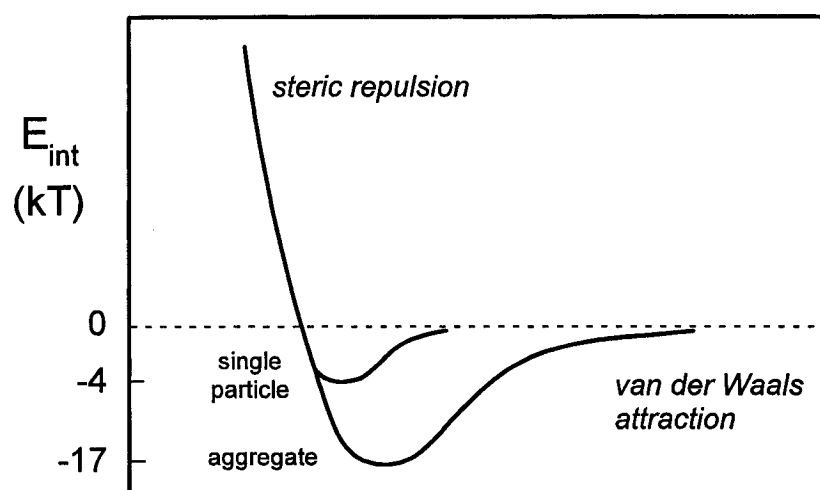


Fig. 3.7: Energy of interaction between a fiber and a pigment both fully coated by polymer (schematic).

fiber. In this case, a dynamic equilibrium is established ($k_1 \neq 0$, $k_2 \neq 0$). The feasibility of such a mechanism can be shown from an evaluation of the attractive van der Waals energy E_A between the fiber and CaCO_3 particle separated by a distance equal to twice the thickness of the polymer layer. The thickness of cPAM adsorbed on clay was reported to be around 100 nm [13]. Assuming the fiber to be a flat surface and the pigment to be a sphere, $E_A = -Aa/6H$ at short separations, where A is the Hamaker constant for a CaCO_3 -fiber interaction in water about 4.10^{-20}J [2], a is the radius of a pigment sphere (taken as 0.5 μm for an individual particle or 2 μm for aggregates), and H is the distance between the pigment and fiber which, assuming the adsorption layers are 100 nm, equals about 200 nm. The attractive energy for single particles is then around -4 kT and for an aggregate around -17 kT. This suggests that the energy minimum in Fig. 3.7 is sufficiently deep to justify the third explanation, i.e. van der Waals forces are sufficiently strong to keep fully coated fibers and fillers in contact.

3.4.5. Retention in Handsheets

At the end of each deposition run, handsheets were formed to see how much of the deposited CaCO_3 remains in the sheet. Since the process requires considerable dilution (500 cm^3 into 8 L) and mixing, some removal of the deposited CaCO_3 from the fiber is expected. Consequently, the amount of CaCO_3 ending up in the sheet will depend on the tenacity of CaCO_3 attachment to the fibers.

In Table 3.4, the CaCO_3 content of handsheets formed from three levels of filler addition and three levels of polymer addition (0.1 mg, 1 mg and 10 mg/g fiber) is shown. The data are approximate average values from a number of experiments

Table 3.4: Comparison of deposition (D) and retention (R) of CaCO₃.

Polymer addition mg/g fiber		CaCO ₃ addition, mg/g fiber					
		125		500		1000	
		D	R	D	R	D	R
PEI	0.1	80	30	200	100	500	140
	1.0	20	40	100	110	400	150
	10.0	0	20	0	40	100	80
cPAM	0.1	110	40	400	80	600	130
	1.0	110	50	400	180	700	280
	10.0	110	50	400	160	800	330

D - CaCO₃ deposition in mg/g fiber after 30 minutes of mixing fiber suspension (1 g/500 cm³) at 80 rpm.

R - CaCO₃ in mg/g fiber in a sheet formed after deposition completed.

with both PCC and GCC and used for illustration. As seen, there is no clear correlation between the amount of CaCO_3 deposited on fibers suspended in water (subjected to gentle stirring) and the amount of CaCO_3 in a sheet formed by the standard method. The efficiency of the two polymers appears to be similar at the lowest levels of addition. However, the difference is apparent at high polymer additions. Excess PEI produces dispersed and positively charged CaCO_3 particles, which do not deposit on positively charged fibers (cf. Fig. 3.5c). Still, some filler particles are retained even when no deposition occurs on fibers. Presumably diluting the suspension with water causes a desorption of PEI from the filler, which can subsequently aggregate and be trapped in the pores of the forming sheet. On the other hand, cPAM flocculates CaCO_3 and the flocs deposit effectively on the fibers. In addition, large flocs can be retained in the forming sheets by entrapment. The different mechanism is the reason why cPAM is more effective as a retention aid than PEI.

3.5. Concluding Remarks

Untreated ground CaCO_3 and precipitated CaCO_3 dispersed in water are similar in their colloidal behavior and in their response to different cationic polyelectrolyte. Their interactions with pulp fibers depend on the mechanism by which the different polymers act. A highly charged polymer of relatively low molar mass, such as PEI, acts as a dispersant producing positively charged single particles, which interact with negatively charged fibers via electrostatic colloidal forces. Therefore, overcharging the system with PEI results in decreased deposition and

retention. A high molar mass polyelectrolyte of low charge density, such as cPAM, produces flocs of CaCO_3 particles which deposit effectively on fibers and are more easily retained. With cPAM, the electrostatic interaction is not a dominant mechanism because overcharging the system does result in decreased deposition and retention. The bridging mechanism, however, is not sufficient to account for the observed interaction between pigment particle and fiber at high cPAM dosage. The overall behavior indicates that cPAM is more effective as a retention aid due to its flocculating ability.

3.6. Acknowledgement

The work was financially supported by a Domtar-NSERC IOR grant.

3.7. References

1. Vanerek, A., Alince, B., and van de Ven, T.G.M., "Colloidal Behavior of Ground and Precipitated Calcium Carbonate Fillers: Effect of Cationic Polyelectrolytes and Water Quality". *J. Pulp Paper Sci.* **26**(4), 135-139 (2000).
2. Fimbel, P., and Siffert, B., "Interaction of Calcium Carbonate (Calcite) with Cellulose Fibers in Aqueous Medium". *Colloids Surf.*, **20**, 1-16 (1986).
3. Kamiti, M., and van de Ven, T.G.M., "Kinetics of Deposition of Calcium Carbonate Particles onto Pulp Fibers". *J. Pulp Pap. Sci.*, **20**(7), J199-J205 (1994).

4. Halab-Kessira, L., and Ricard, A., "Adsorption of CaCO_3 Particles on Cationic Cellulose Graft Copolymers". *J. Colloid Interface Sci.*, **179**, 269-275 (1996).
5. Ono, H., and Deng, Y., "Flocculation and Retention of Precipitated Calcium Carbonate by Cationic Polymeric Microparticle Flocculants". *J. Colloid Interface Sci.*, **188**, 183-192 (1997).
6. Gibbs, A., Xioa, H., Deng, Y., and Pelton, R.H., "Flocculants for Precipitated Calcium Carbonate in Newsprint Pulps". *Tappi*, **80**(4), 163-170 (1997).
7. Alince, B., Petlicki, J., and van de Ven, T.G.M., "Kinetics of Colloidal Particle Deposition on Pulp Fibers. Part I". *Colloids Surf.*, **59**, 265-277 (1991).
8. Petlicki, J., and van de Ven, T.G.M., "Shear-Induced Deposition of Colloidal Particles on Spheroids". *J. Colloid Interface Sci.*, **148**, 14-22 (1992).
9. Alince, B., Vanerek, A., and van de Ven, T.G.M., "Effect of Surface Topography, pH and Salt on the Adsorption of Polydisperse Polyethylenimine onto Pulp Fibers". *Ber. Bunsenges Phys. Chem.*, **100**(6), 954-962 (1996).
10. Suty, S., Alince, B., and van de Ven, T.G.M., "Stability of Ground and Precipitated CaCO_3 Suspensions in the Presence of Polyethylenimine and Salt". *J. Pulp Pap. Sci.*, **22**(9), J321-J326 (1996).
11. Alince, B., and van de Ven, T.G.M., "Kinetics of Colloidal Particle Deposition on Pulp Fibers. Part 2". *Colloids Surf. A*, **71**, 105-114 (1993).
12. Lindström, T., and Wågberg, L., "Effect of pH and Electrolyte Concentration on the Adsorption of Cationic Polyacrylamide on Cellulose". *Tappi* **66**(6), 83-85 (1988).

13. Radeva, T., Petckanchin, I., Varoque, R., and Stoylov, S., "Electro Optical Studies of Kaolinite-Polyacrylamide Suspensions". *Colloids Surf.*, **41**, 353-361 (1989).

Chapter 4

The interaction of mineral pigments with pulp fibers in the presence of cationic polyelectrolytes is greatly affected by the presence of anionic impurities. The general consensus is that the cationic polyelectrolytes have to first neutralize the excess negative charge, and only then the cationic polymers can flocculate the suspension. As shown in Chapter 2, the results do not seem to support this hypothesis. Moreover, it appeared that cationic polyelectrolytes formed complexes with anionic substances, which was the focus in this chapter.

4.1. Abstract

Polyelectrolyte complex formation (PEC) is a common phenomenon occurring when positively charged polymers react with anionic polyelectrolytes and other anionic substances. Our interest is in papermaking, where cationic polyelectrolytes are used as retention aids (floculants) added to papermaking suspensions which contain many dissolved anionic substances. In general, there are three types of polyelectrolyte complexes: soluble, colloidal and coacervate complexes, of which the latter two phase-separate. The formation of each individual type of complex depends on the chemical and physical properties of the two oppositely charged polyelectrolytes. The focus of this study is on the formation of the coacervate complex between various cationic polyacrylamides (cPAM) and anionic sulfonated kraft lignin (SKL). The reaction between cPAM and SKL was found to be nearly stoichiometric. The amount of insoluble PEC (i.e. colloidal and coacervate complex) was found to be constant for a given cPAM charge; however, the ratio between colloidal and coacervate complex varied depending on the molecular weight of cPAM used. The formation of the coacervate complex increased with increasing molecular weight of cPAM while low molecular weight cPAM formed predominantly colloidal complexes with SKL.

4.2. Introduction

Retention aids are widely used in the wet-end of a papermaking machine. In general, they are cationic polyelectrolytes added to a mixture of pulp fibers and mineral pigments with the objective to promote fines and pigment attachment to the

fiber surface. Anionic dissolved and colloidal substances (DCS), which can comprise up to a hundred different compounds including dissolved lignin, hemicelluloses, soluble extractives, colloidal wood resins, etc., compete with fibers and pigment for the retention aids. As a result, the efficiency of the retention aids is substantially decreased [1-3]. The presence of DCS leads to the formation of a polyelectrolyte complex (PEC) between the cationic retention aid and the dissolved anionic and colloidal substances. Three types of polyelectrolyte complexes can form simultaneously: (i) soluble; (ii) colloidal; and (iii) coacervate. The soluble complex will remain in solution where one of the polyelectrolytes acts as a host molecule for the other much smaller polyelectrolyte. The colloidal and coacervate complexes become insoluble and phase-separate where one of the phases is usually concentrated and the other dilute. However, the main characteristic of the polyelectrolyte complex formation is that both phases contain about the same amount of both polymers.

The formation of polyelectrolyte complexes in solution was first studied in detail by Bungenberg de Jong, [4], Michaels [5] and Veis [6] using mostly biological polymers. The PEC formation originates from the electrostatic attraction between polyanions and polycations. The interaction between the two oppositely charged polyelectrolytes results, in most cases, in irreversible complex formation. Many researchers have found reactions between anionic and cationic polyelectrolytes to be non-stoichiometric [7-9], and yet other studies show polyanions and polycations reacting in stoichiometric ratios [5, 10, 11]. Based on these results, it was concluded that the reaction stoichiometry depends on three major factors: (i) polymer flexibility – rigid polymers are likely to form non-stoichiometric PEC because of their inability

to conform; (ii) polymer branching – charged sites in the inner part of molecules can be inaccessible to oppositely charged polymers; and (iii) the uneven distance between charged groups of the two polyelectrolytes. Deviations from the otherwise stoichiometric reaction can also occur in the presence of salt where polyelectrolytes tend to form denser structures [5]. Dautzenberg et al. [12-14] also showed that oppositely charged polyelectrolytes form stable colloidal dispersions at low ionic strength. At high ionic strength, the polyelectrolyte complexes become unstable and undergo secondary macroscopic flocculation due to screening of charges by the electrical double layer. Excellent reviews of recent developments in PEC formation are also reported by Burkart et al. [15], Tsuchida et al. [16] and Weinbreck [17].

Polyelectrolyte complex formation is a very common phenomenon in papermaking. However, very little is known about the precise mechanism of PEC formation as well as the structure and factors influencing the PEC; this is mainly due to the fact that PEC formation occurs in a matter of a few seconds on fast paper machines before paper is made. Some results may suggest that the formation of PEC may not be entirely detrimental to pigment flocculation [18]. The aim of this study is to investigate and characterize the formation of polyelectrolyte complexes between cationic retention aids and a model anionic compound. Determining the factors affecting the formation of polyelectrolyte complexes can lead to a better understanding of mechanisms by which cationic retention aids operate in the presence of DCS.

4.3. Experimental

4.3.1. Materials

A nonionic polyacrylamide (PAM) and various cationic polyacrylamides (cPAM's) were acquired from CIBA Specialty Chemicals Canada Inc. The molecular weight (Mw) and the degree of substitution (DS) of each polymer are summarized in Table 4.1. For future references, the cationic polyacrylamides will be referred to as cPAM followed by two numbers. The first number corresponds to DS (%) and the second number to Mw (MDa). The molecular weight of the cationic polyacrylamides was calculated from intrinsic viscosities using an empirical Mark-Houwink-type equation developed by Mabire et al. [19]. The positive charge of the polyacrylamide is incorporated in the chain during random copolymerization with (N,N,N-trimethyl) aminoethyl chloride acrylate. However, the cationic amino groups are unstable and undergo hydrolysis at $\text{pH} \geq 7$ [19-21]. The hydrolysis renders the polymer negatively charged (see Fig. 4.1).

A solution of a given cPAM was prepared at a concentration of 1 g/L and the pH was adjusted to 5.5 with 0.1 M HCl to prevent the polymer hydrolysis. To ensure proper dissolution of the polymers, each solution was stirred for 2 hrs using a magnetic stirrer. Every day, a fresh stock cPAM solution was prepared in order to avoid intrinsic changes of the polymer solutions with time.

Table 4.1: Summary of used polyacrylamides and their description in terms of degree of substitution (DS) and molecular weight (Mw).

Polymer: cPAM (DS/Mw)	DS (%)	Mw (MDa)	Commercial Name
PAM	0	4	Percol 351 PG
cPAM 5/7	5	7	Percol 455
cPAM 20/2	20	2	Percol 181
cPAM 25/3	25	3	Percol 292
cPAM 25/5	25	5	Percol 175
cPAM 25/6	25	6	Percol 178
cPAM 40/6	40	6	Percol 63
cPAM 40/8	40	8	Organopol 5440
cPAM 60/5	60	5	Organopol 5030
cPAM 80/7	80	7	Organopol 5472
cPAM 100/0.5	100	0.5	Percol 368

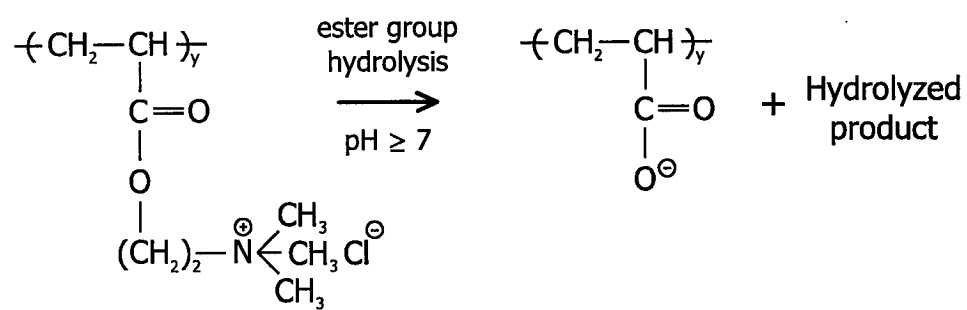


Fig. 4.1: Hydrolysis of cPAM at $\text{pH} \geq 7$ resulting in a negatively charged polyacrylamide.

Water-soluble, sulfonated kraft lignin was used as a model anionic compound in the PEC-formation experiments. The commercially available sodium salt of sulfonated kraft lignin (SKL) Indulin C was obtained from Westvaco Polychemicals. It is a polydisperse polymer with an average molar mass of 20,000 g/mol [22]. Stock solutions of SKL were prepared at a concentration of 10 g/L and a pH of 8. The degree of sulfonation was estimated to be about one sulfonated group per two monomer units with an average Mw of one unit approximately 223 g/mol [23].

4.3.2. Polyelectrolyte complex formation procedure

A stock solution of SKL was transferred into six volumetric flasks (a total volume of 100 cm³ each) so that the final concentration of SKL would be 1 g/L. (The concentration of SKL was constant in all the experiments at 1 g/L). Solutions of cPAM were then introduced to these volumetric flasks. The cPAM additions varied for each flask increasing in concentrations from 0, 3, 5, 10, 20 to 40 mg cPAM. The volume was then adjusted to 100 cm³ using deionized water, and the solutions were gently agitated while the PEC was being formed. The formation of PEC is captured in Fig. 4.2.

The first stage of PEC formation can be described as complex coacervation that was first defined by Bungenberg de Jong [4] as liquid-liquid phase separation (not shown in Fig. 4.2). The complex coacervate stage is then followed by formation of a large-scale network as the polyelectrolyte complexes start to precipitate out (see Fig. 4.2A). At these early stages of PEC formation, the network still contains a substantial amount of water. However, in the case of SKL and cPAM, the solvent is

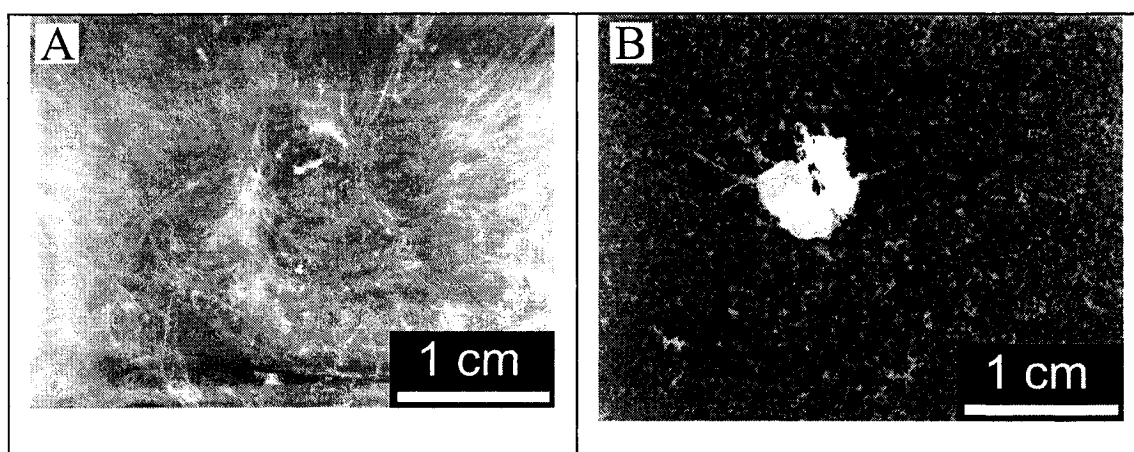


Fig. 4.2: An example of polyelectrolyte complex formation: (A) Formation of a thread-like precipitate that forms a large-scale network (coacervate complex) after cPAM was added to SKL and the solution was gently stirred for about 10 s; (B) The same PEC after 1 min agitation, the network shrank with time, expelling solvent and eventually becoming a single aggregate. The diameter of the aggregate is around 1 cm. The presence of much smaller colloidal complexes is also evident. For better visualization, the concentration of SKL was lowered to 0.5 g/L, cPAM addition was 5 mg and the total volume was 100 cm³.

gradually expelled as the PEC network collapses with time. At the end of the reaction, the network remains as a compact, rubbery-like, single aggregate in solution. Since the aggregates originate from complex coacervation, as described by Bungenberg de Jong [4], the single aggregates at the end of the PEC formation are, for the purpose of this study, referred to as coacervate complexes. Any other insoluble PEC, that is not a part of these single aggregates, is referred to as a colloidal complex. At the end of the complex-formation experiments, the coacervate complex (the aggregate) was removed from each solution, dried in an oven at 105°C for 24 hrs and the mass was determined. From Fig. 4.2B, the formation of colloidal complexes in the form of small particles is also evident. Lu [24] observed similar network formation with systems containing nonionic high molecular weight PEO and a polypeptide cofactor in the presence of Ca^{2+} salt. The size of the PEO/cofactor network was also in the range of 1 μm . These results suggest that coacervate complex formation is not solely restricted to polymers with opposite charges.

4.3.3. Determination of SKL in the supernatant

The amount of SKL, which did not react with cPAM and remained in the supernatant, was determined with a Varian Cary 1E UV/VIS spectrophotometer using a calibration curve. After the polyelectrolyte complexes were formed, all the insoluble PEC's (i.e. colloidal and coacervate complexes) were removed from the supernatant. The samples were first pre-filtered using a 0.45 μm Millipore syringe filter, followed by filtration through a 0.10 μm Cameo syringe filter. No adsorption of SKL on these filters was detected, which means that all unassociated SKL could pass

freely through the filters. The final amount of SKL that associated with cPAM was determined from the difference between the amounts added and detected in the supernatant. However, this technique is insensitive to soluble polyelectrolyte complexes as they could be indistinguishable from solutions of SKL. Therefore, the results presented in this study are only related to SKL being associated within the insoluble, i.e. colloidal and coacervate complexes; and the fraction of SKL that might have been a part of the soluble complex was treated as free SKL.

4.4. Results and Discussion

4.4.1. Reaction stoichiometry between cPAM and SKL

The difference in charge densities between two oppositely charged polyelectrolytes is a crucial factor in determining the driving force for the interaction between anionic and cationic polyelectrolytes [25]. The first step of this study is to determine the reaction stoichiometry and also the effect of increasing charge densities of cPAM on PEC formation.

The composition of the insoluble PEC as a function of increasing cPAM charge densities is shown in Fig. 4.3. The amount of SKL in PEC is expressed in mg SKL/mg cPAM. The graph is a classical example of PEC formation which is driven by electrostatic attraction, i.e. polymers with higher charge densities are capable of reacting with larger amounts of oppositely charged polyelectrolytes. This electrostatically based association appears to be completely independent of the

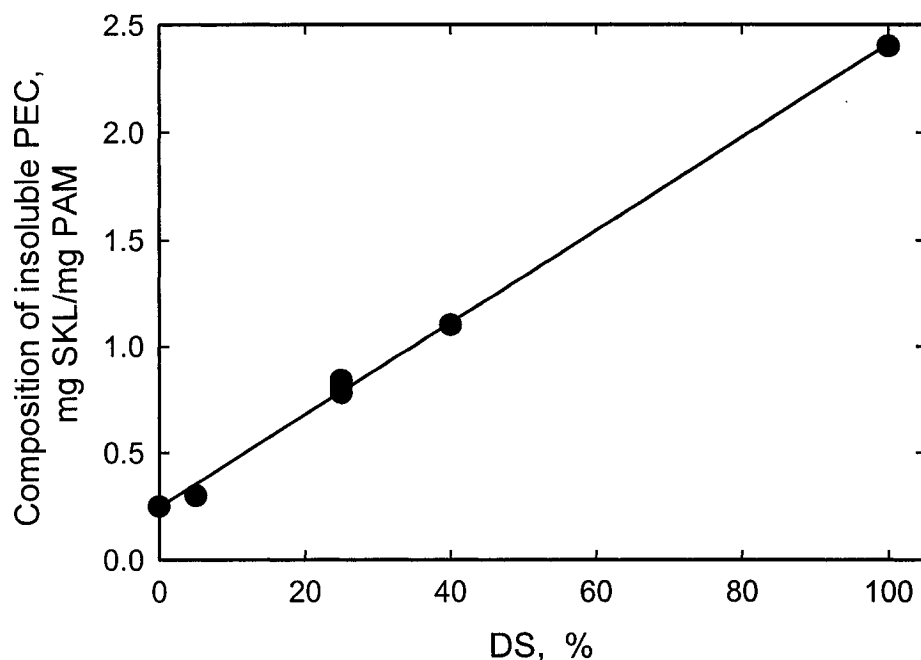


Fig. 4.3: The amount of SKL in insoluble PEC (i.e. colloidal and coacervate complexes combined) as a function of DS of added cPAM determined by light adsorption of supernatants containing unreacted SKL. Each point on the plot represents an average value for cPAM additions of 3, 5, 10, 20 and 40 mg introduced to 100 mg SKL. The total volume was 100 cm³. Experimental errors were within 5%. For DS = 25%, three cPAM's with Mw of 3, 5, and 6 MDa were used. The points are almost superimposed. A nonionic PAM (DS = 0%) was also used as a reference.

molecular weight of the cPAM as three different molecular weights (3, 5 and 6 MDa) with the same charge densities (DS = 25%) interacted with almost the same amount of SKL 0.8 mg/mg cPAM. The three points in Fig. 4.3 are nearly superimposed. In almost all experiments, SKL was always added in excess resulting in an overall negative charge of the colloidal precipitate. The only exception was for the highest addition of 40 mg of cPAM 100/0.5 where the overall PEC charge approached the isoelectric point. These results were obtained by measuring electrophoretic mobilities of PEC using a Rank Bros particle electrophoresis apparatus (Cambridge, UK) equipped with a flat cell.

For a polymer with DS = 100% (i.e. all functional groups were substituted with cationic (N,N,N-trimethyl) aminoethyl chloride acrylate group), around 2.4 mg SKL reacted with 1 mg cPAM 100/0.5 creating the insoluble complexes. The molecular weight of the co-monomer unit of the cPAM 100/0.5 is around 175 g/mol. From the molecular weights and charge densities of SKL [22, 23] and cPAM 100/0.5, one can calculate that SKL has 45 negatively charged groups while cPAM 100/0.5 has 2860 positively charged groups per polymer molecule. It can be then estimated that 3.4×10^{18} negative charges in 2.4 mg SKL reacted with 3.2×10^{18} positive charges in 1 mg cPAM 100/0.5, which is very close to a 1:1 ratio. Since very similar ratios apply to all other cPAM's and SKL, it can be concluded that the overall reaction between anionic SKL and cationic cPAM is nearly stoichiometric. The calculated numbers of charged groups involved in the complex formation are listed in Table 4.2. It can be seen that charge stoichiometry is 0.87 ± 0.14 , i.e. within experimental error, approximately equal to one.

Table 4.2: Reaction stoichiometry of PEC formation between cPAM and SKL.

	POLYMER					
	cPAM 5/7	cPAM 25/3	cPAM 25/5	cPAM 25/6	cPAM 40/6	cPAM 100/0.5
Associated SKL (mg/mg cPAM)	0.30	0.80	0.82	0.83	1.10	2.40
Number of SKL charges*	4.0×10^{17}	1.1×10^{18}	1.1×10^{18}	1.1×10^{18}	2.1×10^{18}	3.4×10^{18}
Number of cPAM charges**	4.1×10^{17}	1.5×10^{18}	1.5×10^{18}	1.5×10^{18}	2.1×10^{18}	3.2×10^{18}
Ratio	0.98	0.73	0.73	0.73	1.0	1.1

* The number of SKL charges was calculated from the amount of SKL that reacted with 1 mg cPAM.

** Number of charges present in 1 mg cPAM.

It should be noted that the intercept on the y-axis has a non-zero value (~ 0.25 mg SKL/mg PAM, which means that the nonionic PAM (DS = 0%) also formed a complex with the anionic SKL. This fact may indicate that the electrostatic interaction is not the only driving force for the SKL association with polyacrylamide-type polymers. The origin of SKL association with nonionic polyacrylamide is most likely due to hydrophobic contributions of the polymer chains [25].

4.4.2. Effect of M_w on coacervate complex formation

The previous graph Fig. 4.3 showed that the overall reaction between SKL and cPAM was nearly stoichiometric. However, it does not give any insight as to how much of the insoluble PEC was in the form of colloidal or coacervate complexes. The majority of studies available in the literature focuses on stable, well-defined colloidal complexes, some of which are between SKL and cPAM [22, 26], or colloidal complexes in general [12-14, 27], but very little has been reported about the actual formation of coacervate complexes. Therefore, the main objective of this study is to shed some light on the formation of the coacervate complex.

Unlike the charge density for the electrostatic interaction between the two oppositely charged polyelectrolytes discussed in the previous section, the most important factor influencing the amount of coacervate complex formed appears to be the molecular weight of cPAM. The effect of molar mass of three cPAM's with identical charge densities (DS = 25%) on the formation of the coacervate complex is plotted in Fig. 4.4. The data show that increasing the molecular weight of cPAM results in increasing amounts of the coacervate complex produced by the

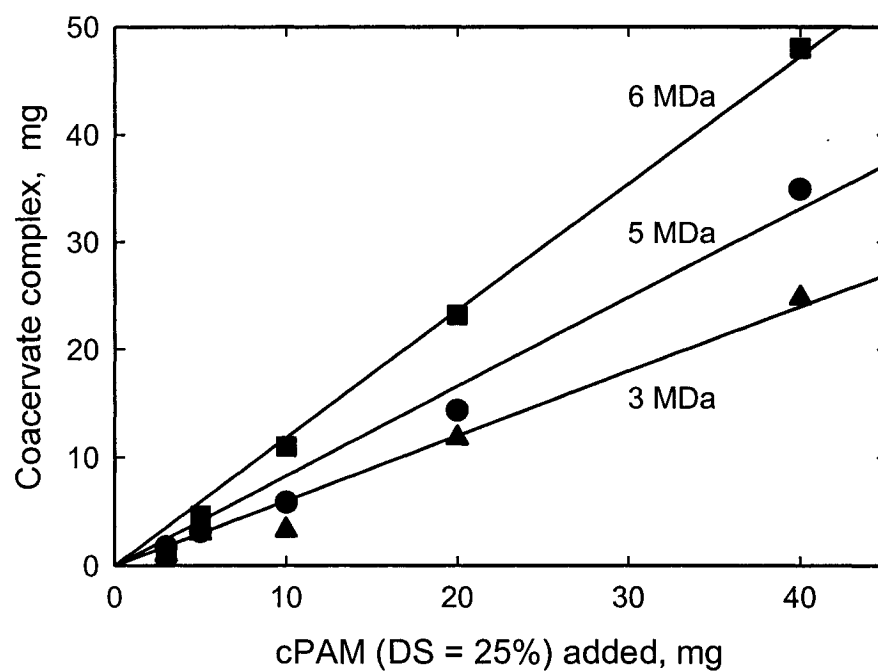


Fig. 4.4: The formation of the coacervate complex as a function of cPAM with DS = 25%. Three molecular weights (3, 5, and 6 MDa) were used. The concentration of SKL was 1 g/L and the total volume was 100 cm³.

reaction. Furthermore, this linear increase shows no effect of the initial polymer concentration on the final amount of coacervate complex formed. This is important because, at very low and at very high polymer concentrations, the coacervate complex formation is likely to be affected by the initial polymer concentration. However, this was not the case for the cPAM/SKL system at chosen experimental conditions.

The highest amount of coacervate complex was formed between SKL and cPAM with a highest molecular weight of 6 MDa. Considering the reaction stoichiometry, one can calculate that nearly 75 % of the added polyelectrolytes precipitated out from solution in the form of a coacervate complex. This trend appears to be consistent with results reported by Li and Pelton [26] who observed that high molecular weight cationic polymers formed larger amounts of coacervate complexes. Similarly, Ström and Stenius [22] fractionated SKL and observed that the highest amount of PEC was formed with the SKL fraction that had the highest molecular weight.

The reason for the increase of PEC with increasing molar mass of cPAM is most likely due to the differences in chain length. The initial formation of the PEC network is triggered by the electrostatic attraction between the two oppositely charged species. At the same time, clustering of cPAM molecules also takes place. From Fig. 4.2A, it appears that the cPAM molecules prefer an extended configuration over a coiled configuration. The formation of thread-like networks in the initial stage of polyelectrolyte complex formation seems to substantiate this hypothesis. Also statistically, longer cPAM molecules have a better chance of being entangled than the short polymer chains. After the initial entanglement, a subsequent bridging of cPAM

molecules by SKL can lead to a formation of large-scale networks. The actual mechanism of PEC formation is discussed in more detail in section 4.4.4.

The effect of Mw on the formation of respective colloidal and coacervate complexes is shown in Fig. 4.5. The insoluble PEC represents the amount of colloidal and coacervate complexes formed per milligram of cPAM added. The graph clearly shows that the total amount of the formed insoluble PEC is virtually the same for all three cPAM's. These results are in accordance with those obtained during stoichiometry experiments where all three polymers associated with almost the same amount of SKL (cf. Fig. 4.3). However, unlike the total amount of the insoluble PEC, the amount of colloidal and the amount of coacervate complexes changed significantly. The ratios of the two complexes vary dramatically depending on the molecular weight of the cPAM. The low molecular weight polymer (cPAM 25/3) forms about 70% colloidal and 30% coacervate complexes with SKL, while the high molecular weight polymers (cPAM 25/5 and cPAM 25/6) have the ratios reversed (i.e. a majority of insoluble PEC is in the form of the coacervate complex). Since the formation of each particular complex varies with Mw, it is of the utmost importance to distinguish clearly between the colloidal and coacervate complexes as they may substantially differ in structure and colloidal behavior in real systems.

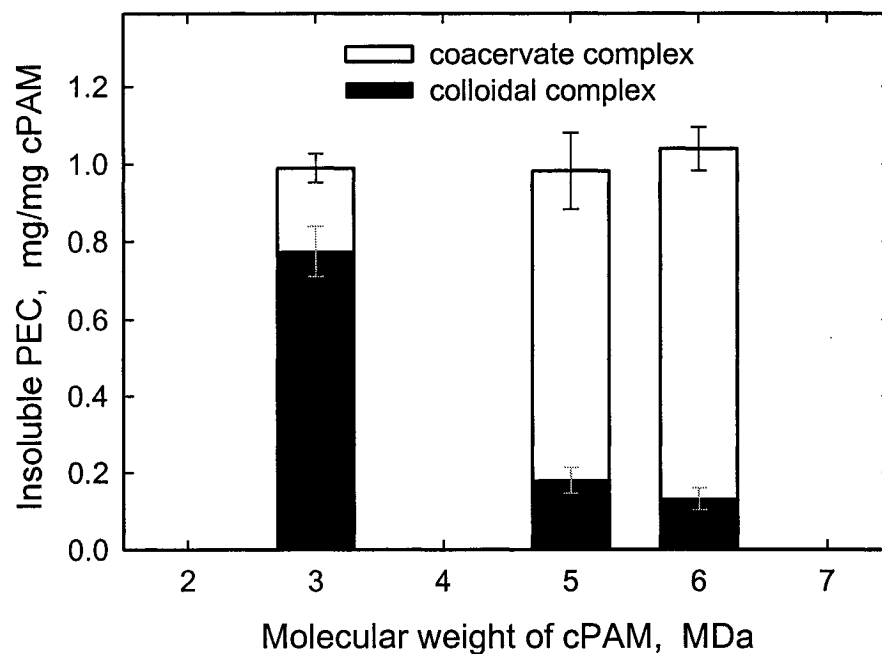


Fig. 4.5: The ratio between the formation of colloidal and coacervate complexes. Three cPAM's with the same DS (25%), but three different Mw (3, 5 and 6 MDa) were used. The white portion of the bar represents the formation of the coacervate complex and the black portion represents the colloidal complex. The bar height represents the total amount of insoluble complex formed per mg cPAM added.

4.4.3. Effect of DS on coacervate complex formation

The formation of the coacervate complex as a function of Mw and DS is shown in Fig. 4.6. Coacervate complex formation increases linearly as a function of Mw of cPAM, and the data fall more or less on the same line despite the different charge densities. This is in agreement with Fig. 4.5 where exactly the same trend of increased coacervate complex formation with increasing Mw was observed, but at constant DS. These results suggest that the coacervate complex formation is almost exclusively a function of Mw, and the polymer charge densities seem to play a minor role. A very different behavior was observed for nonionic PAM where no formation of the coacervate complex occurred despite the high molecular weight (4 MDa). However, as shown previously, the nonionic PAM does form a small amount of colloidal complexes with SKL (cf. Fig. 4.3). Since the high molecular weight nonionic PAM is unable to form a coacervate complex with SKL, it implies that the electrostatic attraction between two polymers is an essential requirement for successful coacervate formation between SKL and cPAM.

It should also be noted that the line does not go through the origin. This may be an indication that a critical chain length of cPAM is required for successful coacervate complex formation. If the polymer size is below this critical chain length, only colloidal complexes can form. This was also observed with cPAM 100/0.5 where all the insoluble precipitate was in the form of a colloidal complex. Thus, for systems consisting of SKL and cPAM, the critical molar mass required for successful coacervate complex formation appears to be around 500,000 g/mol.

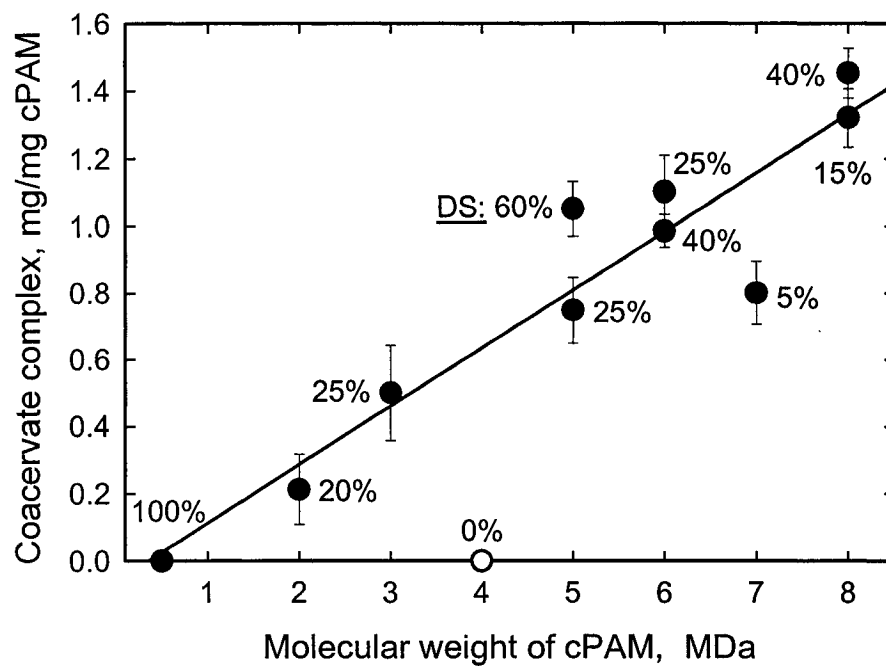


Fig. 4.6: The formation of the coacervate complex as a function of a molecular weight and charge densities of cPAM. Each point on the plot represents an average value for cPAM additions of 3, 5, 10, 20 and 40 mg introduced to 100 mg SKL. The total volume was 100 cm³. A nonionic PAM was also used as a reference (○).

4.4.4. Mechanism of colloidal and coacervate complex formation

The formation of PEC is a process during which cPAM molecules interact not only with SKL molecules, but also with other cPAM molecules. It can be described by two major phenomena: (i) SKL association with cPAM and (ii) clustering of cPAM molecules. The characteristic times of association and clustering can be estimated using the following equations [28, 29]

$$\tau_a = \frac{1}{\alpha_a k_{12} \frac{n_{SKL}}{n_{max}} n_{cPAM}}; \quad \tau_c = \frac{1}{\alpha_c k_{11} n_{cPAM}} \quad (1a,b)$$

where τ_a and τ_c refer to characteristic times of SKL association with cPAM and clustering of cPAM molecules, respectively. The ratio n_{SKL}/n_{max} is the ratio between the number SKL molecules per unit volume and the total number of positive sites available on cPAM. The ratio n_{SKL}/n_{max} varies between 1 and 100 for the highest addition of the highly-charged, low molecular weight polymer (cPAM 100/0.5) and the lowest addition of the weakly-charged, high molecular weight polymer (cPAM 5/7), respectively. The remainder of the polymers and their concentrations fall within this range. The number of cPAM molecules per unit volume is n_{cPAM} ; k_{11} and k_{12} are the diffusion controlled Smoluchowski rate constants modeled as interactions between equal spheres for clustering and unequal spheres for association, respectively; α_a is the association efficiency; and α_c is the clustering efficiency of cPAM molecules. The estimated values for τ_a and τ_c are listed in Table 4.3. The assumptions made were that α_a and α_c are equal to unity and the radii of gyration were 35 nm, 150 nm and 2.5 nm for cPAM 100/0.5, cPAM 5/7 [19] and SKL (determined by dynamic light scattering), respectively.

Table 4.3: Theoretical prediction of characteristic times of association τ_a and clustering τ_c .

Polymer	Addition (mg/L)	$\frac{n_{SKL}}{n_{max}}$	τ_a (s)	τ_c (s)
cPAM 5/7 [*]	30	100	2×10^{-5}	3×10^{-2}
cPAM 100/0.5 ^{**}	400	1	4×10^{-5}	2×10^{-4}

^{*} Forms coacervate and colloidal complexes

^{**} Does not form coacervate, only colloidal complex

The characteristic times in Table 4.3 indicate that the association of SKL with cPAM occurs almost instantaneously. This can explain why no effect of DS was observed during coacervate formation. The association is the fastest phenomenon, and all polymer chains are neutralized almost immediately regardless of the charge densities. Clustering takes place after the association of SKL with cPAM is complete. The size and the type of clusters are therefore determined chiefly by the molecular weight of the cPAM used. The time scales τ_a and τ_c alone cannot explain the formation of colloidal and coacervate complexes with respect to the molecular weight of cPAM. One additional factor, which must be considered, is the characteristic time of polymer reformation τ_r . Einarson et al. [30] measured the reformation times of adsorbed cPAM on carboxymethylated pulp fibers and polystyrene latex in the range of 1 min and 5 s, respectively. The difference is claimed to be due to disparity in porosity of the two substrates. It is expected that the reformation of a free polymer chain in solution is even more rapid. Initially, the cPAM molecules are stretched due to electrostatic repulsion, but after association with SKL, the electrostatic repulsion is diminished due to the stoichiometric, charge-neutralization reaction. These charge-neutralized polymers having a net-zero charge begin to reconfirm (see Fig. 4.7). Shorter polymers can reconfirm at a much faster rate than longer polymers. If the characteristic time of reformation is shorter than the time of clustering $\tau_r < \tau_c$, the cPAM/SKL complexes will tend to form colloidal complexes, which is most likely the case for cPAM 100/0.5. If the characteristic time of reformation is longer than the time of clustering $\tau_r > \tau_c$, the polymers will tend to

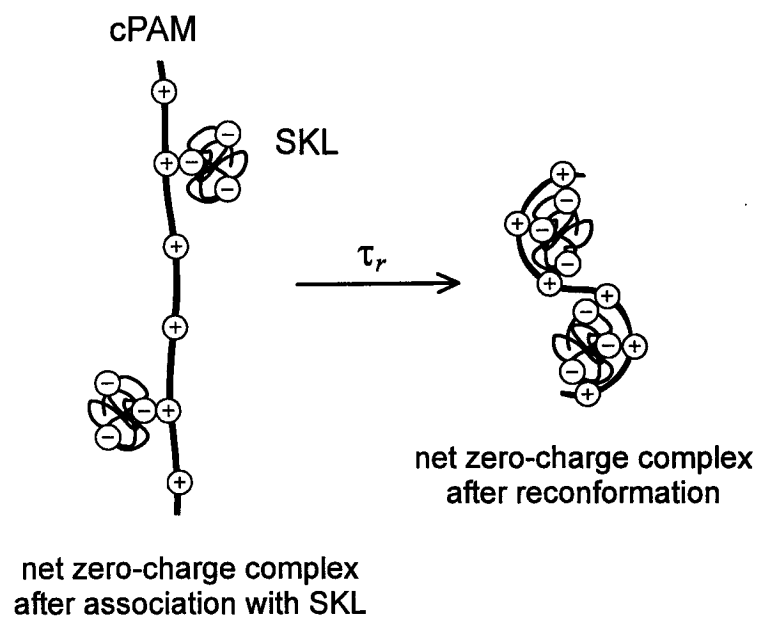


Fig. 4.7: Schematic drawing of reformation of cPAM after association with SKL. After the charge neutralization reaction of cPAM with SKL, the polyelectrolyte complex has an overall net zero charge, and the system tends to reconfirm due to the interaction between the anionic and cationic sites.

form coacervate complexes. Moreover, if the reconfiguration is slow, the polymer is initially stretched and, at the same time, some of the positive sites on neighboring molecules are still unoccupied. This leads to polyelectrolyte complex formation where SKL acts as a bridging agent. As a result, large macroscopic networks (i.e. coacervate complexes) can be formed. This network structure is initially very loose, but starts to contract as cPAM molecules start to reconfigure and form denser structures. As the electrophoretic mobility experiments suggest, after the initial stoichiometric reaction, additional adsorption of SKL on these net zero-charge complexes takes place rendering them eventually negatively charged.

In the presence of mineral pigments, such as precipitated calcium carbonate, it is likely that after the initial stoichiometric reaction, these net zero-charge complexes adsorb on the pigment causing pigment flocculation due to polymer bridging [18]. In high shear, the adsorption of the net zero-charge complexes on the pigment is much faster than the polymer clustering, and hence no extensive formation of coacervate complexes is expected. However, in the case of a pigment fully coated with net zero-charge complexes, the pigment may still flocculate as the electrostatic repulsion is diminished. This is in contrast with steric stability expected for particles fully coated with cPAM [18]. Furthermore, two complex-covered surfaces may bond together due to a complex-complex interaction, which is, in some aspects, reminiscent of the coacervate complex formation. This would also explain the need for increased additions of retention aids in contaminated systems. It is because some of the polymer is lost in the complex-complex interaction, as opposed to polymer-bare surface interactions, which are more efficient and occur mostly in clean systems.

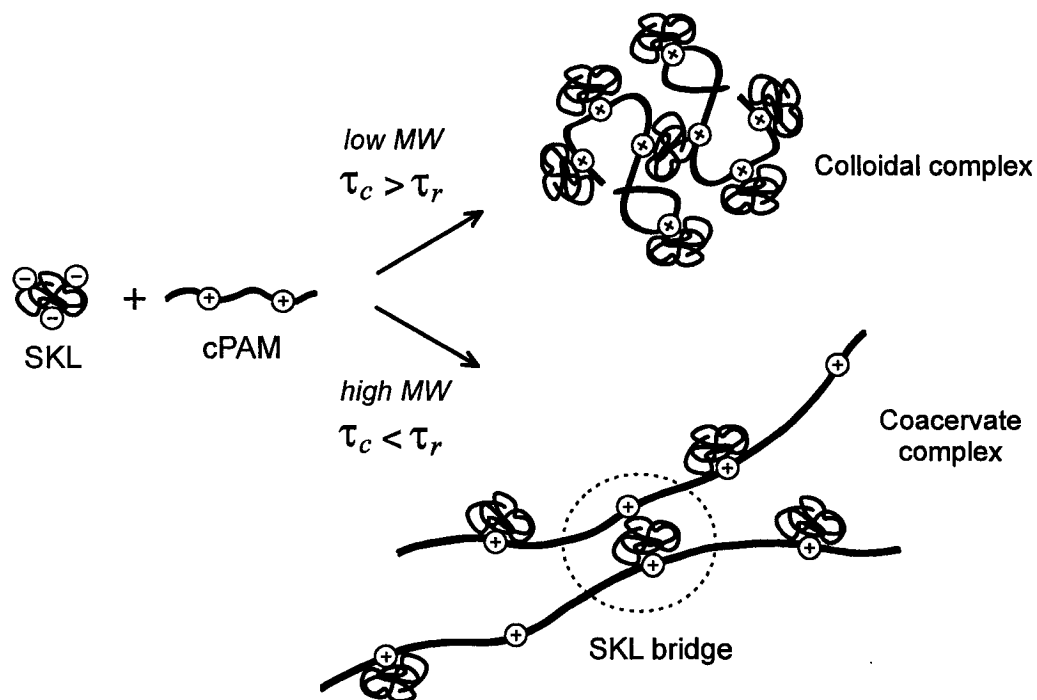


Fig. 4.8: Schematic drawing of the effect of molecular weight of cPAM on the formation of colloidal and coacervate complexes. Low molar mass cPAM forms predominantly colloidal complexes while high molar mass cPAM forms mostly coacervate complexes with SKL.

The formation of colloidal and coacervate complexes is schematically summarized in Fig. 4.8. Due to the different characteristic times of cPAM clustering and cPAM reformation, low molecular weight cPAM forms predominantly colloidal complexes with SKL while high molecular weight cPAM forms coacervate complexes.

4.5. Conclusions

Cationic polacrylamides were found to form polyelectrolyte complexes with anionic sulfonated kraft lignin. The reaction between the two oppositely charged polyelectrolytes is nearly stoichiometric except for a slight excess of SKL, which provided stability to colloidal complexes and accounted for the observed electrophoretic mobility. A highly positively charged cPAM reacts with larger amounts of anionic SKL forming more insoluble PEC, and vice versa. However, varying the charge density of cPAM has virtually no effect on the final formation of the coacervate complex. Coacervate complex formation was found to be mainly determined by the molecular weight of cPAM. The reaction of SKL with high molar mass cPAM resulted in the formation of extensive amounts of coacervate complex, as opposed to the reaction with low molar mass cPAM, which lead to preferential formation of the colloidal complex. The preferential formation of either the colloidal complex for low molar mass cPAM or the coacervate complex for high molar mass cPAM was attributed to a competition between clustering of cPAM molecules and polymer reformation.

4.6. Acknowledgements

The authors would like to thank to Mr. P. Bricault from CIBA Specialty Chemicals Canada Inc. for donating the polyacrylamide samples. Financial support from the Network of Centres of Excellence (NCE) for Mechanical-Wood Pulps and from Paprican/NSERC IRC is also greatly appreciated.

4.7. References

- [1] Alinec, B., "Contaminants, Clay Retention and Polyethylenimine". *Paper Technology* **6**, 27-30 (1991).
- [2] Alinec, B., "Effect of Contaminants on Filler Retention in Mechanical Pulp". *Paperi Ja Puu* **69**(3), 230-233 (1987).
- [3] Sundberg, A., Ekman, R., Holmbom, B. and Grönfors, H., "Interaction of Cationic Polymers with Components in Thermomechanical Pulp Suspensions". *Paperi Ja Puu* **76**(9), 593-598 (1994).
- [4] Bundenberg de Jong, H.C., "Colloid Science", Elsevier, Amsterdam, (1949).
- [5] Michaels, A.S., Mir, L. and Schneider, N.S., "A Conductometric Study of Polycation-Polyanion Reactions in Dilute Aqueous Solution". *J. Phys. Chem.* **69**(5), 1447-1455 (1965).
- [6] Veis, A., "Biological Polyelectrolytes", New York, (1970).
- [7] Polderman, A., "The Interaction between Two Oppositely Charged Polyelectrolytes". *Biopolymers* **14**, 2181-2195 (1975).

- [8] Sato, H. and Nakajima, A., "Formation of Polyelectrolyte Complex from Carboxymethyl Cellulose and Poly(ethylenimine)". *Polymer. J.* **7**(2), 241-247 (1975).
- [9] Ström, G., Barla, P. and Stenius, P., "The Formation of Polyelectrolyte Complexes between Pine Xylan and Cationic Polymers". *Colloid Surf A* **13**, 193-207 (1985).
- [10] Brand, F. and Dautzenberg, H., "Structural Analysis in Interpolyelectrolyte Complex Formation of Sodium Poly(styrenesulfonate) and Diallyldimethylammonium Chloride-Acrylamide Copolymers by Viscometry". *Langmuir* **13**(11), 2905-2910 (1997).
- [11] Horn, D., "Polymeric Amines and Ammonium Salts", Pergamon, Oxford, (1980).
- [12] Dautzenberg, H. and Jaeger, W., "Effect of Charge Density on the Formation and Salt Stability of Polyelectrolyte Complexes". *Macromol. Chem. Phys.* **203**(14), 2095-2102 (2002).
- [13] Dautzenberg, H., "Polyelectrolyte Complex Formation in Highly Aggregating Systems. 1. Effect of Salt: Polyelectrolyte Complex Formation in the Presence of NaCl". *Macromolecules* **30**, 7810-7815 (1997).
- [14] Dautzenberg, H. and Karibyants, N., "Polyelectrolyte Complex Formation in Highly Aggregating Systems. Effect of Salt: Response to Subsequent Addition of NaCl". *Macromol. Chem. Phys.* **200**(1), 118-125 (1999).

- [15] Burkart, P., Dautzenberg, H., Linow, K.-J., Kötzt, J. and Dawydoff, W., "Polyelectrolyte Complexes-Recent Developments and Open Problems". *Prog. Polym. Sci.* **14**, 91-172 (1989).
- [16] Tsuchida, E., Osada, Y. and Ohno, H., "Formation of Interpolymer Complexes". *J. Macromol. Sci.-Phys.* **B17**(4), 683-714 (1980).
- [17] Weinbreck, F., "Whey Protein/Polysaccharide Coacervates: Structure and Dynamics", Utrecht University, The Netherlands, (2004).
- [18] Vanerek, A., Alince, B. and van de Ven, T.G.M., "Colloidal Behaviour of Ground and Precipitated Calcium Carbonate Fillers: Effect of Cationic Polyelectrolytes and Water Quality". *J. Pulp Paper Sci.* **26**(4), 135-139 (2000).
- [19] Mabire, F., Audebert, R. and Quivoron, C., "Synthesis and Solution Properties of Water Soluble Copolymers Based on Acrylamide and Quaternary Ammonium Copolymers". *Polymer* **25**(9), 1317-1322 (1984).
- [20] Aksberg, R. and Wågberg, L., "Hydrolysis of Cationic Polyacrylamides". *J. App. Polym. Sci.* **38**, 297-304 (1989).
- [21] Kamiti, M. and van de Ven, T.G.M., "Impinging Jet Studies of the Kinetics of Deposition and Dissolution of Calcium Carbonate Particles". *Colloid Surf A* **100**, 117-129 (1995).
- [22] Ström, G. and Stenius, P., "Formation of Complexes, Colloids and Precipitates in Aqueous Mixtures of Lignin Sulphonate and Some Cationic Polymers". *Colloid Surf A* **2**, 357-371 (1981).
- [23] Sarkanen, K.V. and Ludwig, H.C., "Lignins", New York, (1971).

- [24] Lu, C., Ph.D. Thesis, McMaster University, (2003).
- [25] Abe, K., Ohno, H., Nii, A. and Tsuchida, E., "Calorimetric Study on the Formation of Polymer Complexes through Electrostatic Interaction and Hydrogen Bonding". *Makromol. Chem.* **179**, 2043-2050 (1978).
- [26] Li, P. and Pelton, R., "Wood Pulp Waching. 1. Complex Formation between Kraft Lignin and Cationic Polymers". *Colloid Surf A* **64**, 217-222 (1992).
- [27] Lappan, R.E., Pelton, R., McLennan, I., Patry, J. and Hrymak, A.N., "Kraft Lignin-Poly(DADMAC) Precipitate Formation". *Ind. Eng. Chem. Res.* **36**, 1171-1175 (1997).
- [28] van de Ven, T.G.M., "Particle Deposition on Pulp Fibers: The Influence of Added Chemicals". *Nord. Pulp Pap. Res. J.* **1**, 130-147 (1993).
- [29] Alince, B. and van de Ven, T.G.M., "Kinetics of Colloidal Particle Deposition on Pulp Fibers. 2. Deposition of Clay on Fibers in the Presence of Poly(ethylenimine)". *Colloid Surf A* **71**, 105-114 (1993).
- [30] Einarson, M., Aksberg, R., Ödberg, L. and Berg, J.C., "Adsorption and Reformation of a Series of Cationic Polyacrylamides on Charged Surfaces". *Colloid Surf A* **53**, 183-191 (1991).

Chapter 5

The interactions of mineral pigments with cationic retention aids and pulp fibers were investigated in Chapters 2 and 3. The cationic polyelectrolytes promote deposition of mineral pigments on pulp fibers. However, the polymeric bond between the pigment and the fiber is usually weak and can be broken by hydrodynamic forces. In real papermaking, a small amount of microparticles is added to the system. The microparticles form a bridge between polymer-covered surfaces of fibers and pigments that is much stronger than simple polymeric bridge. The importance of delamination of microparticles such as bentonite and montmorillonite during pigment deposition on fibers has been long debated and is the prime focus in this chapter.

5.1. Abstract

In papermaking, a microparticulate retention aid system comprising bentonite and high molecular weight cationic polymer is used to incorporate mineral pigments in the fiber web. It is believed that the mechanism by which bentonite operates is based on its ability to form a bridge between polymer-covered fibers and fine particles, i.e. a microparticulate retention aid system promotes heteroflocculation. The performance of kaolin clay and montmorillonite in the role of microparticles was evaluated by observing the deposition of a calcium carbonate pigment on kraft fibers suspended in water. Neither was found to be effective. However, upon treatment with sodium-rich solutions, the montmorillonite delaminated and calcium carbonate deposition increased considerably. The kaolin clay showed only a small degree of delamination after treatment and, as a consequence, calcium carbonate deposition increased only marginally. When commercial bentonite was treated with a strong acid, its particle size increased resulting in decreased deposition of calcium carbonate on fibers. The overall behavior indicates that the flocculation efficiency of microparticles is related to its ability to delaminate.

5.2. Introduction

Clays are abundant, soft, secondary minerals formed by the weathering of parent rocks. Clays are defined as fine grained aluminosilicate minerals which exhibit plastic properties at a certain moisture content, but harden upon drying. These unique properties are often attributed to the presence of clay minerals, such as bentonite [1].

The major component of bentonite is *montmorillonite* (around 90%). A single montmorillonite platelet is composed of three layers: one octahedral aluminum-oxygen layer is sandwiched between two tetrahedral silicon-oxygen layers. The montmorillonite platelets can form large stacks with a general chemical formula $A_{0.6}Al_{2.6}Mg_{1.4}Si_8O_{20}(OH)_4$, where A represents cations such as Na^+ , K^+ and $0.5Ca^{2+}$. The presence of these cations is a result of the so-called isomorphous substitution and these adsorbed cations greatly affect the swelling ability of montmorillonite [2-5], as well as the water content during drying [6, 7]. The presence of the adsorbed cations also increases the basal spacing from 9.1 Å to 9.6 Å [8].

The major component of kaolin clays is *kaolinite*. A kaolinite platelet, with the ideal chemical composition of $Al_2Si_2O_5(OH)_4$, comprises two alternating layers: one tetrahedral silicon-oxygen layer and one octahedral aluminum-oxygen layer. These layers form stacks which are held tightly together by hydrogen bonding [9], with a basal spacing of around 7.1 Å [8]. Unlike in montmorillonite, the lattice structure in kaolinite is nearly perfectly ordered, which leads to relatively low isomorphous substitution. Due to the hydrogen bonding and the low isomorphous substitution, kaolinite swelling in water is limited. Furthermore, kaolinite has been reported to eliminate swelling in interstratified montmorillonites [10].

Both kaolin clays (kaolinite) and bentonite (montmorillonite) are widely used in papermaking. Kaolin pigments are incorporated in paper or used in coating to improve the optical and printing properties of the final product. Bentonite is usually used in two-component microparticulate retention aid systems along with cationic polyacrylamide (cPAM) [11]. The purpose is to increase retention of fine particles,

such as mineral pigments. Initial addition of the cationic polyacrylamide to a suspension of fibers and pigment results in heteroflocculation by a polymer bridging mechanism [12-14]. The suspension is then redispersed by shear generated by fan pumps and/or pressure screens, but ensuing addition of bentonite causes reflocculation. The reflocculation induced by bentonite increases sheet drainage, pigment and fines retention and paper uniformity [15]. The exact flocculation mechanism in pulp suspensions using microparticulate retention aid systems remains unclear, but it is believed that the high surface charge density of montmorillonite platelets promotes the interaction with the adsorbed cationic polyelectrolytes, which results in larger flocs and stronger bonds between the flocs [16-18]. It was shown that in a single-component retention aid (cPAM only), the polymer conformation (trains, loops and tails) is very important for particle flocculation and reflocculation [19]. This is not the case for microparticulate systems, which work almost indiscriminately [19-21].

Wågberg et al. [22] found a maximum deposition of centrifuged bentonite onto cPAM-treated fibers to be around 1.5 mg/g fiber. This result is close to theoretical predictions for completely delaminated bentonite platelets having a thickness of 1 nm and a total surface area of 800 m²/g depositing randomly on fibers with an external surface area of around 1 m²/g [23]. Alince et al. [24] reported a maximum bentonite deposition on cPAM-pretreated fibers to be around 120 mg/g fiber, which is rather high even when accounting for a 10% content of filler-like impurities. From these experimental observations, it was concluded that bentonite can be deposited either in the form of stacks or in the form of single platelets.

The goal of this study is to investigate the possibility of complete delamination (i.e. delamination into single platelets) of kaolin clay and montmorillonite in suspensions with and without an external force. A similar concept was used by Churchman and Weissmann [25], who treated montmorillonite with a sodium salt, which resulted in the formation of fine suspended sols. This study attempts to shed some light on kaolin clay and montmorillonite delamination and the effect of this delamination on the flocculation efficiency, measured by the deposition of a calcium carbonate pigment on pulp fibers.

5.3. Experimental

5.3.1. Materials

A conventional microparticulate retention aid system comprising bentonite (Bnt) Hydrocol 2D7 and cationic polyacrylamide (cPAM) Percol 63 was acquired from CIBA Specialty Chemicals Canada Inc. The commercial cPAM was a copolymer of polyacrylamide with (N,N,N-trimethyl) aminoethyl chloride acrylate with a degree of substitution of 40% and a molecular weight of 6 MDa. A stock solution of cPAM was prepared at a concentration of 1 g/L and pH of 5.5. The performance of this conventional microparticulate retention aid system was compared with systems where bentonite was substituted by either a specialty kaolin clay Hydrate UF (Clay) from ECC (now IMERYS) or two montmorillonite samples Montmorillonite KSF (Mnt 20) and Montmorillonite K-10 (Mnt 200) both from Aldrich. Table 5.1 lists the microparticle systems and their approximate surface areas (SA).

Table 5.1: An overview of the microparticle systems.

Microparticle abbreviation	Commercial Microparticles	Approx. SA (m²/g)
Bnt	Bentonite Hydrocol 2D7	~ 800 ^a
Mnt 20	Montmorillonite KSF	20 – 40 ^b
Mnt 200	Montmorillonite K-10	220 – 270 ^b
Clay	Kaolin Clay Hydrite UF	~ 10 ^c

^aFully delaminated bentonite

^bProvided by Aldrich

^cCalculated using an equivalent spherical diameter of 200 nm [26]

Precipitated calcium carbonate (PCC) Albacar HO from Specialty Minerals was used as a pigment. The calcium carbonate pigment was a scalenohedral type with a particle diameter of 1.3 μm and a surface area of 12 m^2/g . The pigment was dispersed in tap water at a concentration of 50 g/L. The surface charge of PCC is affected by water quality: it is positive in deionized water, but negative in tap or whitewater [27].

Dry, softwood, bleached, kraft pulp Q90 was used as a source of fibers during the PCC deposition experiments. The pulp was immersed overnight in deionized water and then disintegrated in a Standard British Disintegrator using a total of 12,000 revolutions. Fines were removed from the pulp by extensive washing through a 100-mesh screen. The pulp was then redispersed in tap water at a concentration of 2g/L.

5.3.2. Deposition experiments

The experiments consisted of adding 200 mg of PCC to a suspension containing 1 g fiber suspended in 500 cm^3 of tap water. The fiber suspension was agitated in a Waring blender at 1500 rpm using a propeller with rounded edges which prevented damage to the fibers. After 30 s, a sample of supernatant was collected using a syringe with a special tip equipped with a 200-mesh screen. The screen prevented fibers from entering the supernatant. After the first supernatant sample was collected, 2 mg of cPAM were added, allowed to interact with the fibers and pigment for 15 s and followed by another collection of the supernatant. The stirring rate was then increased to 5000 rpm and the microparticles were introduced. The final

supernatant sample was collected 5 s after the microparticulate addition. The content of PCC in the supernatant was determined from light transmittance using a spectrophotometer (Spectronic 20, Bausch&Lomb) at a wavelength of 500 nm. Each supernatant sample was sonicated prior to the transmittance measurement for 30 s in an Ultrasonic Cleaner (Cole-Parmer) using a sound frequency of 40 kHz. The sonication was used as a means of breaking up PCC aggregates formed after the polymer and microparticles were added. The sonication redispersed all aggregated PCC from different addition points to individual particles, and the concentration of these individual particles could be then determined using a single calibration curve (light transmittance vs. concentration). The increase in the agitation from 1500 to 5000 rpm was aimed to simulate industrial conditions where after a retention aid is added to the pulp furnish, the furnish is then exposed to high shear generated by fan pumps and/or pressure screens. The experimental procedure is summarized in Fig. 5.1.

5.3.3. Cation exchange procedure

Clay, Mnt 20, and Mnt 200 were treated with sodium-rich solutions in order to replace existing cations with Na^+ cations. The cation exchange was performed in 100 cm^3 flasks. For a period of five days, 1 g of the microparticles was exposed to sodium-based solutions and gently stirred for 1 min three times a day. After the cation exchange period, the suspensions were centrifuged at a speed of 1000g for 60 min using International Centrifuge, Model K (IEC). The spent supernatants were carefully

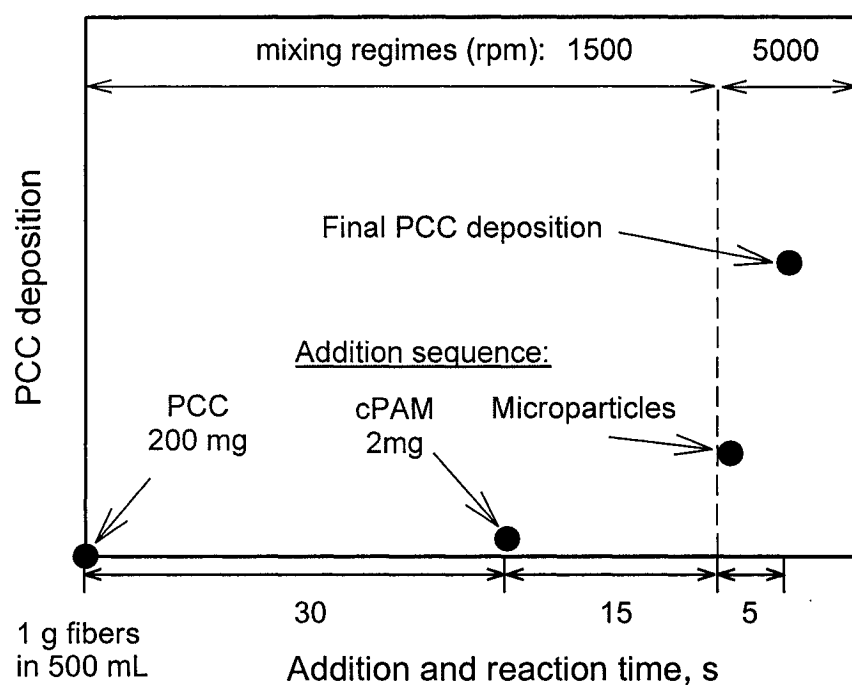


Fig. 5.1: Summary of the experimental procedure. A suspension consisting of 1 g fiber in 500 cm³ of tap water was stirred at 1500 rpm. At given intervals 200 mg PCC and 2 mg cPAM were added and supernatant samples collected. The speed of stirring was increased to 5000 rpm and microparticles were added followed by a supernatant sampling 5 s after the addition.

decanted and the particles, which settled to the bottom due to centrifugal force, were re-suspended using ultra pure water from NANOpure Analytical Deionization System, 851 Series (Barnstead). These treated microparticle suspensions were then used in deposition experiments after one day of ion equilibration. For the elemental analysis, the samples were washed and centrifuged until all free residual ions were removed.

5.3.4. Particle size measurements

Suspensions containing microparticles were thoroughly agitated for 1 min before injecting 15 mL of the suspension into the BI-DCP Disc Centrifuge Particle Size Analyzer (Brookhaven Instruments Corporation). The instrument measured particle settling velocities and average equivalent spherical Stokes diameters (D_{50}).

5.4. Results and discussion

5.4.1. PCC deposition on fibers using various microparticle systems

A comparison between PCC depositions on fibers for various microparticle systems containing Bnt (A), Clay (B), Mnt 20 (C) and Mnt 200 (D) is made in Fig. 5.2. In all four cases, the initial deposition of PCC at 30 s is low because both PCC particles and pulp fibers are negatively charged. The electrostatic repulsion between the two species is overcome with the addition of 2 mg cPAM. The deposition of PCC significantly increases due to polymer bridging between the pigment and the fibers [12-14]. The depositions of PCC alone ($t = 30$ s) and in the presence of cPAM ($t = 45$ s) appear to be constant. The PCC amount that deposits on fibers is controlled by the

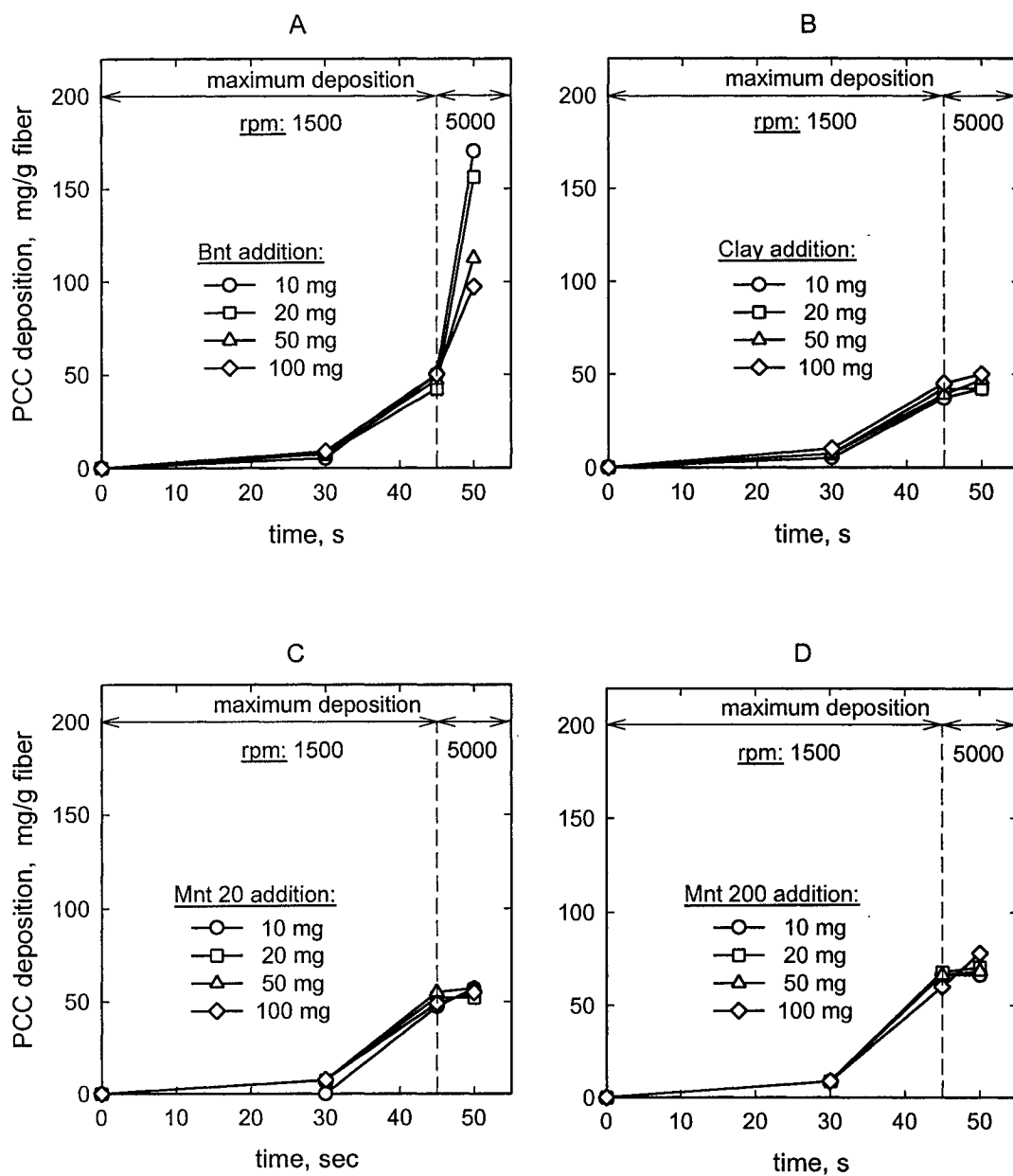


Fig. 5.2: PCC deposition on fibers using various microparticle systems: Bnt (A), Clay (B), Mnt 20 (C) and Mnt 200 (D). The final PCC deposition is determined 5 s after the microparticle addition. The pH of the suspensions was around 8.

dynamic equilibrium between the particle attachment and detachment, which is dependent on hydrodynamic conditions [24]. The addition of Bnt to the system results in dramatic increase in PCC deposition. The lowest addition of 10 mg/g fiber appeared to be the most effective as the PCC deposition is the highest. Further increases of Bnt led to lower PCC depositions. This trend is a direct result of overloading the system with microparticles. Because of their small size and large surface area, even small bentonite additions contain a large number of particles. If added in excess, Bnt deposits on most of the cPAM-covered surfaces on fibers and pigment. This leaves a smaller surface area with adsorbed polymer available for the flocculation, and thus the PCC deposition decreases.

Invariably, additions of Clay, Mnt 20 and Mnt 200 to suspensions containing fibers, PCC and cPAM show very little effect on the final PCC deposition. It is not surprising that this particular clay, although being a special kaolin clay with a much smaller particle size than those usually used in paper loading applications, did not perform well, since kaolin clays do not tend to delaminate and have a low cation exchange capacity [8, 10]. On the other hand, Mnt 20 and Mnt 200 failed to improve PCC deposition, even though montmorillonite is the main component in bentonite, which is renowned for its excellence in wet-end applications.

5.4.2. pH of microparticle suspensions

Measuring the pH of the stock microparticle suspensions (see Table 5.2) revealed that the commercial bentonite, Bnt, had a pH of 9.8. Clay had a more neutral

Table 5.2: pH of microparticle systems at a concentration of 10 g/L.

Microparticulate	pH
Bnt	9.8
Mnt 20	2.6
Mnt 200	2.7
Clay	7.5

pH of 7.5. Both, Mnt 20 and Mnt 200 had extremely low pH values of 2.6 and 2.7, respectively. This suggests that these montmorillonites were treated with an acid. Acid activation is a common process during which the montmorillonite is purified by dissolving undesired impurities. Strong acids also tend to dissolve parts of the montmorillonite structure containing Na^+ , K^+ , Ca^{2+} , Mg^{2+} and Al^{3+} cations, and thus contribute to a development of the surface area [28-32]. By means of acid treatment, montmorillonite is converted to its hydrogenated form, which results in limited swelling [2]. The low degree of swelling was indeed observed during the preparation of the montmorillonite suspensions.

5.4.3. Cation exchange treatment of microparticle suspensions

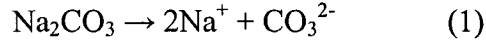
Since Clay, Mnt 20 and Mnt 200 failed to improve PCC deposition on fibers, all three were subjected to cation exchange treatments in order to enrich the microparticle structures with Na^+ cations, and thus enhance swelling and possibly delamination. The first treatment consisted of exposing a given microparticle suspension to 1 M NaCl and 1 M Na_2CO_3 ; the second treatment to 1 M NaCl and 1 M Na_2CO_3 in conjunction with 0.5 M NaOH; and the third treatment to 0.5 M NaOH alone. All the treated samples were compared to a control sample that was left untreated. The list of various cation exchange treatments and pH profiles for treated Mnt 200 are provided in Table 5.3.

The untreated Mnt 200 had a pH of 2.7 at a concentration of 10 g/L. This sample was washed four times where each washing cycle consisted of centrifugation, supernatant decantation and redispersion of the particles in ultra pure water. The final

Table 5.3: The cation exchange treatment of Mnt 200 and pH profiles. Each wash consisted of centrifugation, decanting and redispersion of the microparticles in ultra pure water.

Sample	Chemical Treatment	pH after 1st wash	pH after 2nd wash	pH after 3rd wash	pH after 4th wash
1	untreated (pH 2.7)	3.5	3.7	3.7	3.9
2	1 M NaCl 1 M Na ₂ CO ₃	10.5	10.0	9.8	9.7
3	1 M NaCl 1 M Na ₂ CO ₃ 0.5 M NaOH	11.3	10.0	9.5	9.0
4	0.5 M NaOH	11.0	9.5	9.0	8.4

pH of the untreated Mnt 200 after four washing procedures rose to 3.9. The treatment of Mnt 200 with 1 M NaCl and 1 M Na₂CO₃ increased the pH after the first washing cycle from 2.7 to 10.5. This increase in pH was attributed to a formation of OH⁻ anions during CO₃²⁻ hydrolysis (see Eq. 2):



Further washing reduced the pH only marginally from 10.5 to a final pH of 9.7. The decrease is relatively small considering the dilution and is presumably due to self-buffering effects by the remaining CO₃²⁻ anions. Similar pH behavior was found for the treatment with 1 M NaCl, 1 M Na₂CO₃ and 0.5 M NaOH. The initial high pH of 11.3 was due to the presence of NaOH, and the final pH of 9.0 due to trace amounts of hydrolyzed CO₃²⁻. The treatment of Mnt 200 with 0.5 M NaOH resulted in an initial pH of 11.0 and a final pH of 8.4. The final pH is lower than those of the two previous cases. This is consistent with the occurrence of the hydrolysis of CO₃²⁻ anions, which can substantially influence the pH due to strong self-buffering effects.

The final PCC deposition results (i.e. measured 5 s after microparticles were added) for Mnt 200, Mnt 20 and Clay are shown in Fig. 5.3, 5.4 and 5.5, respectively. The treatment of Mnt 200 with salt only (i.e. 1 M NaCl and 1 M Na₂CO₃) starts to show a slight increase in PCC deposition at additions of 50 and 100 mg/g fiber. The cation exchange treatment using a combination of 1 M NaCl, 1 M Na₂CO₃ and 0.5 M NaOH increased significantly the flocculation efficiency of Mnt 200. The PCC deposition increased with Mnt 200 and seemed to level off at the addition of 100

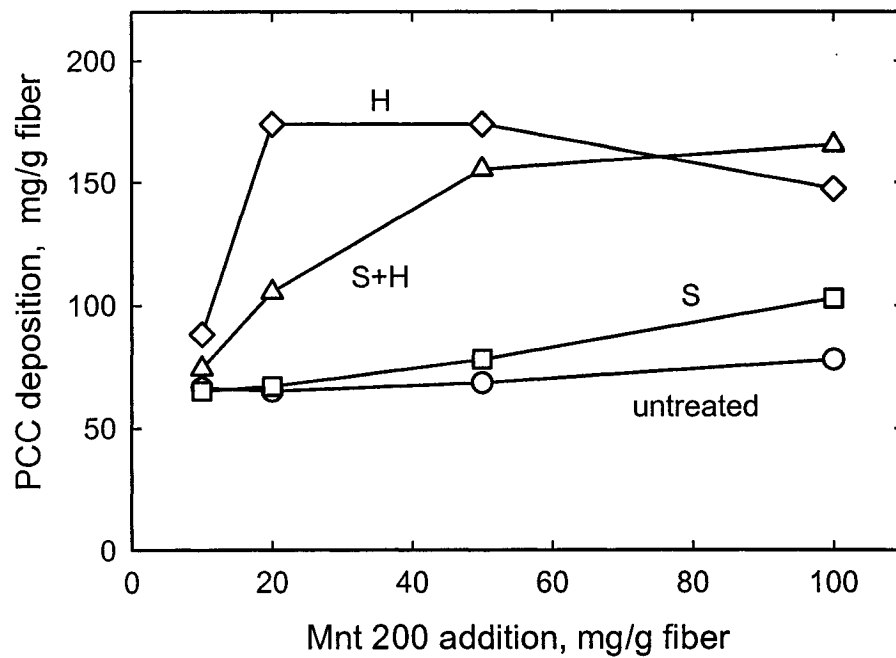


Fig. 5.3: Final PCC deposition on fibers as a function of Mnt 200 addition. (S) refers to ion exchange with 1 M NaCl and 1 M Na₂CO₃; (S+H) to ion exchange with 1 M NaCl, 1 M Na₂CO₃ and 0.5 M NaOH; and (H) to ion exchange with 0.5 M NaOH.

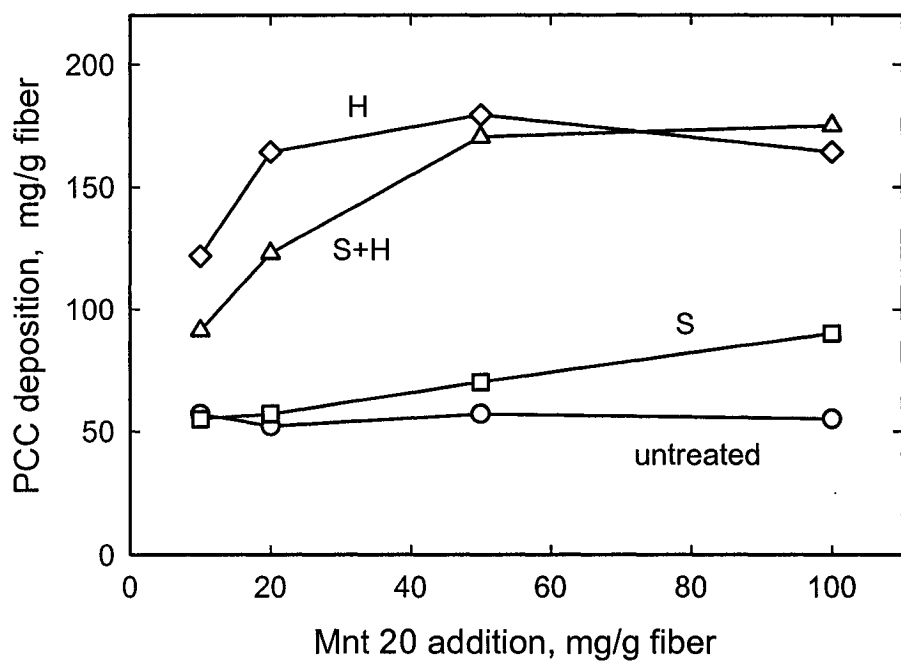


Fig. 5.4: Final PCC deposition on fibers as a function of Mnt 20 addition. (S) refers to ion exchange with 1 M NaCl and 1 M Na₂CO₃; (S+H) to ion exchange with 1 M NaCl, 1 M Na₂CO₃ and 0.5 M NaOH; and (H) to ion exchange with 0.5 M NaOH.

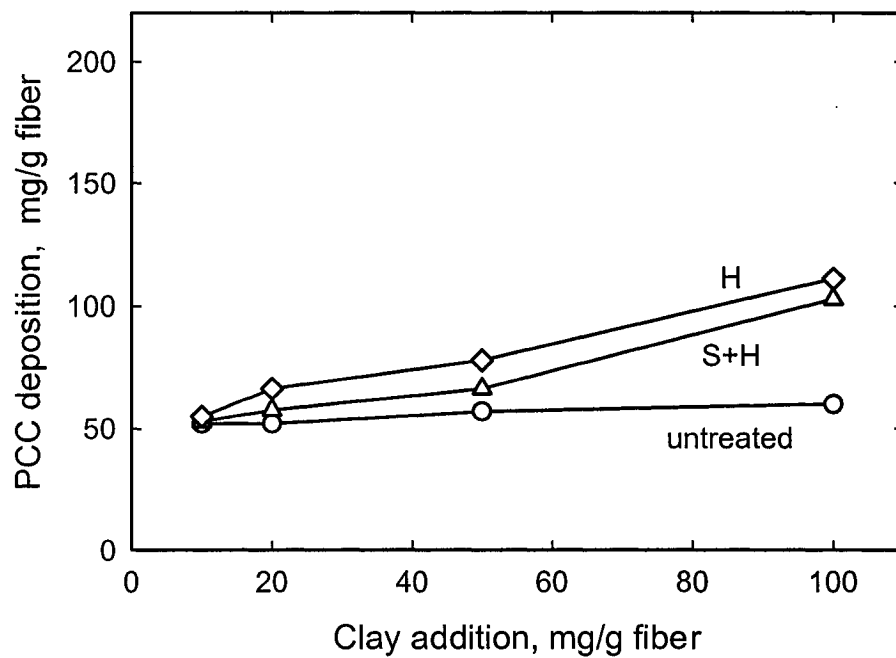


Fig. 5.5: Final PCC deposition on fibers as a function of Clay addition. (S+H) refers to ion exchange with 1 M NaCl, 1 M Na₂CO₃ and 0.5 M NaOH; and (H) to ion exchange with 0.5 M NaOH.

mg/g fiber. However, the best deposition results were obtained with 0.5 M NaOH treatment where the additions of 20 and 50 mg/g fiber resulted in the highest PCC deposition. This is only twice and five times more than the amount that was found to be the most effective with commercial bentonite. At the addition of 100 mg/g fiber, the PCC deposition starts to decline due to an excess of Mnt 200 in the system, which also appears to be analogous to Bnt behavior. The results for Mnt 20 are very similar to those of Mnt 200. Cation exchange using 1 M NaCl and 1 M Na₂CO₃ showed only a marginal increase in PCC deposition. Cation exchange using 0.5 M NaOH was again found to be the most effective as it shows a maximum PCC deposition at an addition of 50 mg/g fiber of Mnt 20. Similar to Mnt 200, the treatment of Mnt 20 with 1 M NaCl, 1 M Na₂CO₃ and 0.5 M NaOH shows a slower initial increase in PCC deposition and the deposition approaches a plateau at the addition of 100 mg/g fiber.

Cation exchange performed on Clay showed a different pattern. The treatment with 1 M NaCl and 1 M Na₂CO₃ resulted only a minor increase in PCC deposition and is not included in Fig. 5.5. The treatments of Clay with 1 M NaCl, 1 M Na₂CO₃ and 0.5 M NaOH and 0.5 M NaOH alone result in a gradual increase in PCC deposition, which is well below the values achieved with Mnt 20 and Mnt 200.

5.4.4. Microparticle delamination during cation exchange

The PCC deposition results for treated Mnt 20 and Mnt 200 seem to suggest that converting the hydrogenated montmorillonite into the sodium form may reduce the number of montmorillonite platelets within a single stack. The results in Fig. 5.3, 5.4 seem to suggest some montmorillonite delamination, as it would explain the great

increase in PCC deposition on fibers after montmorillonite treatments with 0.5 M NaOH alone or in conjunction with 1 M NaCl and 1 M Na₂CO₃. If that is the case and delamination really occurs during cation exchange, it would also imply that delaminated microparticles are more efficient flocculating agents.

In order to substantiate this hypothesis, particle sizes of bentonite, montmorillonite and kaolin clay were measured by the BI-DCP Disk Centrifuge Particle Size Analyzer. During the particle size measurements, the microparticles were modeled as very thin disks which are forced to the perimeter of a rotating disk due to centrifugal forces:

$$F_{cen} = \pi a_d^2 n d \Delta \rho \frac{\omega^2}{r} \quad (1)$$

where F_{cen} is the centrifugal force, a_d is the radius of a disk, n is the number of platelets in a montmorillonite stack, d is the thickness of a single montmorillonite platelet, $\Delta \rho$ is the density difference between the particle and spin fluid, ω is the angular velocity and r is the distance from the centre of the rotating disk to the detector. The centrifugal force acting on a montmorillonite particle is the same whether the particle is in a swollen or a non-swollen state because the water between the platelets does not contribute to the force.

Happel and Brenner [33] showed that the drag forces acting on extremely narrow disks with a broadside parallel to the centrifugal force, $F_{||}$, and perpendicular to the centrifugal force, F_{\perp} , are nearly independent of the disk thicknesses (i.e. only a weak dependence on swelling), which could be an adequate approximation for montmorillonite stacks.

$$F_{||} \cong 16 \eta u a_d \quad (2)$$

$$F_{\perp} \cong \frac{32}{3} \eta u a_d \quad (3)$$

Here η is the viscosity of the spin fluid and u is the velocity of a settling particle. Since the particles are randomly oriented in a suspension, the random drag force, F_r , equals to

$$F_r = \frac{l}{3} (2F_{\perp} + F_{\parallel}) \quad (4)$$

Because the centrifugal force and the drag force are in balance,

$$F_{drag} = F_r \quad (5)$$

the thickness of microparticle stacks, h , can be expressed as

$$h a_d \approx 4 \frac{\eta u r}{\Delta \rho \omega^2} \quad (6)$$

where the stack thickness, h , is defined as

$$h = n d \quad (7)$$

The settling velocity, u , was determined from the data obtained by the BI-DCP Disk Centrifuge Particle Size Analyzer and the particle radius, a_d , was assumed to be 300 nm for montmorillonite and bentonite and 100 nm for clay. The other parameters in Eq. 6 are known and remain constant. Since all forces acting on a montmorillonite particle during centrifugation experiments are almost independent of the state of swelling, the thickness, h , corresponds almost entirely to the contracted montmorillonite (i.e. no swelling). Thus it appears that the BI-DCP Disk Centrifuge Particle Size Analyzer is a useful instrument in determining dimensions of swollen non-spherical particles.

Table 5.4: The number of platelets, n , in montmorillonite stacks as a function of Mnt 200 cation exchange treatment. The radius of montmorillonite, a_d , is assumed to be 300 nm.

Chemical Treatment	ha_d (μm^2)	n
Untreated (D_{50}) = 1850 nm	0.200	332
1 M NaCl 1 M Na_2CO_3	0.130	221
1 M NaCl 1 M Na_2CO_3 0.5 M NaOH	0.099	165
0.5 M NaOH	0.049	82

The results listed in Table 5.4 show an estimated number of platelet, n , in Mnt 200. As suggested, the number of platelets changes with cation exchange treatment of Mnt 200 from 332 for untreated Mnt 200; to 221 (reduction by ~30%) for treatment with 1 M NaCl and 1 M Na₂CO₃; to 165 (reduction by ~50%) for treatment with 1 M NaCl, 1 M Na₂CO₃ and 0.5 M NaOH; and finally to 82 (reduction by ~75%) for treatment with 0.5 M NaOH. Since the number of montmorillonite platelets decreases from 332 for untreated Mnt 200 to 82 for Mnt 200 treated with NaOH only, the data suggest that, upon NaOH treatment, the untreated Mnt 200 delaminated to form new stacks, which contained approximately four times fewer platelets. The other cation exchange treatments were less efficient in Mnt 200 delamination.

One interesting aspect, which is not apparent from Table 5.4, are the opposite effects of delamination (size reduction) and swelling (increase in the size of montmorillonite stacks). The thickness, h , of non-swollen untreated Mnt 200 is 664 nm. On the other hand, Mnt 200 swells greatly in water and the interlayer spacing may increase from 1 nm (non-swollen state) to approximately 10 nm (swollen state). This would suggest that the thickness corresponding to 82 platelets for contracted montmorillonite will increase to around 820 nm after the montmorillonite swells in water, which is around 25% larger than the untreated Mnt 200.

It should be noted that the thicknesses of microparticulate platelets are underestimated when calculating the drag forces using Eq. 2,3 (i.e. neglecting axis ratios). On the other hand, the drag force for random orientation overestimates the force in the perpendicular direction as the microparticulates platelets are likely to orient parallel to the flow when the suspension is injected to the BI-DCP Disk

Centrifuge Particle Size Analyzer. Since the results are consistent with the expected trends, it is possible that these two phenomena balance each other.

5.4.5. Effect of shear on microparticle delamination

Although the montmorillonite stacks appear to delaminate after cation exchange, the possibility of extending the delamination by exposing the stacks to shear was also studied. Clay and Mnt 20 were treated with 1 M NaCl, 1 M Na₂CO₃ and 0.5 M NaOH and then subjected to a high shear prior to their additions to the pulp furnish. The microparticles were subjected to shear using a high-shear mixer Polytron, Kinematica GMBH, Luzern-Schweiz and the shear was estimated to be around $5 \times 10^3 \text{ s}^{-1}$. The PCC deposition results are shown in Fig. 5.6. The non-sheared Mnt 20 is compared with three samples subjected to the shear for a period of 1, 3 and 5 min, respectively. The PCC deposition curves appear to be identical within experimental error. These results suggest that converting Mnt 20 to the sodium form may have caused montmorillonite delamination to a certain degree, and additional shear treatment of the microparticles appears to be ineffective. A similar trend was also observed for Clay.

The results in Table 5.5 seem to support the PCC deposition experiments. The treated and sheared Clay and Mnt 20 are compared with untreated and non-sheared counterparts, and also with non-sheared Clay and Mnt 20 treated with 0.5 M NaOH. Initially, the untreated and non-sheared Mnt 20 and Clay had Stokes diameters of 5230 nm and 414 nm, which represent around 1105 platelets in a single stack for Mnt

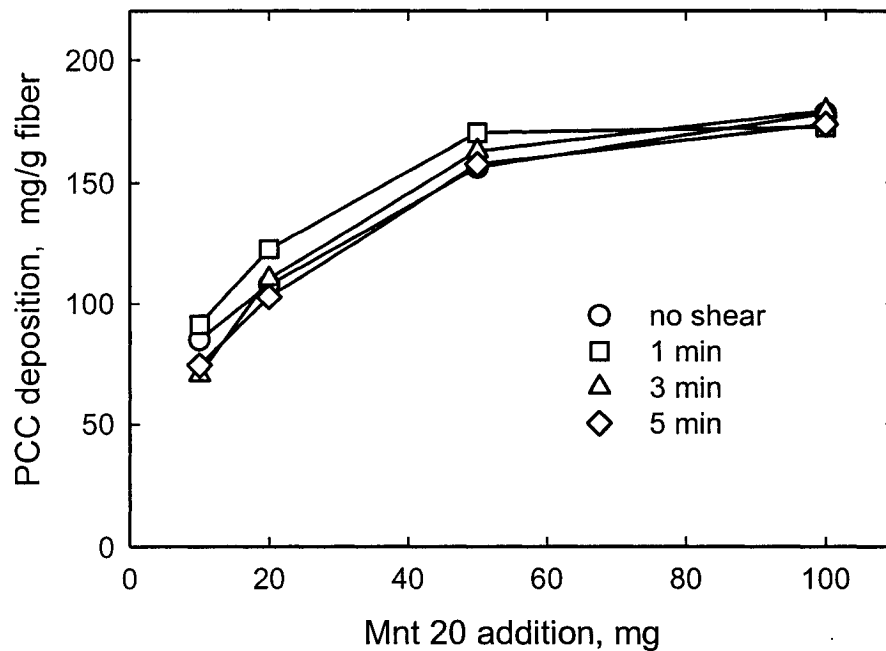


Fig. 5.6: Final PCC deposition on fibers as a function of Mnt 20 addition. Mnt 20 was treated with 1 M NaCl, 1 M Na₂CO₃ and 0.5 M NaOH and then subjected to a high shear before its addition to the suspension of fibers, PCC and cPAM.

Table 5.5: The number of platelets, n , in montmorillonite and bentonite stacks as a function of shearing time. Both, Mnt 20 and Clay were treated with 1 M NaCl, 1 M Na₂CO₃ and 0.5 M NaOH. The shaded rows represent untreated Mnt 20 and Clay and Mnt 20 and Clay treated with 0.5 M NaOH, respectively. The radii of the montmorillonite and clay, a_d , are assumed to be 300 nm and 100 nm, respectively.

Shearing (min)	Mnt 20		Clay	
	ha_d (μm^2)	n	ha_d (μm^2)	n
0 (untreated)	0.660	1105	0.040	285
0	0.066	111	0.050	357
1	0.057	95	0.040	285
5	0.062	104	0.044	314
0 (NaOH-treated)	0.050	83	0.033	235

20 and around 285 for Clay, respectively. The thickness of a kaolinite layer and interlayer spacing were assumed to be 0.7 Å each. The cation exchange treatment decreased the number of platelet in Mnt 20 to 111. Shearing Mnt 20 for 1 min reduced the number of platelets to 95, but the number remained almost the same even after 5 min of shearing (104). As a comparison, the number of platelets in non-sheared Mnt 20 treated with 0.5 M NaOH was 83. The data seem to indicate that shearing of Mnt 20 did not result in a reduction of the number of platelets.

Several possible explanations why a complete montmorillonite delamination was not observed are: (i) it is very difficult to delaminate already very thin montmorillonite stacks; (ii) sheared Mnt 20 might have reaggregated during particle size measurements and increased the thickness of the stacks due to face-to-face aggregation, which is a common phenomenon at higher ionic strength [34]; and (iii) the treated Mnt 20 might have further delaminated to a higher degree in the presence of fibers during PCC deposition experiments.

Unlike for Mnt 20, the number of platelets in a single Clay stack remained nearly constant despite the cation exchange and shear exposure, except for the case when Clay was treated with 0.5 M NaOH. These results support the general belief that kaolin clays do not readily delaminate, and they can also explain the poor performance of Clay during PCC deposition on fibers.

5.4.6. Acid treatment of bentonite

Based on the experimental results, montmorillonite becomes effective after cation exchange apparently due to its ability to swell and delaminate. The question,

which remains to be answered regarding the reversibility of this process, is whether delaminated montmorillonite platelets in bentonite can stack up, if exposed to a strong acid, which will likely transform the sodium bentonite into the hydrogenated form. For this purpose, Bnt was treated with 0.5 M HCl before being used in PCC deposition experiments. The performance of the treated Bnt is compared with untreated Bnt in Fig. 5.7.

The untreated Bnt was most effective at the addition of 10 mg/g fiber. The effectiveness decreased with further Bnt additions as the system became overloaded with an excess of Bnt. Bentonite treated with 0.5 M HCl had a pH of 1.5 prior to addition to the suspension containing fibers, PCC and cPAM. The graph shows a maximum PCC deposition at the addition of 50 mg/g fiber, which is five times more than for the untreated Bnt. The deposition starts to decline at the addition of 100 mg/g fiber. However, these results may be misleading because Bnt became unstable and aggregated due to protonation of the edges at low pH [35]. This behavior is also reflected in the particle size measurements listed in Table 5.6. To redisperse Bnt treated with HCl, the pH of the suspension was adjusted to pH 7. The higher pH reversed the positive charge of the edges and provided enough electrostatic repulsion to prevent the edge-to-face coagulation. The curve in Fig. 5.7 shows a marked improvement in PCC deposition. However, the effectiveness was still well below that of the untreated Bnt (10 mg/g fiber).

The results in Table 5.6 are in accordance with the results in Fig. 5.7. The number of platelets in untreated Bnt was 34 compared to 40 nm for acid-treated Bnt

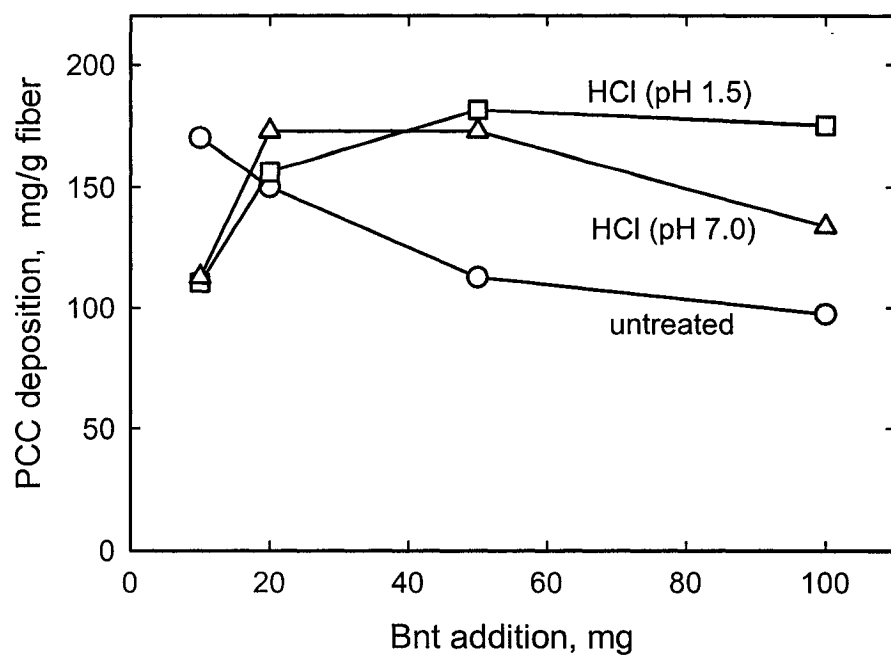


Fig. 5.7: Final PCC deposition as a function of addition of untreated Bnt and Bnt treated with 0.5 M HCl. The pH of the treated Bnt suspensions is indicated in parentheses.

Table 5.6: The number of platelets, n , for untreated Bnt and Bnt treated with 0.5 M HCl. The pH of the treated Bnt suspensions is indicated in parentheses. The radius of bentonite, a_d , is assumed to be 300 nm.

Chemical Treatment	ha_d (μm^2)	n
untreated	0.020	34
<i>HCl (pH 1.5) *</i>	<i>0.200*</i>	<i>333*</i>
HCl (pH 7.0)	0.024	40

*Bnt coagulates due to edge-to-face interactions. Therefore the presented numbers just merely indicate that the system is unstable and aggregates.

at pH 7. The acid activation of Bnt appears to increase the particle size of Bnt, which is in agreement with PCC deposition. However, the increase in number of platelets per stack does not seem to correspond with the pronounced effect on PCC deposition. A possible explanation is that the acid treatment strengthened the forces keeping these platelets together, while the actual stack thickness remained almost unchanged, and as a consequence, the ability of bentonite to delaminate was greatly reduced.

5.4.7. Elemental analysis

Untreated Mnt 200; Mnt 200 treated with 1 M NaCl and 1 M Na₂CO₃; Mnt 200 treated with 1 M NaCl, 1 M Na₂CO₃ and 0.5 M NaOH; and Mnt 200 treated with 0.5 M NaOH were analyzed for content of Na, Ca, Mg, Al and Si. The concentration of Ca, Mg, Al and Si in all four samples appears to be constant regardless of chemical treatment as it remains virtually unchanged. The changes in the concentration of Na are listed in Table 5.7. The amount of Na in untreated Mnt 200 was found to be 0.246%, which is about 7.5 times lower than the theoretical amount (~1.9%) based on the general montmorillonite formula. These results substantiate the original assumption that Mnt 200 had been treated with a strong acid, which removed most of the sodium ions, and consequently limited the montmorillonite swelling. The Na content in Mnt 200 treated with 1 M NaCl and 1 M Na₂CO₃ increased to 1.570%, which is very close to the theoretical amount. The Na contents in Mnt 200 treated with 1 M NaCl, 1 M Na₂CO₃ and 0.5 M NaOH and NaOH alone were 0.704% and 0.751%, respectively. This represents about one half of the theoretical amount.

Table 5.7: The sodium content in untreated Mnt 200; Mnt 200 treated with 1 M NaCl and 1 M Na₂CO₃; Mnt 200 treated with 1 M NaCl, 1 M Na₂CO₃ and 0.5 M NaOH; and Mnt 200 treated with 0.5 M NaOH.

Chemical treatment	Untreated	1 M NaCl 1 M Na ₂ CO ₃	1 M NaCl 1 M Na ₂ CO ₃ 0.5 M NaOH	0.5 M NaOH
Na content (%)	0.246	1.570	0.704	0.751

These results illustrate that the cation exchange treatment of montmorillonite with sodium-rich solutions can lead to an increase of Na in the montmorillonite structure. However, one discrepancy has to be noted. The Na content in Mnt 200 treated with salt only (i.e. 1 M NaCl and 1 M Na₂CO₃) was the highest, yet the PCC deposition and particle size measurements show that the extent of delamination was not as pronounced as for Mnt 200 which was exposed to NaOH. These findings may indicate that treatment with NaOH is more beneficial to delamination than using sodium-based salt solutions.

5.5. Conclusions

Two acid-treated montmorillonite products, which differed in particle size and surface area, showed no significant improvement in PCC deposition. After cation exchange with sodium salts and NaOH, both montmorillonite samples increased deposition of PCC on fibers dramatically. Particle size measurements indicated that montmorillonite partly delaminated after the cation exchange (especially when treated with NaOH), and this delaminated montmorillonite was much more effective during the PCC deposition on fibers. A high shear was applied to Clay and Mnt 20 treated with 1 M NaCl, 1 M Na₂CO₃ and NaOH, which did not appear to reduce the number of platelets per stack and also the deposition of PCC on fibers remained almost the same.

A microparticle systems containing kaolin clay had no significant effect on PCC deposition. Even after cation exchange treatment with sodium-rich solutions and NaOH, PCC deposition on fibers increased only marginally. The particle size

measurements showed that the size of clay remains almost constant, which is another proof that kaolin clays do not delaminate.

The deposition of PCC on pulp fibers was greatly improved with low additions of commercial bentonite. An acid treatment converted this bentonite into the hydrogenated form and increased the Bnt particle size. As a consequence, the effectiveness of Bnt during PCC deposition on fibers decreased.

The results presented in this study suggest that the flocculation efficiency of microparticles is related to their ability to swell and delaminate.

5. 6. Acknowledgements

The authors would like to thank to Ms Josée Tessier from Paprican at Pointe-Claire for performing the elemental analysis. Financial support from the Network of Centres of Excellence (NCE) for Mechanical-Wood Pulps and from Paprican/NSERC IRC is also greatly appreciated.

5.7. References

- [1] Bailey, S.W., "Summary of Recommendations of AIPEA Nomenclature Committee". *Clays Clay Miner.* **28**, 73 (1980).
- [2] Yamada, H., Nakazawa, H., Hashizume, H., Shimomura, S. and Watanabe, T., "Hydration Behaviour of Na-Smectite Crystals Synthesized at High Pressure and High Temperature". *Clays Clay Miner.* **42**(1), 77 (1994).
- [3] Suquet, H., de la Calle, C. and Pezart, H., "Swelling and Structure Organization of Saponite". *Clays Clay Miner.* **23**, 1 (1975).

- [4] Erdogan, B. and Demirci, S., "Activation of Some Turkish Bentonites to Improve Their Drilling Fluid Properties". *Appl. Clay Sci.* **10**, 401 (1996).
- [5] Volzone, C. and Garrido, L.B., "The Effect of Some Physico-Chemical and Mineralogical Properties on the Na₂CO₃ Activation of Argentine Bentonites". *Appl. Clay Sci.* **6**, 143 (1991).
- [6] Bishop, J.L., Pieters, C.M. and Edwards, J.O., "Infrared Spectroscopic Analysis on the Nature of Water in Montmorillonite". *Clays Clay Miner.* **42**(6), 702 (1994).
- [7] Hall, P.L. and Astill, D.M., "Adsorption of Water by Homoionic Exchange Forms of Wyoming Montmorillonite (SWY-1)". *Clays Clay Miner.* **37**(4), 355 (1989).
- [8] van Olphen, H., "An Introduction to Clay Colloid Chemistry", Interscience Publishers John Wiley & Sons, New York, London, (1963).
- [9] Benco, L., Tunega, D., Hafner, J. and Lischka, H., "Upper Limit of the O-H...H Hydrogen Bond. Ab Initio Study of the Kaolinite Structure". *J. Phys. Chem. B* **105**, 10812 (2001).
- [10] Cuadros, J., Delgado, A., Cardenete, A., Reyes, E. and Linares, J., "Kaolinite/Montmorillonite Resembles Beidellite". *Clays Clay Miner.* **42**(5), 643 (1994).
- [11] Langley, J.G. and Lichfield, E., "Papermaking Conference Proceedings, " Tappi Press, Atlanta, (1986).
- [12] Dickinson, E. and Eriksson, L., "Particle Flocculation by Adsorbing Polymers". *Adv. Colloid Interface Sci.* **34**, 1 (1991).

- [13] van de Ven, T.G.M., "Kinetic Aspects of Polymer and Polyelectrolyte Adsorption on Surfaces". *Adv. Colloid Interface Sci.* **48**, 121 (1994).
- [14] Swerin, A., Ödberg, L. and Wågberg, L., "An Extended Model for the Estimation of Flocculation Efficiency Factors in Multicomponent Flocculant Systems". *Colloids Surf. A* **113**, 25 (1996).
- [15] Covarrubias, R.M., Paracki, J. and Mirza, S., "New Advances in Microparticle Retention Technologies". *Appita J.* **55**(4), 272 (2002).
- [16] Swerin, A., Sjödin, U. and Ödberg, L., "Flocculation of Cellulosic Fibre Suspensions by Model Microparticulate Retention Aid Systems". *Nordic Pulp Paper Res. J.* **4**, 398 (1993).
- [17] Swerin, A. and Ödberg, L., "Flocculation of Cellulosic Fibre Suspensions by a Microparticulate Retention Aid System Consisting of Cationic Polyacrylamide and Anionic Montmorillonite". *Nordic Pulp Paper Res. J.* **1**, 22 (1996).
- [18] Swerin, A., Risinger, G. and Ödberg, L., "Shear Strength in Papermaking Suspensions Flocculated by Retention Aid Systems". *Nordic Pulp Paper Res. J.* **1**, 30 (1996).
- [19] Swerin, A., Risinger, G. and Ödberg, L., "Flocculation in Suspensions of Microcrystalline Cellulose by Microparticle Retention Aid Systems". *J. Pulp Paper Sci.* **23**(8), J374 (1997).
- [20] Asselman, T., Alince, B., Garnier, G. and van de Ven, T.G.M., "Mechanism of Polyacrylamide-Bentonite-Microparticulate Retention Aids". *Nordic Pulp Paper Res. J.* **15**(5), 515 (2000).

- [21] Asselman, T. and Garnier, G., "The Role of Anionic Microparticles in a Poly(acrylamide)-Montmorillonite Flocculation Aid Systems". *Colloids Surf. A* **170**, 79 (2000).
- [22] Wågberg, L., Björklund, M., Åsell, I. and Swerin, A., "On the Mechanism of Flocculation by Microparticle Retention-Aid Systems". *Tappi J.* **79**(6), 157 (1996).
- [23] Stamm, A.J., "Wood and Cellulose Science", Ronald Press, New York, (1964).
- [24] Alince, B., Bednar, F. and van de Ven, T.G.M., "Deposition of Calcium Carbonate Particles on Fiber Surfaces Induced by Cationic Polyelectrolyte and Bentonite". *Colloids Surf. A* **190**, 71 (2001).
- [25] Churchman, G.J. and Weissmann, D.A., "Separation of Sub-Micron Particles from Soils and Sediments without Mechanical Disturbance". *Clays Clay Miner.* **43**(1), 85 (1995).
- [26] Alince, B., Petlicki, J. and van de Ven, T.G.M., "Kinetics of Colloidal Particle Deposition on Pulp Fibers 1. Deposition of Clay on Fibers of Opposite Charge". *Colloids Surf.* **59**, 265-277 (1991).
- [27] Vanerek, A., Alince, B. and van de Ven, T.G.M., "Colloidal Behavior of Ground and Precipitated Calcium Carbonate Fillers: Effects of Cationic Polyelectrolytes and Water Quality". *J. Pulp Paper Sci.* **26**(4), 135-139 (2000).

- [28] Espantaleón, A.G., Nieto, J.A., Fernández, M. and Marsal, A., "Use of Activated Clay in Removal of Dyes and Surfactants Form Tannery Waste Waters". *Appl. Clay Sci.* **24**, 105 (2003).
- [29] Srasra, E., Bergaya, F., van Damme, H. and Ariguib, N.K., "Surface Properties of an Activated Bentonite - Decolorization of Rape-Seed Oils". *Appl. Clay Sci.* **4**, 411 (1989).
- [30] Mourad, W.E., "The Effect of Compaction on the Surface Characteristics of Activated Ventonite". *Surface Technology* **11**, 457 (1980).
- [31] Gates, W.P., Anderson, J.S., Raven, M.D. and Churchman, G.J., "Mineralogy of Bentonite from Miles, Queensland, Australia and Characterization of Its Activation Products". *Appl. Clay Sci.* **20**, 189 (2002).
- [32] Maurice, P.A., Hochella, M.F., Parks, G.A., Sposito, G. and Schwertmann, U., "Evolution of Hematite Surface Microtopography Upon Dissolution by Simple Organic Acids". *Clays Clay Miner.* **43**(1), 29 (1995).
- [33] Happel, J. and Brenner, H., "Low Reynolds Number Hydrodynamics with Special Applications to Particulate Media", Prentice-Hall, Inc., Englewood Cliffs, N.J., (1965).
- [34] Lagaly, G. and Ziesmer, S., "Colloid Chemistry of Clay Minerals: The Coagulation of Montmorillonite Dispersions". *Adv. Colloid Interface Sci.* **100**(102), 105 (2003).
- [35] Rand, B., Pekenc, E., Goodwin, J.W. and Smith, R.W., "Investigation into the Existence of Edge-Face Coagulated Structures in Na-Montmorillonite Suspensions". *J. Chem. Soc. Faraday I* **76**, 225 (1980).

Chapter 6

In Chapter 5, it was shown that delamination of montmorillonite resulted in a greater deposition of a mineral pigment on pulp fibers. Many researchers raised questions about complete delamination. Because of the thickness of montmorillonite platelets ($\sim 1\text{ nm}$), the delaminated microparticles are difficult to determine, especially in suspensions that contain pulp fibers, mineral pigment and cationic polyelectrolyte.

6.1. Abstract

Bentonite in combination with cationic polyacrylamide is used to incorporate mineral pigments into paper. It is believed that bentonite acts as a bridge between polymer-coated pulp fibers and pigment and its performance appears to be related to its ability to delaminate. The possibility of enhanced bentonite delamination induced by pulp fibers coated with cationic polyacrylamide was studied. The extent of bentonite delamination was evaluated by measuring the deposition of a calcium carbonate pigment on fibers suspended in water. When a mixture of polymer-treated fibers and bentonite is exposed to high shear before calcium carbonate addition, almost complete bentonite delamination takes place. At low shear, a similar delamination is achieved, but at a much longer stirring time. Adding bentonite to a mixture of untreated fibers, calcium carbonate and cationic polyacrylamide results only in partial delamination, and consequently, more bentonite is required to achieve the maximum calcium carbonate deposition. The results suggest that in this case the bentonite bridge contains on average four platelets.

6.2. Introduction

Bentonite is widely used in papermaking as part of two-component microparticulate retention aid system alongside with a cationic polyacrylamide (cPAM) [1]. The role of retention aid systems is to improve retention of fine particles, namely fines and mineral pigments, in paper. Since pulp fibers and most fillers are negatively charged when suspended in water, initial additions of cationic polyelectrolytes causes heteroflocculation by a polymeric bridging mechanism [2-4].

The system is then subjected to high shear generated by fan pumps and/or pressure screens which breaks up the flocs. Bentonite is introduced to the system at this point, which leads to reflocculation where bentonite acts as a bridge between polymer-coated surfaces of fibers, fines and pigments [5]. The exact flocculation mechanism in pulp suspensions using microparticulate retention aid systems is still unclear, but it is believed that the high surface charge density of bentonite platelets is the driving force for the interaction with the adsorbed cationic polyelectrolytes. The formation of bentonite bridges between polymer-covered surfaces of fibers and mineral pigment results in larger, more uniform and stronger flocs [6-9]. In addition, it has been shown that nonionic polyacrylamide is also capable of adsorbing on bentonite surfaces [6]. However, it is known that for the maximum efficiency, the amount of both bentonite and cationic polyacrylamide is limited. Too much of either component is detrimental. Excess of polymer means that all the components, i.e. fibers, pigment and bentonite become positively charged, and consequently, the bentonite particles fail to act as a bridge. Excess of bentonite means that fibers become fully coated with bentonite and thus will not attract negatively charged pigment, which may also be coated with bentonite. The optimum amount of bentonite may differ depending on its degree of delamination into single platelets. The main advantage of using microparticle retention aids in paper manufacturing is that the bentonite-induced flocculation increases simultaneously sheet drainage and pigment retention [10], which for most other retention aids negatively affect one another.

Bentonite is composed mainly of *montmorillonite* (~90%). A single montmorillonite platelet is composed of three layers where one octahedral aluminum-

oxygen layer placed between two tetrahedral silicon-oxygen layers with an interlayer spacing of 9.1 Å [11]. The sheets can stack up on top of each other to form large stacks. The general chemical formula of montmorillonite is $A_{0.6}Al_{2.6}Mg_{1.4}Si_8O_{20}(OH)_4$, where A represents adsorbed cations such as Na^+ , K^+ and $0.5Ca^{2+}$. The presence of these adsorbed cations is a result of isomorphous substitution during which some tetravalent Si^{4+} cations in the tetrahedral layers are replaced with trivalent Al^{3+} cations, and Al^{3+} cations in the octahedral layers are replaced with divalent Mg^{2+} cations. The adsorbed cations in the interlayer spacing also provide montmorillonites with an extremely high cation exchange capacity (CEC) of around 100 µeq/g [11] and increase the interlayer spacing to 9.6 Å [11]. The presence of these adsorbed cations also greatly affects the ability of montmorillonite to swell [12, 13]. Heat dehydration is also a function of the specific cations and the amount of water loss decreases in the order $Mg > Ca > Fe > Na$ [14, 15].

Wågberg et al. [5] reported a maximum deposition of centrifuged bentonite onto cPAM-treated fibers to be around 1.5 mg/g fibers. This result is close to the theoretical predictions for completely delaminated bentonite platelets having a thickness of 1 nm and a total surface area of 800 m²/g depositing randomly onto fibers with an external surface area of 1 m²/g [16]. Alince et al. [17] reported a maximum bentonite deposition on cPAM-pretreated fibers of around 120 mg/g fibers, which is extremely large even when accounting for filler-like impurities. From these experimental observations, it was concluded that in the former case, bentonite must have deposited in the form of single platelets while in the latter case, bentonite deposited in the form of stacks of platelets.

In its role as a bridging agent, bentonite performance appears to be related to its ability to delaminate [18]. However, the extent of bentonite delamination is extremely difficult to determine in complex papermaking suspensions. The intent here is to investigate the possibility of more effective bentonite delamination using fibers which were pretreated with cPAM. To evaluate its performance, the extent of bentonite delamination is monitored by calcium carbonate deposition on these pretreated fibers. This is compared with the deposition under conventional procedure where bentonite is added to a suspension containing fibers, calcium carbonate pigment and cPAM.

6.3. Experimental

6.3.1. Materials

Dry, softwood, bleached, kraft pulp Q90 from Domtar was used. The pulp was immersed overnight in deionized water and then disintegrated in the Standard British Disintegrator using a total of 12,000 revolutions. Fines were removed by intensive washing of the pulp through a 100-mesh screen. The pulp was then diluted with tap water to a concentration of 2 g/L. Prior to deposition experiments, 500 cm³ of pulp slurry (1 g fiber) was poured over a 200-mesh screen to separate the fibers. The fibers were then transferred into a Waring blender already containing 500 cm³ of fresh tap water.

Precipitated calcium carbonate (PCC) Albacar HO from Specialty Minerals was used as a mineral pigment in the deposition experiments. The pigment was scalenohedral-shaped calcite with an average particle size of 1.3 µm and a surface

area of $12 \text{ m}^2/\text{g}$. A stock suspension of PCC was prepared in tap water to a concentration of 50 g/L . PCC dispersed in tap or white waters becomes negatively charged due to adsorption of impurities and the electrophoretic mobility of both was determined to be $-2 \times 10^{-8} \text{ m}^2 \text{ s}^{-1} \text{ V}^{-1}$ [19]. During deposition experiments, 4 mL of the stock suspension (i.e. 200 mg) was added to the fibers already suspended in the Waring blender.

A microparticulate retention aid system consisting of a cationic polyacrylamide (cPAM) Percol 63 and bentonite Hydrocol 2D7 were obtained from CIBA Specialty Chemicals Canada Inc. The commercial cPAM is a random copolymer of polyacrylamide with (N,N,N-trimethyl) aminoethyl chloride acrylate. The positive charge of cPAM originates from the quaternary amino groups. The degree of substitution of the polyacrylamide (i.e. substitution with positive amino groups) was 40% and the molecular weight was 6 MDa . A stock solution of cPAM was prepared in deionized water at a concentration of 1 g/L . Since the positively charged groups are unstable and hydrolyze at $\text{pH} \geq 7$ [20-22], the pH of the stock cPAM solution was adjusted to a pH of 5.5 with 0.1 M HCl .

Bentonite suspensions were prepared in deionized water at a concentration of 1 g/L . Bentonite was allowed to swell and equilibrate overnight prior to deposition experiments. Some of the bentonite suspensions were fractionated using International Centrifuge, Model K from IEC at a speed of 1000g for 30 min . Two fractions were obtained by centrifugation: (i) a high surface area (HSA) and (ii) low surface area (LSA).

6.3.2. Deposition of PCC on fibers

Deposition experiments consisted of adding 200 mg of PCC to a suspension consisting of 1 g of fibers in 500 cm³ of tap water. The suspension was agitated in a Waring blender at 1500 rpm using a propeller with rounded edges which prevented damage to the fibers. After 30 s of stirring, a sample of supernatant was collected using a syringe equipped with a special tip utilizing a 200-mesh screen. The screen prevented fibers from entering the syringe. After the supernatant sample was collected, 2 mg of cPAM was added and allowed to interact with the fibers and pigment for 15 s followed by another collection of the supernatant. The stirring rate was then increased to 5000 rpm and the microparticles were added. The last supernatant sample was collected 5 s after the microparticulate addition. The content of PCC in the supernatant was then determined from light transmittance using a spectrophotometer (Spectronic 20, Bausch&Lomb) at a wavelength of 500 nm. Each supernatant sample was sonicated prior to the light transmittance measurement for 30 s in an Ultrasonic Cleaner (Cole-Parmer) at a sound frequency of 40 kHz. Sonication was used as a means of breaking up PCC aggregates, formed after the polymer and microparticles were added, into individual particles. This allowed for all PCC samples from different addition points to be compared to a single calibration curve for well dispersed PCC. The increase in agitation from 1500 to 5000 rpm was aimed to simulate industrial conditions where after a retention aid is added to pulp furnish, the furnish is subjected to high shear by fan pumps and/or pressure screens. Following the shear exposure, the microparticles are introduced. The experimental procedure is summarized in Fig. 6.1.

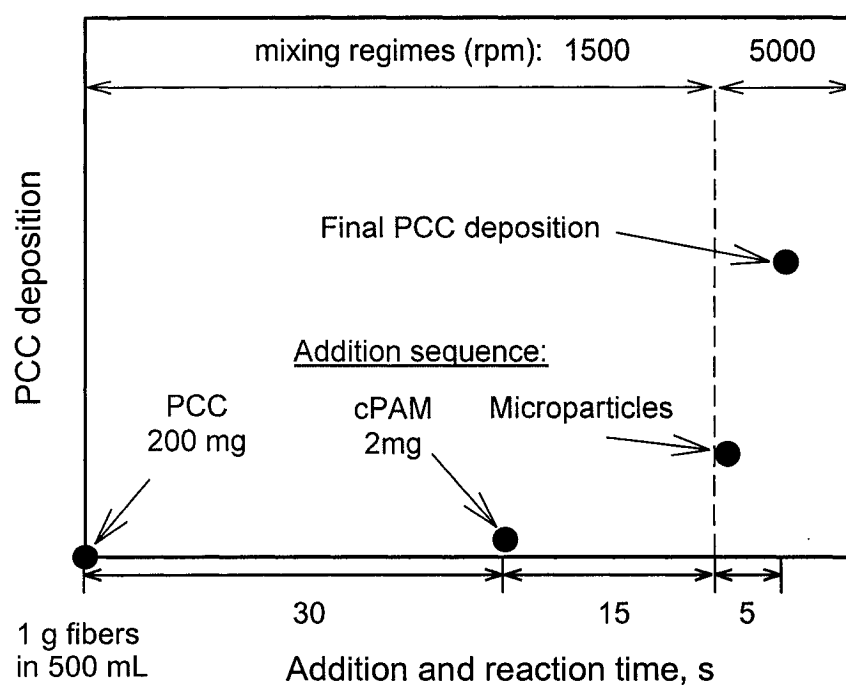


Fig. 6.1: Summary of the experimental procedure. A suspension of 1 g of fibers dispersed in 500 cm³ of tap water was stirred at 1500 rpm. At given intervals 200 mg of PCC, 2 mg of cPAM were added and supernatant samples were collected. The speed of stirring was increased to 5000 rpm followed by bentonite addition and supernatant sampling 5 s after the bentonite addition.

6.3.3. Deposition of PCC on fibers pretreated with cPAM and bentonite

The cationic polymer at a concentration of 10 mg/g fiber was allowed to adsorb on 1 g of fibers suspended in 500 cm³ of deionized water for a period of 5min. The suspension was agitated by a paddle stirrer (Phipps & Bird) operating at a speed of 100 rpm. The pH of all water used during pretreatment and washing was always adjusted to 5.5, which prevented cPAM hydrolysis during fiber pretreatment. After the cPAM adsorption, the excess of polymer was removed by washing the fibers through a 200-mesh screen with deionized water. The fibers treated with cPAM were then drained and 1 g of fibers was redispersed in 500 cm³ of deionized water followed by an appropriate bentonite addition. The polymer-treated fibers were exposed to bentonite for a period of 15 s. For two fiber suspensions, which contained the same amount of bentonite, one suspension was stirred at 100 rpm using the paddle stirrer and the second suspension was agitated at 5000 rpm using a Waring blender. Next, the excess of bentonite was removed following the same procedure as in the case of fiber treatment with cPAM. Fibers pretreated with cPAM and bentonite were again redispersed in 500 cm³ of fresh tap water, and 200 mg of PCC was introduced and allowed to deposit. The speed of agitation during PCC deposition on pretreated fibers was maintained constant for all experiments at 100 rpm using the paddle stirrer.

6.4. Results and discussion

6.4.1. Deposition of PCC on fibers

Addition of bentonite to the system consisting of fibers, mineral pigment and cPAM caused an increase in PCC deposition at a high shear rate (5000 rpm). The highest deposition was achieved with the bentonite addition of 10 mg/g fiber (see Fig. 6.2). Further bentonite additions led to lower PCC depositions. This can be explained by limitations in the available surface area. Because of their small size and large surface area ($\sim 800 \text{ m}^2/\text{g}$ for fully delaminated bentonite), even low bentonite additions contain a large number of particles. If added in excess, bentonite begins to cover most of the cPAM-coated surfaces on fibers and the pigment, which results in electrostatic repulsion between bentonite-covered surfaces. Consequently, a smaller surface area with the adsorbed cPAM remains available for flocculation, and thus PCC deposition decreases. This is exactly the case for bentonite additions of 50 and 100 mg/g fiber. At low bentonite additions, too few bentonite particles may be present, which also results in a lower degree of flocculation, and hence lower PCC deposition (bentonite additions of 1 and 5 mg/g fiber).

6.4.2. PCC deposition on fibers using fractionated bentonite

Although the main component of bentonite is montmorillonite, non-swelling impurities such as illite, kaolinite, calcite, anatase, hematite, feldspar, quartz, etc., can also be present [23]. The amount of impurities will depend on the origin of a particular bentonite. The bentonite used in this study contained around 10% of non-swelling material, which was determined by a BI-DCP Disc Centrifuge Particle Size

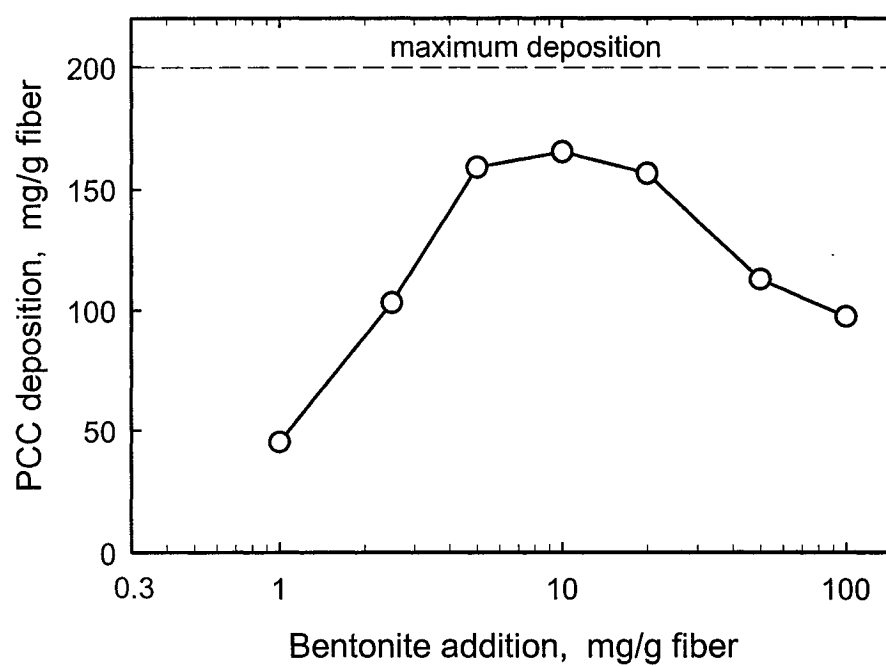


Fig. 6.2: PCC deposition on fibers using a microparticulate retention aid system consisting of 2 mg/g fiber cPAM and various amounts of bentonite. The graph shows the final PCC deposition, i.e. 5 s after bentonite addition.

Analyzer from Brookhaven Instruments Corporation. In order to investigate the effect of non-swelling contaminants on PCC deposition, a suspension of bentonite was fractionated by centrifugation to obtain a high surface area (HSA) and low surface area (LSA) bentonite fractions.

The results in Fig. 6.3 show the difference in PCC deposition using HSA bentonite, which most likely consists almost entirely of montmorillonite, and LSA fraction, which mainly consists of non-swelling impurities. The deposition of PCC using the HSA bentonite is reminiscent of the PCC deposition using un-fractionated bentonite (cf. Fig. 6.2) except, the peak appears to be narrower and more PCC was found to deposit on fibers for bentonite additions of 5, 10 and 20 mg/g fiber. The maximum PCC deposition was also found for the bentonite addition of 10 mg/g fiber. Lower PCC depositions at additions above and below 10 mg/g fiber indicate either excess or lack of bentonite, respectively.

Unlike in the case of HSA bentonite, the deposition of PCC using LSA bentonite is initially very low and starts to increase only after the addition of 20 mg/g fiber. The addition of 100 mg/g fiber of LSA bentonite results in high PCC deposition that is comparable to that of 5 mg/g fiber of HSA bentonite. These results suggest that LSA bentonite is a less effective bridging agent when bridging polymer-covered surfaces between fibers and PCC, which also appears to be in good agreement with a previous study [18] where non-delaminated montmorillonite was less effective in PCC deposition than delaminated montmorillonite. Since during the bentonite fractionation, a decantation technique was used to separate HSA fraction from LSA sediment, it is very likely that the LSA fraction is contaminated by a small amount of

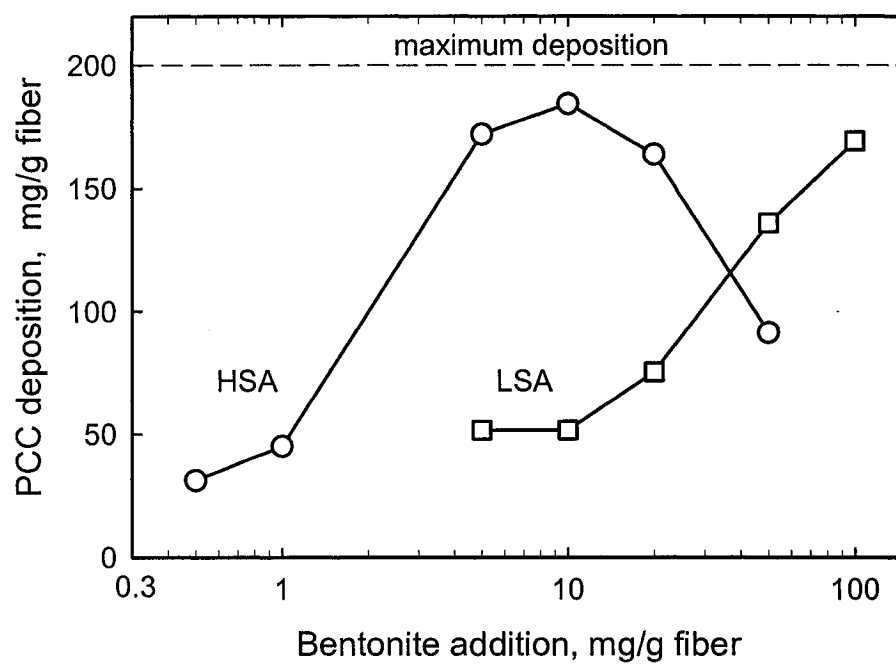


Fig. 6.3: Final PCC deposition on fibers (i.e. 5 s after bentonite addition) using high surface area (HSA) and low surface area (LSA) bentonite fractions. The cPAM concentration was 2 mg/g fiber.

HSA bentonite. In this case, it appears that around 5% HSA bentonite was present in LSA fraction. Based on these observations, one can conclude that non-swelling impurities in the bentonite fraction, in fact, do not contribute to PCC deposition; only the HSA fraction containing delaminated montmorillonite is efficient in bridging cPAM-coated fibers and PCC.

6.4.3. PCC deposition on fibers pretreated with cPAM and HSA bentonite

It has been shown that bentonite can partly delaminate under favorable conditions [18, 24]. However, the extent of delamination is extremely difficult to determine in complicated papermaking suspensions. The intent here is to investigate indirectly the possibility of delamination of bentonite by fibers which were pretreated with cPAM.

The results in Fig. 6.4 show the kinetics of PCC deposition on fibers pretreated with cPAM and bentonite at 100 rpm. The highest PCC deposition was observed for a system consisting of fibers pretreated with cPAM only (i.e. 0 mg bentonite). The maximum PCC deposition occurred between 3 and 5 min reaching around 170 mg/g fiber. Beyond the 5 minute period, the PCC particles start to detach from the fibers most likely due to polymer rearrangement and polymer transfer from fibers to PCC [25-27]. Bentonite inclusion in the fiber pretreatment resulted in a lower PCC deposition. This behavior is expected because bentonite deposits onto cPAM-treated fibers and blocks the polymer-covered areas otherwise available for PCC deposition (see Fig. 6.5). Since both PCC and bentonite are negatively charged,

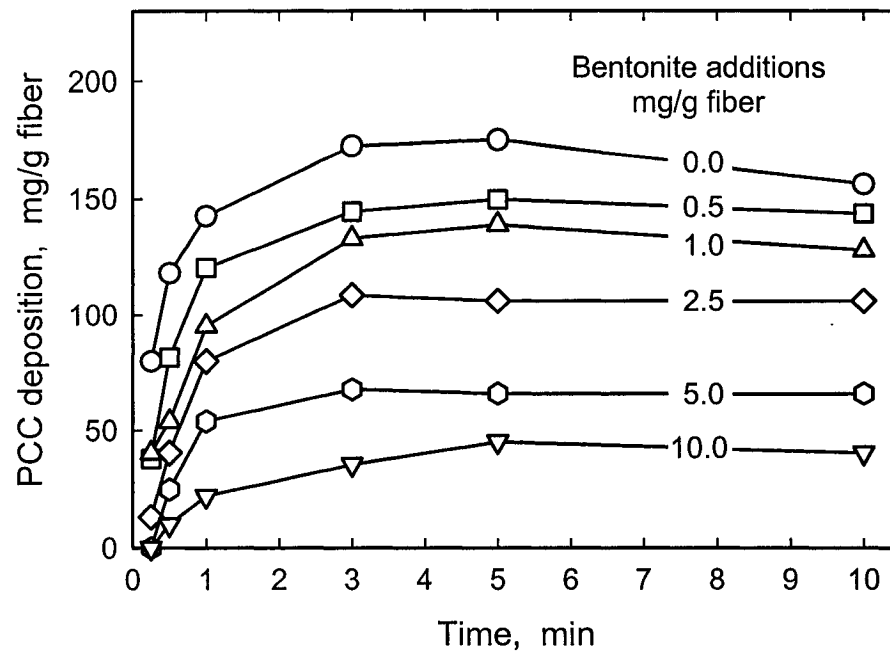


Fig. 6.4: Kinetics of PCC deposition on fibers pretreated with cPAM and various amounts of HSA bentonite. The speeds of stirring during both fiber pretreatment with bentonite and PCC deposition were 100 rpm.

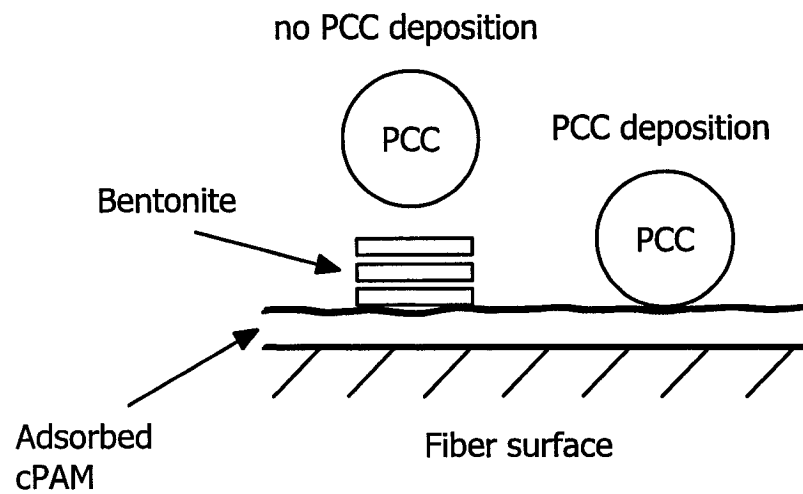


Fig. 6.5: Bentonite blocks the surface of cPAM-treated fibers, and hence, prevents PCC deposition.

PCC cannot deposit on top of the bentonite layer due to electrostatic repulsion, and therefore remains in the supernatant [17, 28].

The deposition of PCC on fibers pretreated with cPAM and bentonite at 5000 rpm is shown in Fig. 6.6. The PCC deposition on fibers pretreated with cPAM only (i.e. 0 mg bentonite) at 5000 rpm is similar to PCC deposition on fibers pretreated with cPAM only (i.e. 0 mg bentonite) at 100 rpm. The difference in shear during the fiber pretreatment does not appear to affect PCC deposition; both curves in Fig. 6.4 and Fig. 6.6 appear to be almost identical. Therefore, these results suggest that the pre-adsorbed polymer was not damaged by the increase in stirring from 100 rpm to 5000 rpm during fiber pretreatment.

The major difference in PCC deposition becomes evident with the addition of bentonite. The PCC deposition on fibers pretreated with bentonite at 5000 rpm is significantly lower than those pretreated at 100 rpm.

6.4.4. Delamination of HSA bentonite induced by fibers pretreated with cPAM

The PCC deposition on fibers pretreated with cPAM and bentonite shows a dependence on the rate of stirring during fiber pretreatment. In order to better illustrate this dependence, the deposition of PCC on pretreated fibers as a function of bentonite addition for the low and high shear rates is summarized in Fig. 6.7. Maximum PCC deposition, in this case, represents the maximum observed value (i.e. PCC deposition after 5 min) during investigation of the kinetics of PCC deposition on fibers (cf. Fig 6.4, 6.6). Figure 6.7 shows a gradual decrease in PCC deposition on pretreated fibers with cPAM and bentonite at the low shear rates (100 rpm). This

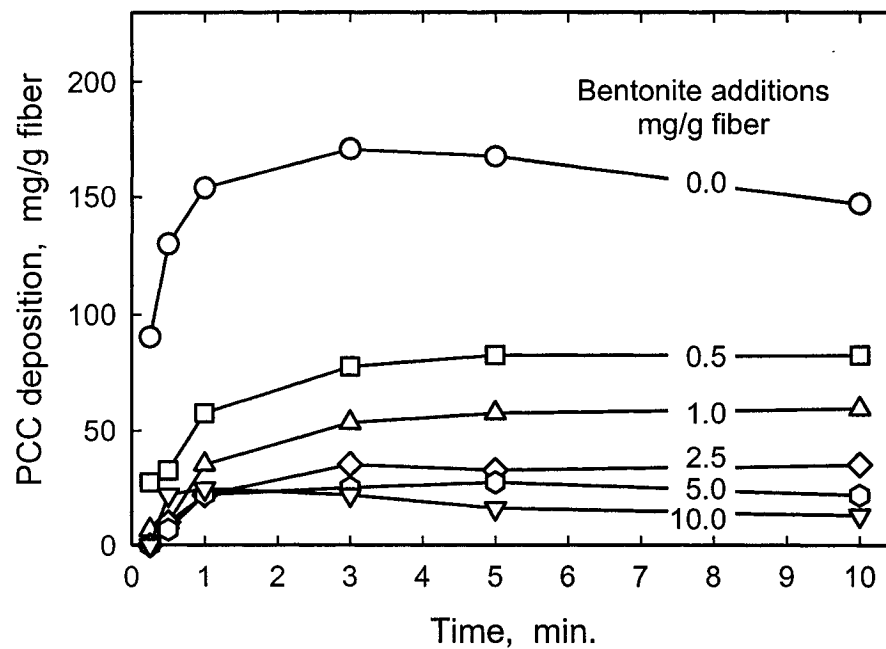


Fig. 6.6: Kinetics of PCC deposition on fibers pretreated with cPAM and various amounts of HSA bentonite. The speeds of stirring during fiber pretreatment with bentonite and during PCC deposition were 5000 rpm and 100 rpm, respectively.

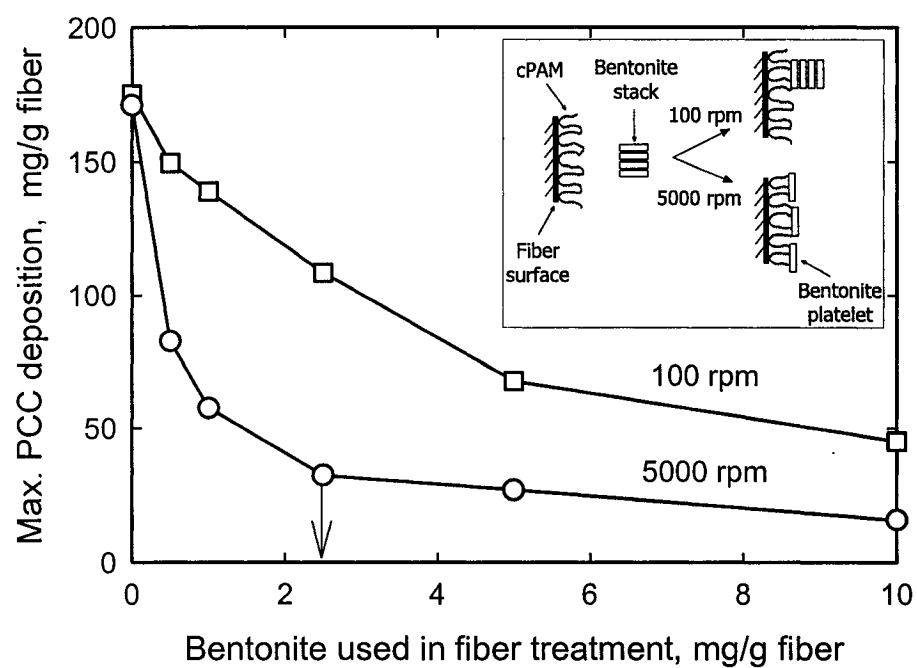


Fig. 6.7: Maximum PCC deposition on fibers pretreated with cPAM and HSA bentonite. After bentonite was added, fibers coated with cPAM were subjected to either a low shear (100 rpm) or a high shear (5000 rpm). The arrow indicates monolayer coverage of bentonite on cPAM-treated fibers (~2.5 mg/g fiber).

decrease in PCC deposition is due to the blocking action of bentonite during its deposition on fiber surfaces already covered with cPAM (see Fig. 6.5). The fiber surface with the adsorbed polymer, which is now covered with bentonite, becomes thus inaccessible to PCC particles. The same mechanism applies to fibers pretreated with bentonite at high shear rate (5000 rpm). However, the data show a sharp decrease in PCC deposition at already low bentonite additions. Assuming that the bentonite blocking of the fiber surfaces is the only mechanism leading to low PCC deposition, the results suggest that at high stirring rates, a much lower amount of bentonite is required to cover the cPAM-coated fiber surface and, consequently, prevent PCC deposition. The addition of 2.5 mg/g fiber was found to be a critical bentonite concentration beyond which PCC deposition remained almost unchanged. It should also be noted that PCC deposition was never reduced to zero. A small amount of PCC (~15 mg/g fiber) seems to deposit on fibers, even though the fibers are protected by a monolayer of bentonite platelets. This might be caused by the weak charge of PCC particles dispersed in tap water [19].

These findings may indicate that bentonite delaminated completely in the presence of cPAM-coated fibers at high shear rates. The critical bentonite addition of 2.5 mg/g fiber is very close to the theoretical value as well as to the value of 1.5 mg/g fiber obtained by Wågberg et al. [5], who also used fractionated bentonite. To explain this delamination phenomenon, one has to assume that at low bentonite additions, bentonite stacks deposit only on a fraction of the fiber surface while there is still a large surface area unoccupied by bentonite, and hence available for bentonite deposition. Since there is no free bentonite in the supernatant, the only bentonite

which can deposit on the available surface is the one that is already attached to another fiber. This leads to flocculation of the fiber suspension, which was also experimentally observed. The bridging of fibers by bentonite particles occurs as the fibers collide in a turbulent flow. However, the fibers tend to separate due to hydrodynamic forces acting upon them. These forces are transferred to the bentonite stacks, which bridge the fibers together. Based on the experimental results, it appears that the forces created by the parting fibers on the bentonite cause the bentonite stacks to delaminate rather than detach from the fiber surfaces. The feasibility of bentonite delamination is also substantiated by results obtained in a previous study, which showed that montmorillonite stacks can partly delaminate under favorable conditions without the use of any external forces [18].

Delamination at the low shear rate (100 rpm) is also expected. However, due to kinetic effects, delamination of bentonite occurs at a much slower rate. A proof of this phenomenon is shown in Fig. 6.8. In this case, a constant bentonite addition of 2.5 mg/g fiber was introduced to cPAM-treated fibers, and the speed of stirring was maintained also constant at 100 rpm. The bentonite was then allowed to interact with the fibers for various times ranging from 5 s to 20 min. The data in Fig. 6.8 clearly show that PCC deposition decreases as the bentonite reaction time with cPAM-treated fibers increases. With increasing interaction times between cPAM-treated fibers and bentonite, more bentonite stacks get progressively delaminated by fiber-fiber collisions and departures, which eventually leads to the formation of a monolayer of bentonite platelets on top of the cPAM-treated fibers.

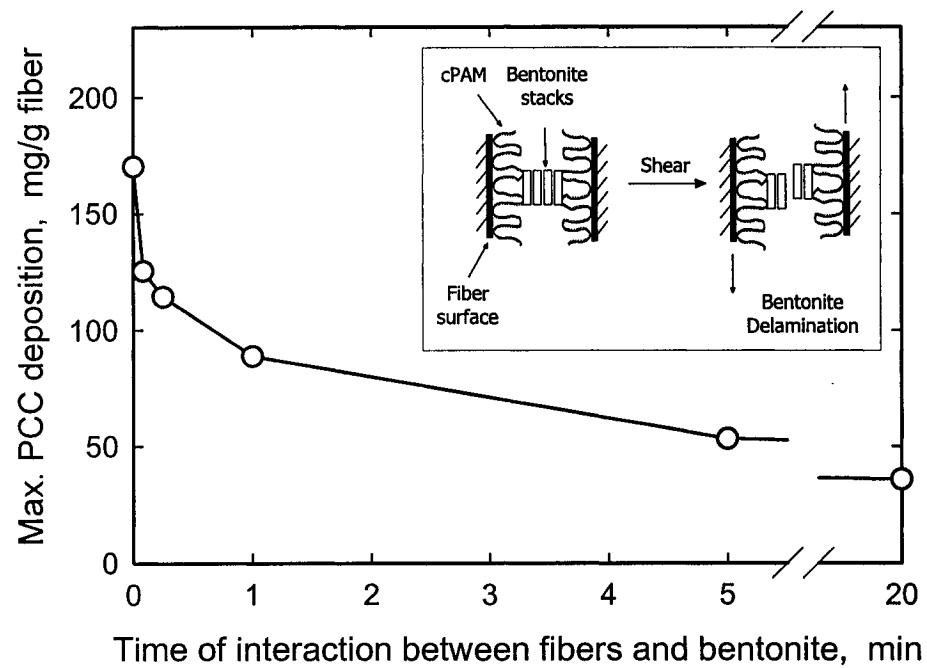


Fig. 6.8: Maximum PCC deposition on pretreated fibers with cPAM and HSA bentonite. During fiber pretreatment, the addition of bentonite and the stirring speed were kept constant at 2.5 mg/g fibers and 100 rpm, respectively.

The last aspect that may influence PCC deposition on cPAM-treated fibers is the reconfiguration of polymer chains adsorbed on the fiber surfaces. A high molecular weight cPAM with low charge density is known to adsorb in an extended conformation with a large number of loops and tails, but with time, the polymer tends to adopt a flatter conformation [29]. This alone could have a potential influence on PCC deposition. For this reason, two experiments aimed to investigate the reconfiguration effects were performed. The first experiment included extended periods of mixing of pretreated fibers with cPAM alone (i.e. 0 mg bentonite) prior to PCC additions. The mixing of the cPAM-treated fiber suspensions was performed at 100 rpm and ranged from 5 s to 30 min. The maximum PCC deposition on these pretreated fibers was found to be independent of the prestirring times with an average PCC deposition of around 170 mg/g fiber. The second experiment consisted of prestirring the cPAM-treated fibers prior to bentonite additions. The fibers were pre-stirred at a speed of 100 rpm for 10 min before bentonite was introduced to the system and allowed to interact with the fibers for 15 s. The maximum PCC deposition was compared to conventional experiments (i.e. without pre-stirring), and again the two sets of experiments showed very little disparity. Furthermore, Einarson et al. [29] measured the reconfiguration time of cPAM on cellulose fibers and found it to be around 1 min. During the fiber pretreatment, cPAM was allowed to adsorb on the fibers for a period of 5 min before the excess was removed. It is possible that the polymer had already adopted a flatter conformation, which further remained unchanged. In addition, the polymer additions used during the fiber pretreatment were high at 10 mg/g fiber. This high polymer concentration (~ ten times more than

monolayer coverage) forces the polymer to adsorb in an extended conformation with a part of the molecule adsorbed on the fiber surface and a part extending into solution. Due to the presence of numerous neighboring cPAM molecules adsorbed on the fiber surfaces, the reformation or flattening of the polymer loops and tails may therefore be limited, as there is no room for the adsorbed polymer to rearrange. This phenomenon was observed by van de Ven and Aline [30], who studied polyethylene oxide adsorption on clay particles.

6.4.5. Delamination of HSA bentonite during PCC deposition

Deposition of PCC on fibers, when bentonite is added to the suspension containing fibers, PCC and cPAM (in the Waring blender at 5000 rpm), reached a maximum at a bentonite addition of 10 mg/g fiber (cf. Fig. 6.2, 6.3). On the other hand, experiments involving fiber pretreatment with cPAM and bentonite revealed that monolayer coverage of bentonite on fibers occurs at a bentonite addition of 2.5 mg/g fiber (cf. Fig. 6.7). The results seem to suggest that bentonite added to a suspension of fibers, PCC and cPAM, which was stirred at 5000 rpm in the Waring blender, did not delaminate completely, but remained in the form of stacks containing on average four platelets provided that bentonite deposits on fibers first. This assumption is based on Smoluchowski theory [31] according to which bentonite first deposits on fibers due to the fact that the volume fraction of fibers is much larger than the volume fraction of the pigment.

In order to investigate the kinetics of bentonite delamination, PCC deposition at 5000 rpm was compared to PCC deposition in the Waring blender at 1500 rpm (i.e.

no increase in the speed of stirring before the bentonite addition). The results are shown in Fig. 6.9. Unlike at 5000 rpm, the final PCC depositions at 1500 rpm are nearly complete (i.e. all 200 mg PCC deposited) for bentonite additions of 5, 10 and 20 mg/g fiber. This is mainly due to the lower shear rate at 1500 rpm which affects the rates of attachment and detachment of PCC particles. In this particular case, the shear appears to reduce the particle detachment as more PCC particles remain attached to the fibers. Although it is not immediately obvious from this graph because of the logarithmic scale, the optimum bentonite addition also appears to be slightly higher around 13 mg/g fiber, which would represent bentonite stacks that contain on average five platelets. This result appears to be consistent with a lower degree of delamination at lower shear rates due to fewer particle-particle collisions leading to successful bentonite delamination. However, the combined effects of lower shear rate and increased PCC deposition make a precise comparison of the optimum bentonite addition at 1500 rpm and 5000 rpm very difficult.

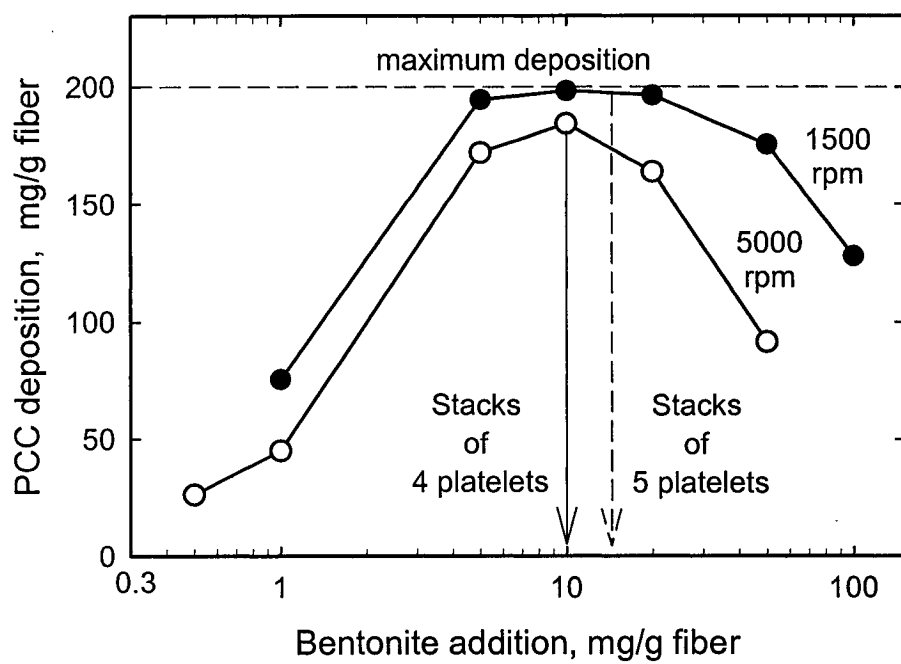


Fig. 6.9: Final PCC deposition on fibers using HSA bentonite at 1500 rpm and 5000 rpm.

6.5. Conclusions

A microparticulate retention aid system comprising a cationic polyacrylamide and bentonite significantly improved PCC deposition on pulp fibers. The most effective bentonite addition introduced to 500 cm³ of suspension consisting of 1 g of fibers, 200 mg of PCC and 2 mg of cPAM was determined to be 10 mg. The bentonite was then fractionated by centrifugation and high surface area (HSA) and low surface area (LSA) bentonite fractions were obtained. The HSA fraction behaved similarly as the un-fractionated bentonite. The LSA bentonite appeared ineffective in PCC deposition; the deposition was improved by HSA bentonite, which was present in the LSA fraction as impurities at a content of around 5%.

Delamination of bentonite was studied by pretreating the pulp fibers with cPAM and bentonite before PCC was added. The results for cPAM-treated fibers with bentonite at high shear suggested rapid bentonite delamination with a monolayer coverage of around 2.5 mg/g fiber. The actual delamination of bentonite occurred when fibers were pushed apart due to hydrodynamic shear and caused delamination of bentonite which acted as a bridge between the fibers. A similar degree of bentonite delamination induced by fibers was also observed at the low shear. However, prolonged stirring times were required.

Since the highest PCC deposition occurred at an addition of 10 mg/g fiber of HSA bentonite and the bentonite monolayer coverage of fiber surfaces was found to be 2.5 mg/g fiber, it was estimated that during the PCC deposition experiments performed at 5000 rpm, bentonite was in the form of stacks containing on average four platelets.

6.6. Acknowledgments

Financial support from the Network of Centres of Excellence (NCE) for Mechanical-Wood Pulps and from Paprican/NSERC IRC is also greatly appreciated.

6.7. References

- [1] Langley, J.G. and Lichfield, E., "Dewatering Aid for Paper Applications", Papermaking Conference Proceedings, Tappi Press, Atlanta, (1986).
- [2] Dickinson, E. and Eriksson, L., "Particle Flocculation by Adsorbing Polymers". *Adv. Colloid Interface Sci.* **34**, 1 (1991).
- [3] van de Ven, T.G.M., "Kinetic Aspects of Polymer and Polyelectrolyte Adsorption on Surfaces". *Adv. Colloid Interface Sci.* **48**, 121 (1994).
- [4] Swerin, A., Ödberg, L. and Wågberg, L., "An Extended Model for the Estimation of Flocculation Efficiency Factors in Multicomponent Flocculant Systems". *Colloids Surf. A* **113**, 25 (1996).
- [5] Wågberg, L., Björklund, M., Åsell, I. and Swerin, A., "On the Mechanism of Flocculation by Microparticle Retention-Aid Systems". *Tappi J.* **79**(6), 157 (1996).
- [6] Swerin, A., Sjödin, U. and Ödberg, L., "Flocculation of Cellulosic Fibre Suspensions by Model Microparticulate Retention Aid Systems". *Nordic Pulp Pap. Res. J.* **4**, 398 (1993).
- [7] Swerin, A. and Ödberg, L., "Flocculation of Cellulosic Fibre Suspensions by a Microparticulate Retention Aid System Consisting of Cationic

- Polyacrylamide and Anionic Montmorillonite". *Nordic Pulp Pap. Res. J.* **1**, 22 (1996).
- [8] Swerin, A., Risinger, G. and Ödberg, L., "Shear Strength in Papermaking Suspensions Flocculated by Retention Aid Systems". *Nordic Pulp Pap. Res. J.* **1**, 30 (1996).
- [9] Swerin, A., Risinger, G. and Ödberg, L., "Flocculation in Suspensions of Microcrystalline Cellulose by Microparticle Retention Aid Systems". *J. Pulp Pap. Sci.* **23**(8), J374 (1997).
- [10] Covarrubias, R.M., Paracki, J. and Mirza, S., "New Advances in Microparticle Retention Technologies". *Appita J.* **55**(4), 272 (2002).
- [11] van Olphen, H., "An Introduction to Clay Colloid Chemistry", Interscience Publishers John Wiley & Sons, New York, London, (1963).
- [12] Erdogan, B. and Demirci, S., "Activation of Some Turkish Bentonites to Improve Their Drilling Fluid Properties". *Appl. Clay Sci.* **10**, 401 (1996).
- [13] Volzone, C. and Garrido, L.B., "The Effect of Some Physico-Chemical and Mineralogical Properties on the Na₂CO₃ Activation of Argentine Bentonites". *Appl. Clay Sci.* **6**, 143 (1991).
- [14] Bishop, J.L., Pieters, C.M. and Edwards, J.O., "Infrared Spectroscopic Analysis on the Nature of Water in Montmorillonite". *Clays Clay Min.* **42**(6), 702 (1994).
- [15] Hall, P.L. and Astill, D.M., "Adsorption of Water by Homoionic Exchange Forms of Wyoming Montmorillonite (SWY-1)". *Clays Clay Min.* **37**(4), 355 (1989).

- [16] Stamm, A.J., "Wood and Cellulose Science", Ronald Press, New York, (1964).
- [17] Alince, B., Bednar, F. and van de Ven, T.G.M., "Deposition of Calcium Carbonate Particles on Fiber Surfaces Induced by Cationic Polyelectrolyte and Bentonite". *Colloids Surf. A* **190**, 71 (2001).
- [18] Vanerek, A., Alince, B. and van de Ven, T.G.M., "Delamination and Flocculation Efficiency of Sodium-Activated Kaolin and Montmorillonite". *to be published*.
- [19] Vanerek, A., Alince, B. and van de Ven, T.G.M., "Colloidal Behaviour of Ground and Precipitated Calcium Carbonate Fillers: Effects of Cationic Polyelectrolytes and Water Quality". *J. Pulp Pap. Sci.* **26**(4), 135 (2000).
- [20] Mabire, F., Audebert, R. and Quivoron, C., "Synthesis and Solution Properties of Water Soluble Copolymers Based on Acrylamide and Quaternary Ammonium Acrylic Comonomer". *Polymer* **25**, 1317 (1984).
- [21] Aksberg, R. and Wågberg, L., "Hydrolysis of Cationic Polyacrylamides". *J. Appl. Polym. Sci.* **38**, 297 (1989).
- [22] Kamiti, M. and van de Ven, T.G.M., "Impinging Jet Studies of the Kinetics of Deposition and Dissolution of Calcium Carbonate Particles". *Colloids Surf. A* **100**, 117 (1995).
- [23] Bulandr, J. and Dudek, J., "Mechanical Processing of Bentonites". *Ceramics International* **9**(4), 132 (1983).

- [24] Churchman, G.J. and Weissmann, D.A., "Separation of Sub-Micron Particles from Soils and Sediments without Mechanical Disturbance". *Clays Clay Min.* **43**(1), 85 (1995).
- [25] Asselman, T. and Garnier, G., "Mechanism of Polyelectrolyte Transfer During Heteroflocculation". *Langmuir* **16**, 4871 (2000).
- [26] Ödberg, L., Tanaka, H., Glad-Nordmark, G. and Swerin, A., "Transfer of Polymers from Cellulosic Fibers to Filler Particles". *Colloids Surf. A* **86**, 201 (1994).
- [27] Tanaka, H., Swerin, A. and Ödberg, L., "Cleavage of Polymer Chains During Polymer Transfer of Cationic Polyacrylamide from Cellulose Fibers to Polystyrene Latex". *J. Colloid Interface Sci.* **153**(1)(1992).
- [28] Asselman, T., Alince, B., Garnier, G. and van de Ven, T.G.M., "Mechanism of Polyacrylamide-Bentonite-Microparticulate Retention Aids". *Nordic Pulp Pap. Res. J.* **15**(5), 515 (2000).
- [29] Einarson, M., Aksberg, R., Ödberg, L. and Berg, J.C., "Adsorption and Reformation of a Series of Cationic Polyacrylamides on Charged Surfaces". *Colloids Surf. A* **53**, 183 (1991).
- [30] van de Ven, T.G.M. and Alince, B., "Heteroflocculation by Asymmetric Polymer Bridging". *J. Colloid Interface Sci.* **181**(1), 73-78 (1996).
- [31] Smoluchowski, M., "Versuch Einer Mathematischen Theorie Der Koagulationskinetik Kolloider Lösungen". *Z. Phys. Chem.* **92**(29), 129 (1917).

Chapter 7

The strength of paper is greatly reduced when a mineral pigment is introduced to paper. The paper strength is believed to come from hydrogen bonding of cellulose fibers after the fibers come in contact during drying. Introduction of mineral pigments, studied previously in Chapters 2, 3, 5 and 6, causes the pigment to deposit with the help of retention aids on fiber surfaces preventing hydrogen bonding between fibers, thus reducing the paper strength. To circumvent this phenomenon, an alternative way to introduce the mineral pigments to paper was devised, which was based on passing concentrated pigment suspension through wet sheets where the fibers already in contact with each other.

7.1. Abstract

The introduction of filler into paper can be achieved by passing a clay suspension through a wet fiber web, thus replacing water with the suspension. When both the fiber and the clay have a similar charge, negative or positive, the clay does not deposit on the fiber and can be removed by washing. Fast deposition, due to electrostatic attraction, takes place when either the pulp or the clay is made positive by adsorbing polyethylenimine while the other component remains negative. Providing enough clay is available, the clay particles fully cover the fiber and, consequently, the distribution of the clay throughout the sheet is uniform. Depending on the pH of the clay suspension, the clay may form a monolayer of dispersed particles, or deposit as aggregates.

7.2. Introduction

Problems associated with filler introduction into paper are numerous. To start with, fibers and most fillers are both negatively charged when dispersed in water. Consequently, they repel each other, and only particles larger than the openings in the forming web are retained by mechanical entrapment. Since most dispersed filler particles are very small, this filtration mechanism is not effective. Retention aids are therefore used to increase the efficiency of filler retention. Although many types of retention aids are available, their operational mechanisms are based on simple principles of colloidal interactions. Being mostly cationic polyelectrolytes, they adsorb onto anionic fibers and fillers. Depending on the type, several things can happen:

- (i) Elimination of repulsion between fiber and filler by modifying or reversing the negative charge of either one or both components. The result is a deposition of filler particle on the fiber due to electrostatic attraction, or due to van der Waals attraction when electrostatic interactions are negligible;
- (ii) Formation of a polymeric bridge between the fiber and the filler particle due to polymer macromolecules being adsorbed onto both;
- (iii) Flocculation of filler particles alone without deposition on the fibers, thus increasing their size and the probability of being captured in the forming web of fibers.

Which of these mechanisms operates depends largely on the type of polyelectrolyte, mainly its molar mass, its charge density and whether it is linear or branched. Although the three cases are quite distinguishable, in reality the process of retention is more likely a combination of them. The reason is that kinetic, colloidal and hydrodynamic factors are involved, making the situation rather complicated. To appreciate the complexity, van de Ven [1] provided a full account of the parameters to be considered.

The effect of hydrodynamic forces is demonstrated clearly by measuring the deposition of filler particles on fibers suspended in water at different speeds of mixing and in the presence of a retention aid. With increased stirring, the rate of deposition increases due to increased frequency of collision, but the amount of deposited filler decreases because hydrodynamic forces increase particle detachment faster than the deposition. Therefore, a process which could be dominated by colloidal forces at slow stirring may become dominated by hydrodynamic forces at

faster stirring. The result is a considerable drop in retention due to colloidal interactions, and the main mechanism becomes the capture of flocculated filler particles within the forming sheet. But again, the size of the flocs decreases with increasing hydrodynamic shear, with the consequence of less effective capture. Moreover, there is a dilemma to be considered. Although larger filler flocs might be entrapped more easily, their optical efficiency decreases. Also of concern is the uneven distribution of fillers throughout the sheet due to the process of filtration.

There is another problem associated with cationic retention aids. The presence of anionic substances in the process water renders the cationic polyelectrolytes ineffective simply by consuming them. The problem is well known in unwashed mechanical-type furnishes containing considerable amounts of anionic trash. Similarly, by closing up the water system, the concentration of anionics increases and becomes a nuisance. To overcome this problem by using an excessive amount of cationic retention aids leads to overflocculation, inferior formation, loss of strength and difficulties with machine runnability.

The question then arises: is there some way of increasing first-pass retention to prevent the accumulation of fillers in the process water and to eliminate the detrimental effect of the anionics? The answer has been sought by using two-component retention aids:

- (i) A combination of cationic and anionic polyelectrolytes;
- (ii) Anionic microparticles and cationic polyelectrolytes;
- (iii) Nonionic polymer and phenolic resin.

There is, however, a possibility, at least in principle, of introducing fillers into paper by passing filler suspensions through an assembly of fibers already formed on a wire. The idea comes from a study dealing with deposition of pigment particles within a pad of fibers [2, 3]. Several arguments would support such a process:

1. Most of the water containing the detrimental anionics has already gone.
2. The interfiber bonding might not be affected by the presence of filler particles since they should deposit only outside the area of fiber crossing.
3. The filler may deposit in the form of individual particles and, consequently, be more effective in scattering light.
4. Cationic polyelectrolytes can be used to pretreat the filler to introduce a positive charge and thus encourage its attraction to negative fibers.
5. No loss of filler into white water will occur if the suspension, which passes through the web, is collected under the wire and recirculated.
6. Sizing of the fibers in the absence of fillers could be more effective, although it is not known how particles depositing on sized fibers affect the sizing properties of paper.

The obvious problem, of course, is how to prevent disturbance of the fiber assembly when passing the filler suspension through the wet web of low solids content. Perhaps a top wire with a filler slurry being delivered by spraying or by a second headbox could provide the solution; however, this is beyond the scope of this paper.

The main objective here is to test the applicability of theoretical predictions based on the principles of colloidal interactions. This is done by observing the

behavior of systems in which the fibers and clay have either the same or opposite surface charge. When oppositely charged, the clay particles should deposit on the fiber because of electrostatic attraction. If of the same charge, no deposition of clay should take place.

7.3. Procedure

Four different systems were investigated in which fibers and clay were either of the same or of opposite charge. Since the intention was to verify that the deposition of clay is governed by colloidal electrostatic interactions, the bleached kraft fibers used were unbeaten and washed free of fines. This prevents complications arising from clay particles being either captured within fibrils formed by beating or by interacting with fines. The clay used had an average equivalent hydrodynamic diameter of 0.2 μm . A fiber mat, of intended basis weight 100 g/m^2 and consistency of $\sim 10\%$, was formed on a screen and secured in position by another screen placed on top. An outlet located under the bottom screen was connected to a vacuum through a cut-off valve. With the valve closed, a suspension of either 1% or 10% clay adjusted to a given pH was introduced on top of the fiber mat, representing an addition of 0.4 and 4 g clay/g fiber. Then the vacuum was applied so that the clay suspension passed through the mat in a fraction of a second. In one set of experiments, the wet web was analyzed for ash content, and in another set pure water adjusted to a given pH was passed through the web several times before analysis. This means that in the first case all the clay remaining in the sheet was detected, while in the second case only the clay attached to the fibers was detected. Besides the retention of the clay, we also

determined its distribution within the web by observing the top and bottom of the sheets by scanning electron microscopy (SEM). From analysis of SEM photographs, it was concluded that negligible particle detachment occurred during washing.

The four systems were composed of: (1) negative fibers, negative clay; (2) positive fibers, positive clay; (3) negative fibers, positive clay; and (4) positive fibers, negative clay.

In system (1), both the fibers and the clay were untreated and they thus acquired a negative charge when dispersed in water. Their charge, however, is a function of pH, as shown in Fig. 7.1 where the charge is represented by the experimentally measured electrophoretic mobility. The fibers are negatively charged over the whole region of pH and the charge increases with increasing pH. The clay used in this study is positively charged at low pH, but becomes negative above pH 4.5 and more so as pH increases. It is of interest to realize that the colloidal behavior, particularly the stability of the clay dispersion, reflects the change in charge. The pronounced charge at high pH results in a strong repulsion between the clay particles, which remain well dispersed. When the charge and, consequently, the mutual repulsion decreases as pH is lowered, the tendency to aggregate increases. At a pH of ~ 4.5 , the repulsion is diminished to the point where spontaneous aggregation (also called coagulation or flocculation) takes place.

In system (2), both the fibers and the clay were made positive by pretreatment with polyethylenimine (PEI). The PEI used (Polymin P, BASF) is a highly branched polyelectrolyte containing primary, secondary and tertiary amino groups in the ratio 1:2:1 with molar mass $M_m = 6 \times 10^5$ Da and $M_n < 3.5 \times 10^4$ Da. As shown in Fig. 7.2,

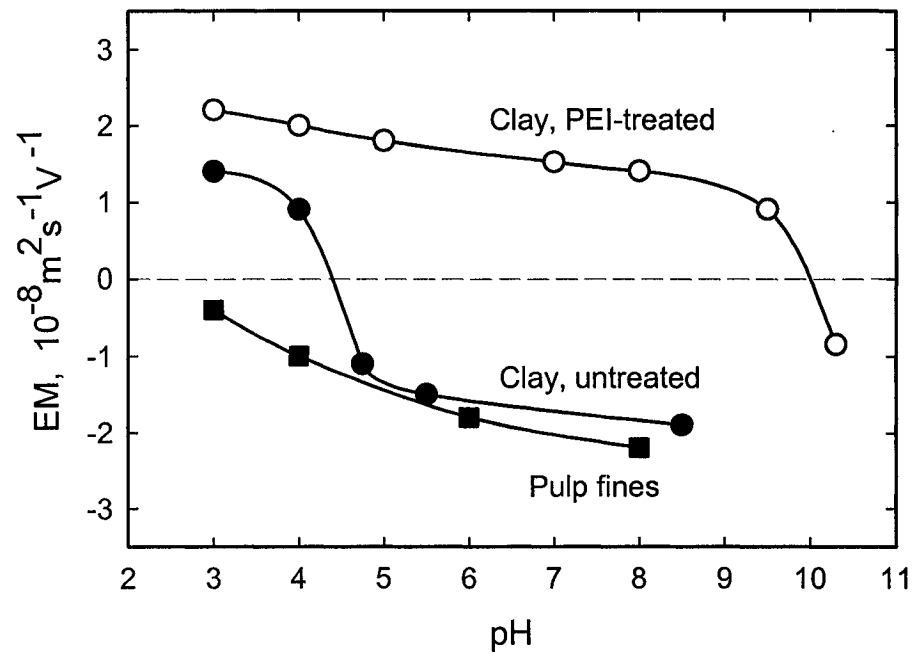


Fig. 7.1: Electrophoretic mobility (EM) as a function of pH of pulp fibers (measured on fines derived from and believed to represent the fibers), untreated clay and clay treated with PEI.

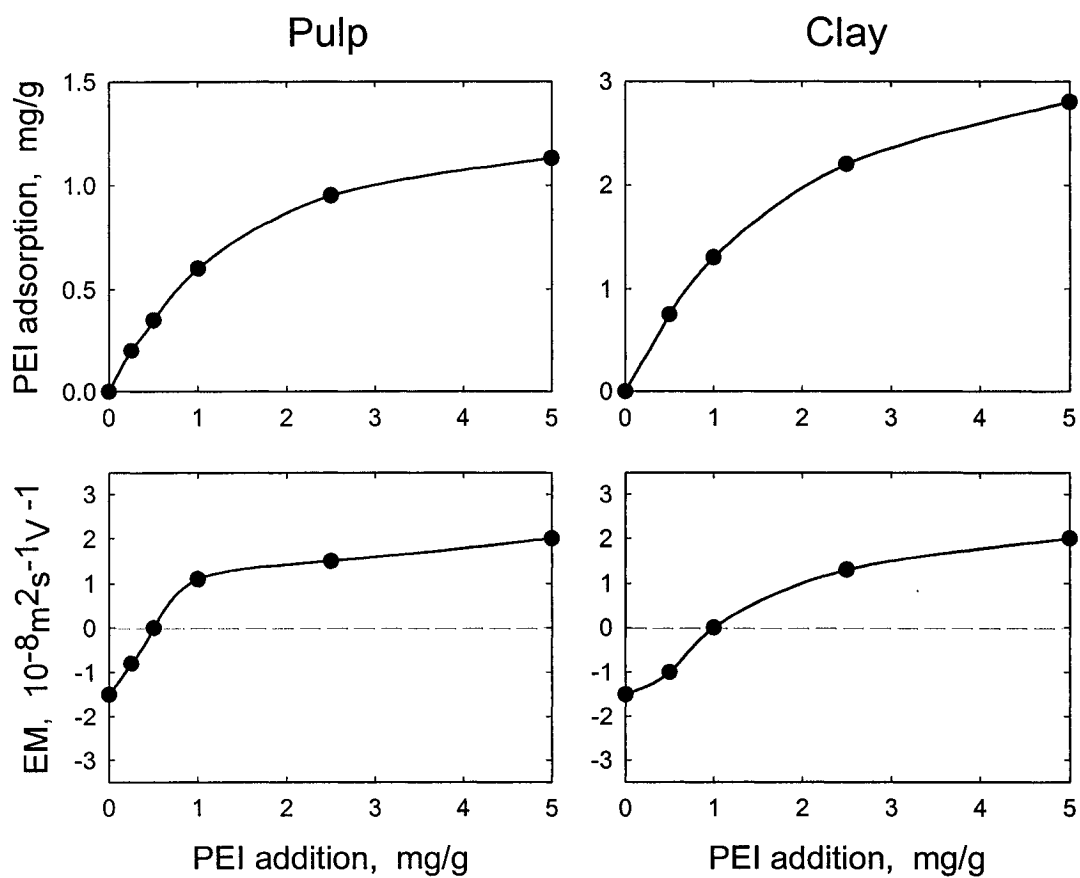


Fig. 7.2: PEI adsorption and electrophoretic mobility of fibers and clay.

when PEI is adsorbed, the charge is reversed. For the treatment of fibers and clay, an excess of PEI was used to achieve maximum adsorption and the unadsorbed PEI was removed by multiple washing. As seen in Fig. 7.1, the charge of pretreated clay remains positive up to pH 9, which is a natural consequence of dissociation of amino groups of PEI ($pK \approx 10-11$). The response of the treated fibers would be similar because the same polyelectrolyte would be adsorbed onto the fiber surface. The stability of the treated clay reflects the observed charge. The clay remains dispersed and positively charged up to pH 8, but at higher pH it starts to aggregate because the charge and the resulting repulsion between the clay particles decreases.

In systems (3) and (4), the systems were composed of either treated fibers and untreated clay, or vice versa.

7.4. Results

In Fig. 7.3, results are shown for a system of untreated fibers and untreated clay obtained at pH 6, 8 and 10 to which the clay suspension was adjusted. The open bars represent the content of clay found in the wet fiber mat after passing either 1% or 10% clay suspensions. The amount of clay was either 0.4 or 4 g/g fiber. The clay remains within the mat as a result of both replacement of water with a clay suspension, and clay deposition on fibers. This is shown as open bars. By passing pure water (adjusted to a given pH) through the mat until the effluent is clear, the amount of clay deposited can be determined, and this is shown as the full bars. It is not surprising to see that, in the system where both components are negatively

Negative Clay - Negative Fiber

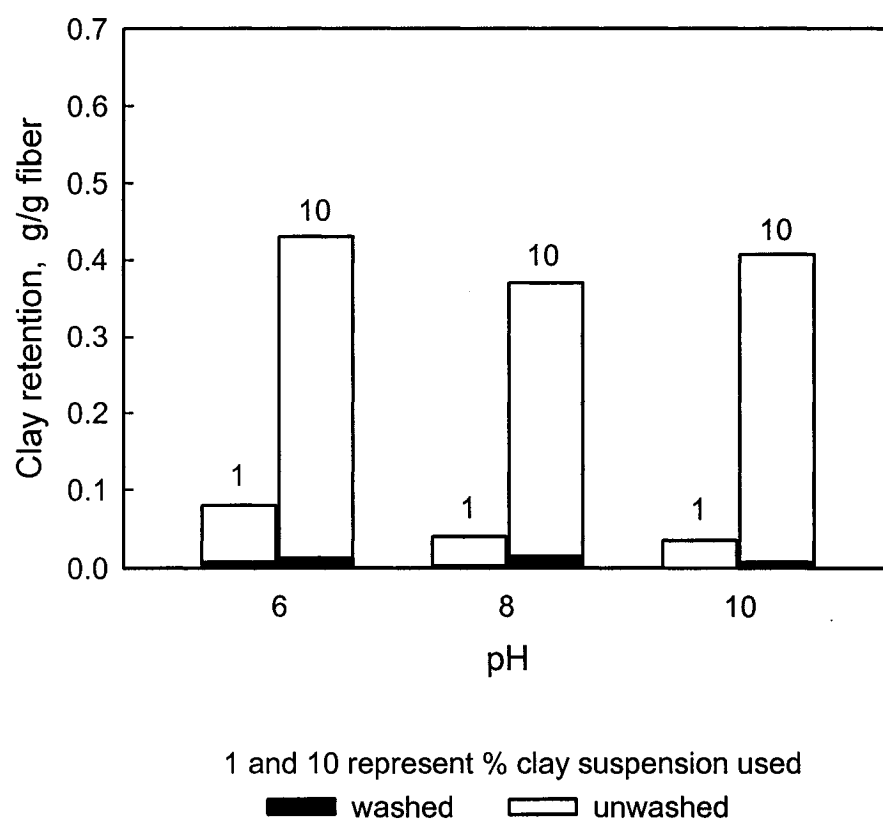


Fig. 7.3: Clay content of sheets after passing 1% and 10% clay suspensions adjusted to pH 6, 8 and 10 before (open bars) and after (full bars) washing with pure water (adjusted to pH 6, 8 and 10). Fiber negative, clay negative.

charged, only a small amount of clay is left within the sheet after washing. This is also observed by SEM in Fig. 7.4. When we look at both the top and the bottom of the washed sheets at two magnifications, it is obvious that only a few clay particles are attached to the fiber surface.

From Fig. 7.3 it can be seen that, at a clay concentration of 10%, ~ 0.4 g clay/g fiber ends up in the unwashed sheet, while for the 1% clay dispersion the amount is ~ 0.05 g/g fiber. The 10% clay dispersion consists of 36 g water and 4 g clay/g fiber in the web and, since most of the retained clay is suspended in the water in the fiber web, 0.4 g clay/g fiber retained corresponds to a water content of $\sim 80\%$. The same is true for the 1% clay dispersion. Thus, during drainage under vacuum, web contraction occurs and the consistency of the web increases from its initial value of $\sim 10\%$ to $\sim 20\%$.

Figure 7.5 shows the results obtained in a system composed of both fibers and clay that are positive. At pH 6 and 8, the situation is similar to the preceding case, apparently because there is no attraction between the similarly charged components. At pH 10, however, a considerable amount of clay is left in the sheet after washing. The reason appears to be the tendency of the cationic clay to flocculate at this pH and, therefore, larger flocs are captured within the fiber net. For such mechanical entrapment, there is no need for electrostatic attraction between fibers and clay.

The effect of electrostatic attraction is shown in Fig. 7.6, where a suspension of untreated negative clay was passed through positive fibers. Because of mutual attraction, the clay particles deposit on fibers. Providing there are sufficient amounts of clay available, full coverage of the fibers can be achieved. Such a situation is

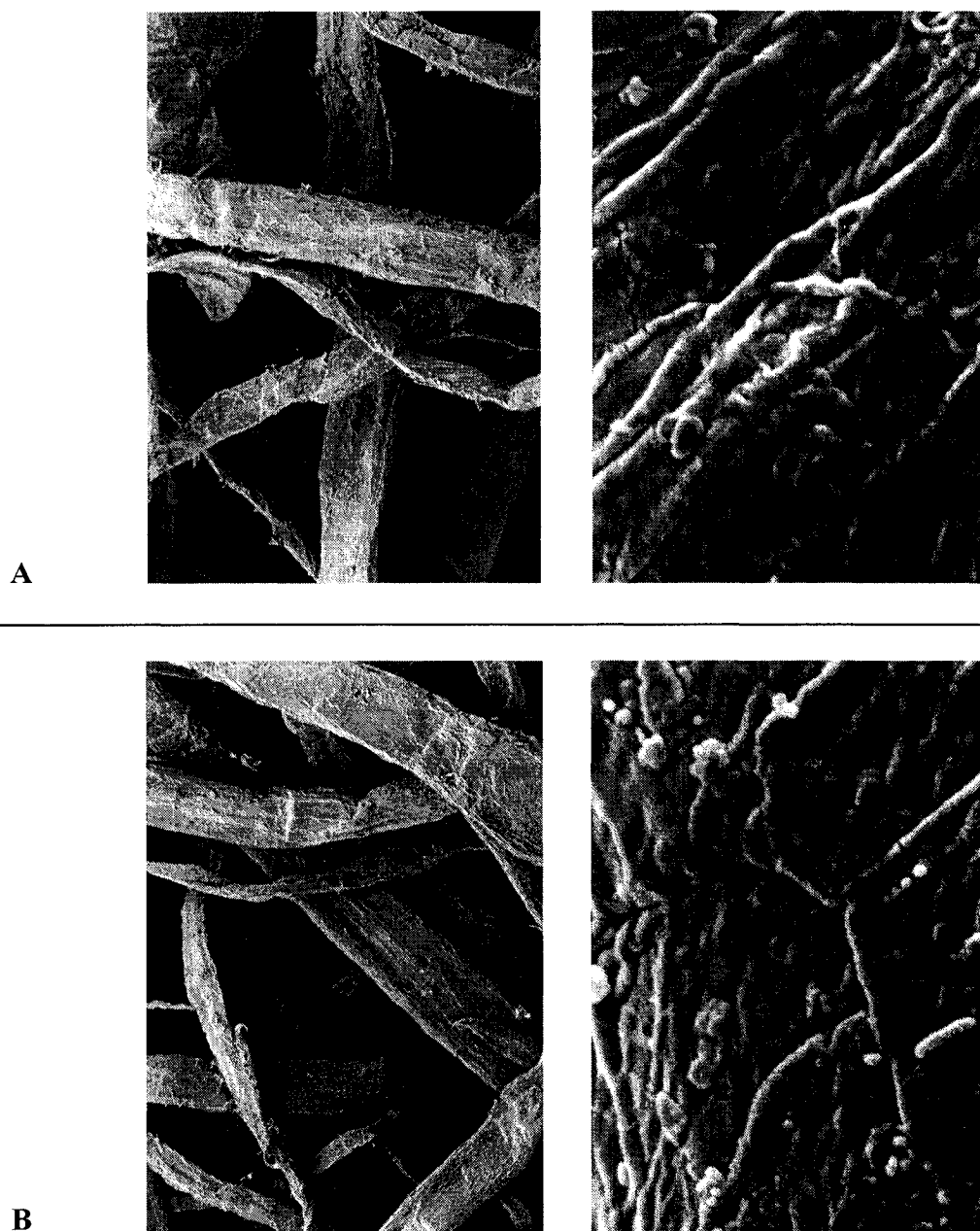


Fig. 7.4: SEM at X900 and X14 500 magnification of top (A) and bottom (B) of sheets after washing. Fiber negative, clay negative.

Positive Clay - Positive Fiber

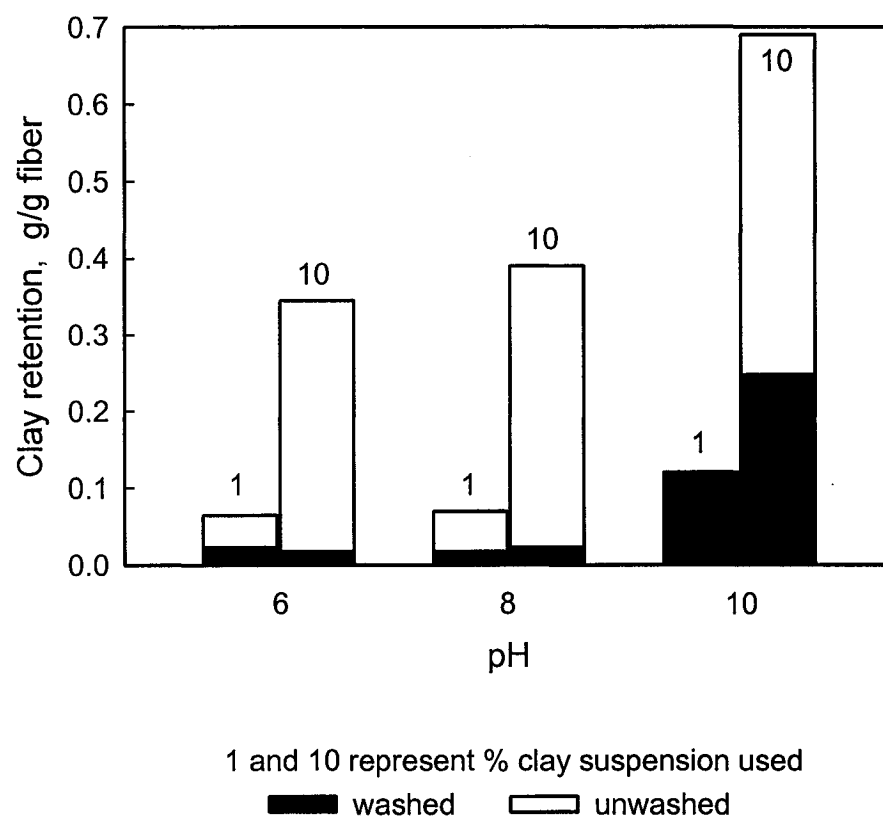


Fig. 7.5: Clay content of sheets after passing 1% and 10% clay suspensions at pH 6, 8 and 10 before (open bars) and after (full bars) washing with pure water. Fiber positive, clay positive.

Negative Clay - Positive Fiber

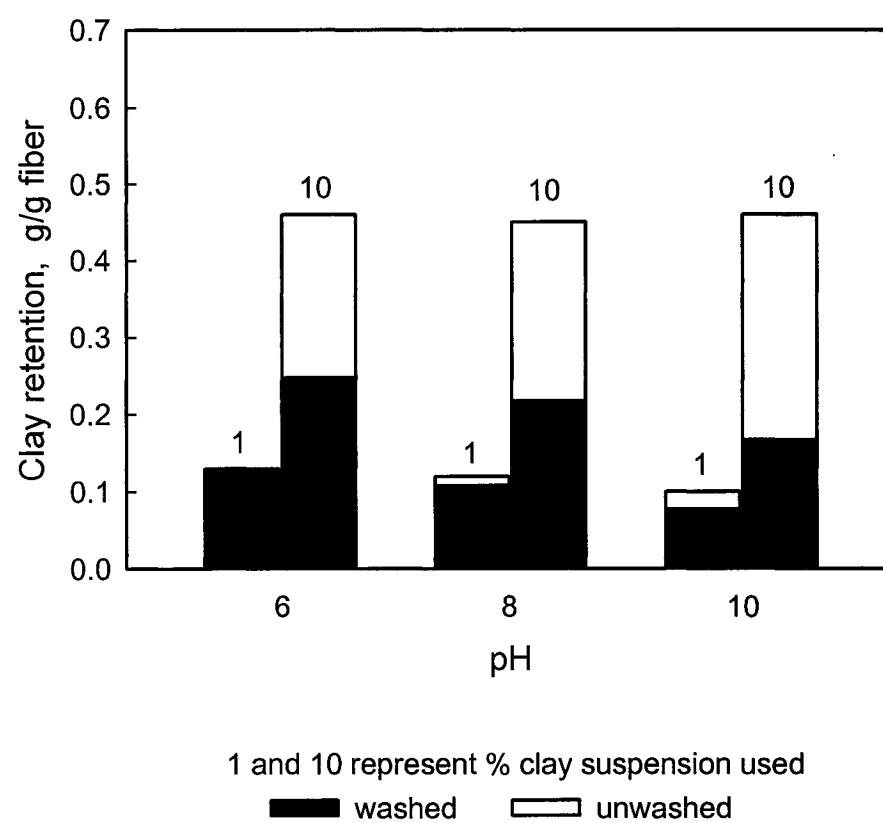


Fig. 7.6: Clay content of sheets. Fiber positive, clay negative.

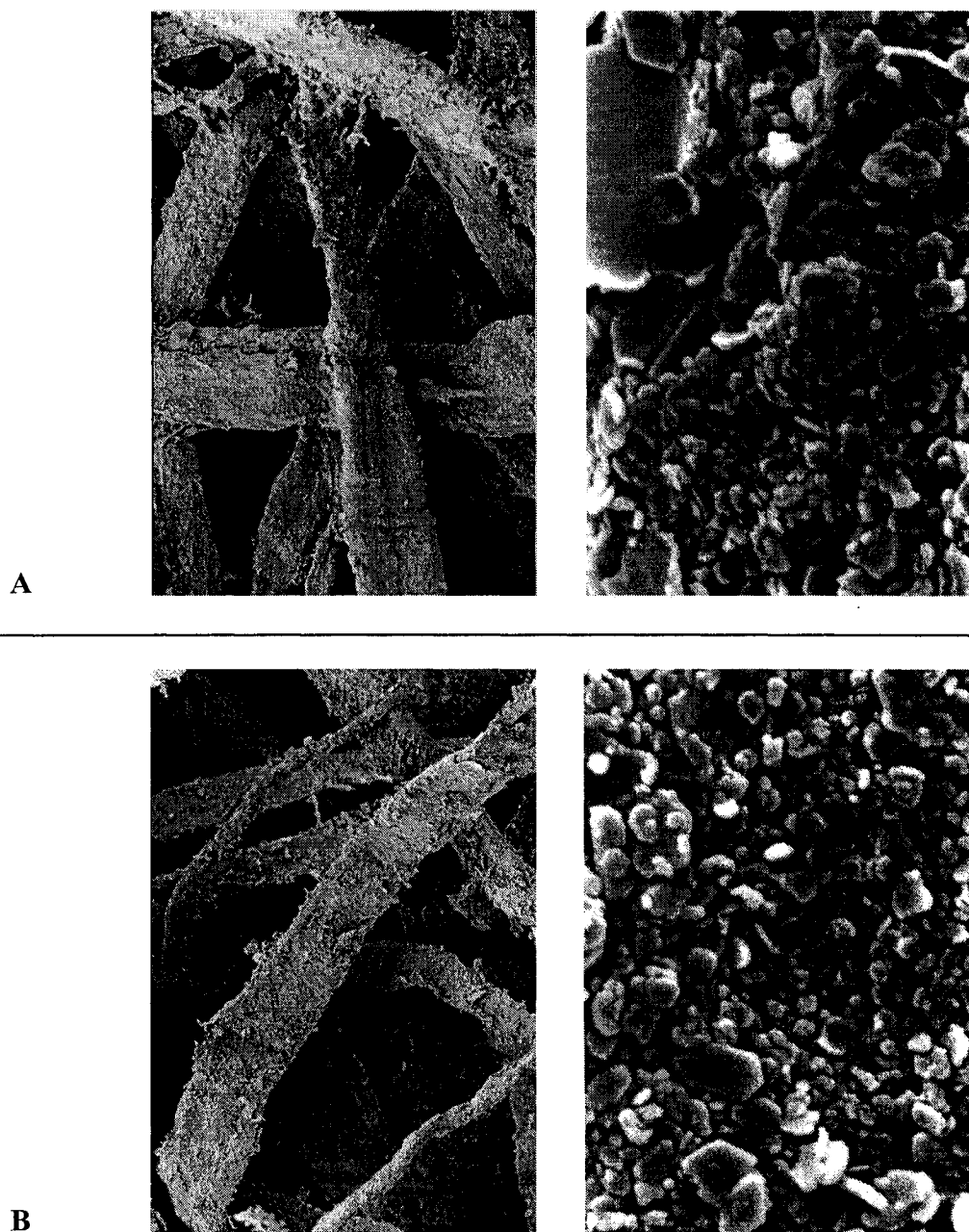


Fig. 7.7: SEM at X900 and X14 500 magnification of top (A) and bottom (B) of sheets after passing 10% clay suspensions and washing with pure water at pH 6. Fiber positive, clay negative.

shown in Fig. 7.7 on micrographs taken of the top and the bottom sides of the washed pads obtained at pH 6 and clay concentration 10%. The clay particles are sufficiently charged to be dispersed (cf. Fig. 7.1) and, therefore, deposit as individual particles forming a quasi-monolayer on the fiber surface. The observed amount of ~ 250 mg/g fiber is close to the value required for full coverage of fibers by dispersed particles, which was found to be in the range of 250–280 mg/g fiber for this particular clay [4]. This proves, by the way, that there is negligible particle detachment during the filling and washing procedures. There is, however, a tendency for the amount of deposited clay to decrease with increasing pH, as seen in Fig. 7.6. This can be attributed to a stronger lateral repulsion between clay particles with increasing pH (negative charge increases as seen in Fig. 7.1), which would result in particles packing on the fiber surface at a lower density [5, 6]. Thus, on a given surface, fewer particles can be accommodated.

The amounts of clay deposited on the fibers can be predicted, in principle, by the theory describing the deposition of fillers in pads of fibers [2] and with extrapolations of the experimental results of clay deposition in such pads [3]. Exact comparisons with theory are difficult, since not all parameters involved with the theory are known. The drainage velocity is difficult to estimate because the duration of the experiment is extremely short. Assuming all drainage occurs in ~ 0.1 s, the drainage velocity, U , is of the order of a few cm/s. The thickness of the wet web is about 1 mm and, since the amount of water used in each experiment is about 4 times the amount of water in the sheet, the experiments lasted a duration corresponding to about 4 times the residence time, t_r , of the clay in the web. We assume further that the

deposition rate increases as $U^{1/3}$ [7] and extrapolate from the deposition rates observed at $U = 4$ cm/min [3], and we neglect the detachment rate since the average time a clay particle spends on the fiber is much larger (about two orders of magnitude) than the time of an experiment. We estimate that, at $t = 4t_r$ (the end of the experiment), the concentration of clay in the water exiting the web, for an initial clay concentration of 1%, is less than 0.8%. This implies that more than 20% of the clay is adsorbed onto the fibers, since at shorter times the adsorption is larger. The actual amount of clay deposited on the fibers is ~25% (cf. Fig. 7.6; 0.1 g clay/g fiber out of the initial 0.4 g clay/g fiber), which is consistent with the estimate. Although crude, these estimates suggest that the theory developed for the deposition of fillers in a fiber web is useful in understanding the process of filling paper the way we propose.

Despite the fact that the duration of the experiment is extremely short, it lasts long enough to attain almost full coverage of the fiber by clay at 10% clay concentration.

Based on these estimates, the kinetics of deposition of clay in the web can be schematically visualized (see Fig. 7.8). The initial kinetics are 10 times as fast when using 10% clay compared than when using 1% clay. The plateau values are expected to be almost the same since particle detachment is negligible. At the end of the experiment (at $t = t_f$), the plateau value is (nearly) reached for the 10% clay dispersion, while the deposited amount is probably still determined by the initial deposition kinetics for the 1% dispersion.

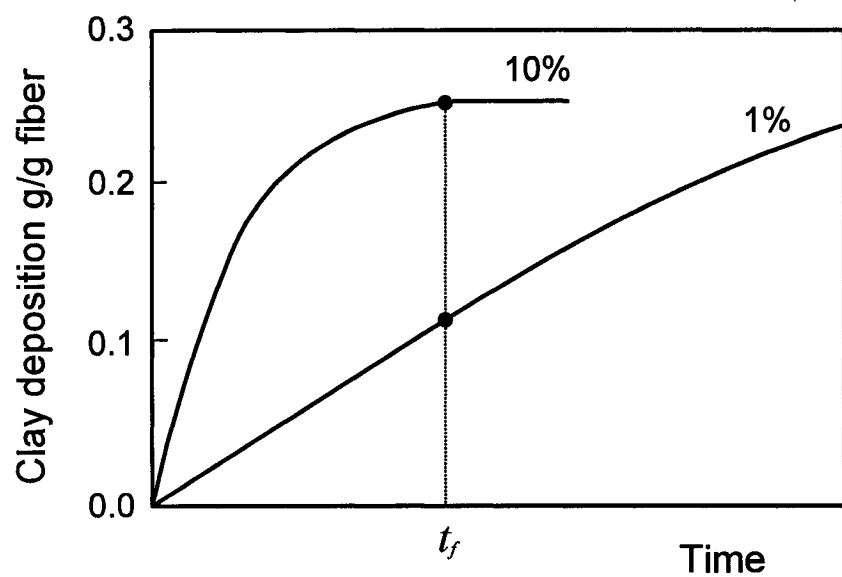


Fig. 7.8: Schematic representation of the kinetics of clay particles depositing on fibers in a wet sheet for 1% and 10% clay dispersion. t_f is the time at the end of the experiment.

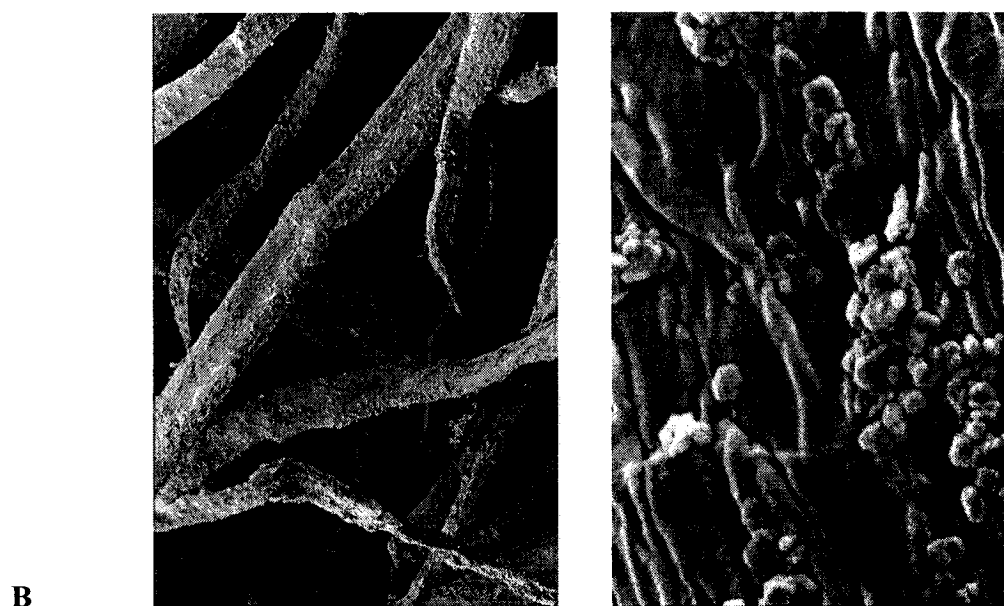
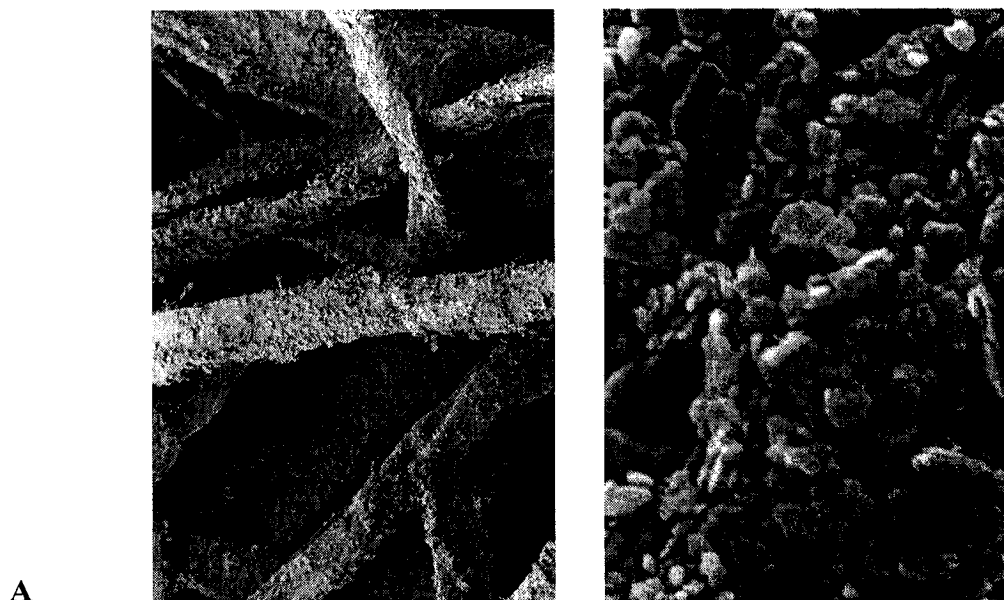


Fig. 7.9: SEM at X900 and X14 500 magnification of the top (A) and bottom (B) of sheets after passing 1% clay suspension and washing with pure water. Fiber positive, clay negative.

Positive Clay - Negative Fiber

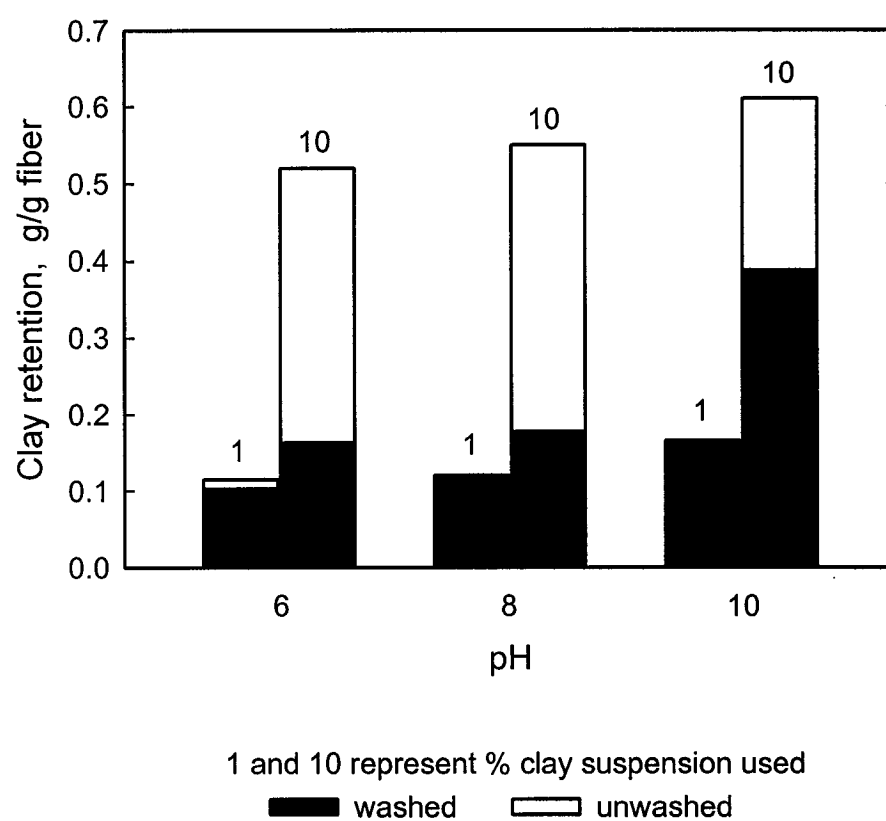


Fig. 7.10: Clay content of sheet. Clay positive, fiber negative.

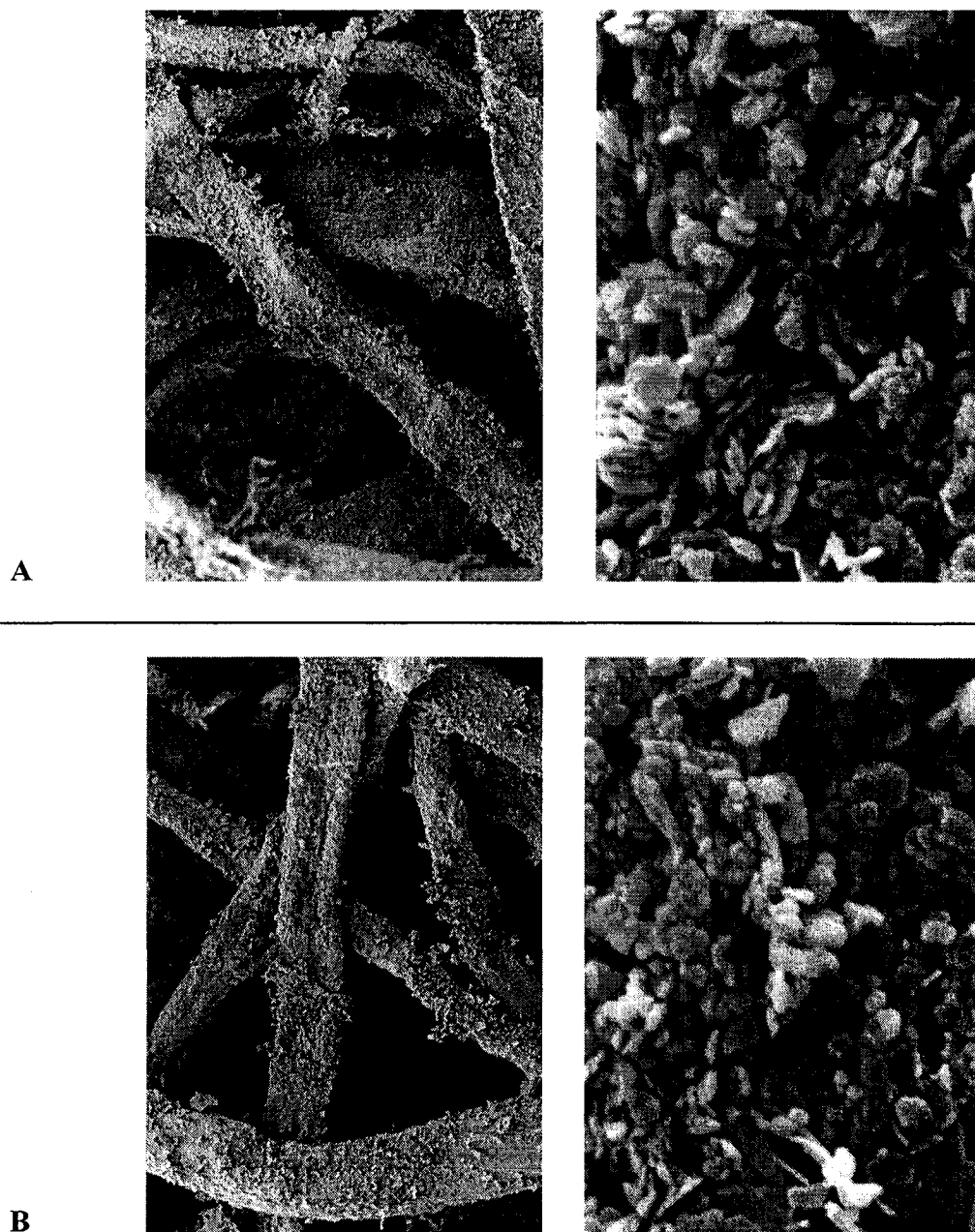


Fig. 7.11: SEM at X900 and X14 500 magnification of top (A) and bottom (B) of sheets after passing 10% of clay suspensions and washing with pure water at pH 10. Fiber negative, clay positive.

Prior to reaching a uniform distribution of particles on the fibers at the plateau, theory predicts [2] that the distribution of clay will be uneven, with the coverage of fibers decreasing from top to bottom. This is indeed observed in Fig. 7.9, which shows SEM photographs of the top and the bottom of the washed pads after passing the 1% clay.

The results of the system composed of positive clay and negative fibers are shown in Fig. 7.10. The repulsion between clay particles now decreases with increasing pH (positive charge decreases as seen in Fig. 7.1). Consequently, more particles can deposit on a given surface as pH increases. At pH 10, an additional mechanism should be considered. Because of diminished repulsion between particles, the clay flocculates. Retention increases because of more effective capture of the flocs and the clay orientation on the fiber surface. In Fig. 7.11A, at larger magnification, it is clearly seen that the orientation of plate-like particles of clay towards the fiber surface is different from that seen in Fig. 7.7. Due to the tendency to flocculate, the clay appears to be attached by the edges while, in Fig. 7.7, particles are deposited face-down. This difference in orientation would account for the attachment of a larger number of particles.

7.5. Conclusions

The mutual electrostatic attraction between oppositely charged fibers and clay particles results in fast and full coverage of the fibers when a clay suspension is passed through an assembly of wet fiber web. When the fibers are positively charged, maximum deposition of negatively charged clay is achieved at a lower pH when the

diminished lateral repulsion between clay particles allows closer packing on the fiber surface. When the clay is positive, deposition on the negative fibers is enhanced at a higher pH due to clay flocculation. Uniform distribution and full coverage of all fibers can be achieved, providing a sufficient amount of clay passes through the fiber mat.

Even without electrostatic attraction, a considerable amount of clay is retained in a wet web because of the replacement of water by the clay suspension. The actual amount will depend on the concentration of the clay suspension, its state of dispersion and the solids content of the wet web.

7.6. Acknowledgements

Many thanks to Mr. James Drummond, Paprican, Vancouver, BC, Canada for his substantial contribution by providing the SEM pictures. We would like to acknowledge funding from NSERC's National Centres of Excellence program.

7.7. References

1. van de Ven, T.G.M., "Particle Deposition on Pulp Fibers. The Influence of Added Chemicals", *Nordic Pulp Pap. Res. J.* **8**(1), 130–134 (1993).
2. Al-Jabari, M., van Heiningen, A.R.P. and van de Ven, T.G.M., "Modeling the Flow and Deposition of Filler in Packed Beds of Pulp Fibers", *J. Pulp Pap. Sci.* **20**(9), J249–J253 (1994).

3. Al-Jabari, M., van Heiningen, A.R.P. and van de Ven, T.G.M., "Experimental Study of Deposition of Clay Particles in Packed Beds of Pulp Fibers", *J. Pulp Pap. Sci.* **20**(10), J289–J295 (1994).
4. Alince, B., Petlicki, J. and van de Ven, T.G.M., "Kinetics of Colloidal Particle Deposition on Pulp Fibers. I. Deposition of Clay on Fibers of Opposite Charge", *Colloids Surf. A* **59**, 265–277 (1991).
5. Alince, B., "Colloidal Particle Deposition on Pulp Fibers", *Colloids Surf. A* **39**, 39–51 (1989).
6. Vincent, B., Young, C.A. and Tadros, T.F., "Equilibrium Aspects of Heteroflocculation in Mixed Sterically-Stabilized Dispersions", *Faraday Disc. Chem. Soc.* **65**, 296–305 (1978).
7. Adamczyk, Z. and van de Ven, T.G.M., "Deposition of Brownian Particles onto Cylindrical Collectors", *J. Colloid Interface Sci.* **89**, 497–518 (1981).

Chapter 8

In Chapter 7, paper was filled by passing clay suspensions through wet web which was stationary. In this chapter the research was extended to more dynamic conditions using two pilot paper machines. Mill trials on these two pilot paper machines (one slow and one fast) were performed to establish the feasibility of this process on a moving wet web, which was also much closer to the real industrial conditions.

8.1. Abstract

Pilot-scale trials on slow and fast Fourdrinier paper machines have shown that a sheet can be filled with clay and calcium carbonate by passing a concentrated filler suspension through a wet sheet. The suspension was supplied from a secondary headbox located at the dryline. The trials showed that no damage to the sheet occurs when the filler suspension is applied to the wet sheet. At low filler concentrations, an uneven distribution of filler in the sheet was observed in the z direction, but at high filler levels, the unevenness in filler distribution decreased. The strength of the paper decreased with increasing filler concentration, as is the case in conventionally filled paper. Aside from fillers, other chemicals can be retained by this process as well. Polyethylenimine (PEI) showed an increase in the dry strength of paper on the slow Fourdrinier machine, but not on the fast one. The main advantage of this method is that the filling process can be completely separated from the wet-end chemistry.

8.2. Introduction

Fillers are added to paper to improve various paper properties and to reduce cost. They are traditionally added to the papermaking furnish prior to the formation of the sheet, and additional additives, such as retention aids, must be used to efficiently incorporate fillers into a sheet. As a consequence, the use of fillers leads to more complex wet-end chemistry, and their limited retention causes an accumulation of fillers and other additives in the whitewater. Additional problems are that the efficiency of retention aids is often reduced by dissolved and colloidal substances

present in the whitewater. Fillers in process water can also contribute to the stabilization of unwanted foams.

For all of these reasons, it would be desirable if the filling of paper could be achieved in a unit operation that is completely separated from the wet-end processing. In this article, we report on a new way to achieve this separation, namely, by filling paper after the sheet is formed and while it is still wet before it enters the press section. Similar concepts in the wet-end processing of the paper machine involve the manufacturing of laminated cardboards, the spraying of starch, and the curtain coating. A secondary headbox is used for laminated cardboards to apply a fiber suspension onto a preformed base sheet. The base sheet has usually inferior optical properties, and the aim of the secondary layer is to improve the properties while reducing the production costs by using a minimum amount of expensive high-quality fibers. The curtain-coating technology uses a free-falling flat jet called a curtain as a single or multiple-layer coating of photographic films and papers, magnetic recording tapes, etc. [1-3]. Curtain coating is not used for pigment coating because of paper machine runnability problems under high-speed conditions [4]. The starch-spraying process can be used either in conjunction with a size press or as an alternative to conventional sizing. During the treatment, the starch granules are applied to paper in the form of a spray [5, 6]. The main advantage is high starch retention (excess of 90%). Both techniques, curtain coating and spraying, have many similarities with the proposed novel method to paper loading, as the amount of additives and the penetration depth can be varied.

The filling of a paper sheet using a secondary headbox is based on replacing the water in the wet sheet with a suspension of fillers. The advantage is that this process is insensitive to the quality of the water in the sheet and that the filler that passes through the sheet can be collected and fed back to the filler suspension. This leads to two completely separate recirculation loops, one for each fibers and pigment. The actual filling of the wet paper can be done with or without the use of retention aids. The use of surface-treated fillers that have favorable fiber-filler interactions is also straightforward. Because most of the water is already removed when the sheet is formed, little of dissolved material is left to interact with the polymers used for the surface treatment. Aside from filling the sheet with pigments, this process can be used to apply any other additives, such as strength agents, sizing agents, yellowing inhibitors, etc. The method of filling wet paper has already been successfully studied under stationary conditions (with a nonmoving sheet) [7]. A disadvantage of displacement filling is that the sheet is wetter when entering the press section of the paper machine, which might necessitate increased nip loads. Alternatively, an additional vacuum section could be installed before the press section.

8.3. Filling wet paper using a secondary headbox

The principle of filling wet paper is shown schematically in Fig. 8.1. In essence, it consists of the displacement of water in the sheet by a suspension containing fillers. A concentrated suspension of fillers flows out of the slice of a secondary headbox with a velocity of v_s , whereas the paper moves through the paper machine with the velocity v_p . If the differential velocity, $v_p - v_s$, is too large, the

possibility exists that the impingement of the suspension on top of the sheet will rupture the sheet. However, this was not found to be the case, even for $v_p = 2v_s$. If suction is applied from below, water from the sheet will be removed and replaced by a filler suspension. Eventually, the filler suspension will be sucked through the sheet as well.

Filler will reach the other side of the sheet when it has traveled a distance l' (see Fig. 8.1), which is approximately given by

$$l' = \frac{hv_p}{u} \quad (1)$$

where h is the thickness of the sheet and u is the average drainage velocity in the filling section. Because of continuity, the velocity u is also related to the height, s , of the slice opening of the secondary headbox

$$s = \frac{lu}{v_s} \quad (2)$$

where l is the location of the dryline of the filler suspension. Combining Eqs. 1 and 2 yields

$$\frac{l'}{l} = \frac{hv_p}{sv_s} \quad (3)$$

For displacement filling to occur, the amount of liquid entering the sheet from above, ul , must be larger than or equal to the amount leaving the sheet at the bottom, ul' ; hence, $l > l'$, which implies $v_s > hv_p/s$. Thus, for low application velocities, such as those used in spraying and curtain coating, the applied liquid does not penetrate the sheet fully, but is confined to the surface layer. In this respect, displacement filling is

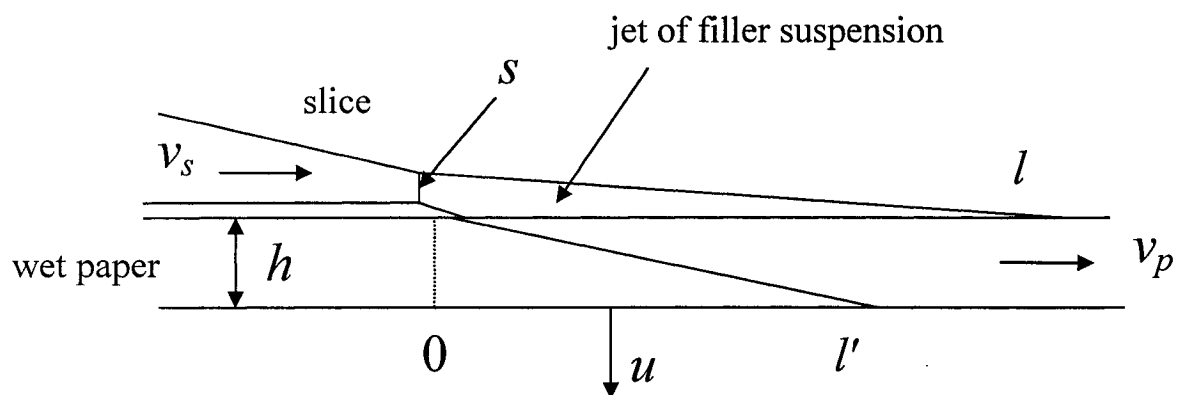


Fig. 8.1: Schematic drawing of water replacement in a wet sheet with a filler suspension.

different from other wet-sheet applications. When $v_s = v_p$, s must be larger than h , whereas when $v_s = 0.5 v_p$, s must be larger than $2h$. These two conditions apply to the two pilot machines discussed below. Given that h is typically about 1 mm at the (secondary) dryline, a slice opening of 3 mm was chosen for all trials. Equations 1-3 can be used to estimate the location of the dryline for given drainage conditions.

Obviously, the description of displacement filling given here is highly approximate. First, the drainage velocity is not constant, but varies along the machine. Also, channeling can occur [8], which can result in the bypassing of certain water regions in the sheet. Nevertheless, the description provides us with approximate values of required slice openings of the secondary headbox and the corresponding dryline locations.

We decided to place the secondary headbox at the dryline. Locating it before this position makes no sense, because one would also have to displace the water on top of the sheet. Placing it further down the drainage section could be considered, but higher solid contents lead to a higher resistance to flow through the sheet. Also air entrainment in the sheet would result in an uneven distribution of filler.

8.4. Materials

8.4.1. Slow Fourdrinier machine

Unbeaten, bleached, softwood kraft pulp was used for the formation of a base sheet. The consistency of the pulp in the primary headbox was 1%.

Alkaline kaolin clay was used as a pigment. This clay was comparable in size (equivalent spherical diameter of 200 nm) and properties to the clay used in

preliminary experiments on a stationary sheet [7]. The clay was introduced to the formed sheet of paper either untreated or treated with polyethylenimine (PEI).

Polyethylenimine under the commercial name of Polymin P was utilized for the clay treatment. Given that PEI is cationic, the role of PEI was to render the clay positive and, therefore, to enhance the mutual electrostatic attraction between the pigment and the negatively charged fibers. The PEI was also passed through the formed wet sheet to study the possibility of applying polymers through the secondary headbox and also to determine the effect of PEI on strength properties.

8.4.2. Fast Fourdrinier machine

Never-dried, unbleached, softwood kraft pulp was beaten to 550 mL CSF (Canadian standard freeness) to achieve optimum runnability of the pilot machine (as determined from prior experience). The pulp consistency in the primary headbox was 1%.

The precipitated calcium carbonate (PCC) Albacar HO was used as a filler. The filler has a diameter about 1 μm and a surface area of 12 m^2/g . The surface charge of PCC suspended in deionized water is slightly positive; however, it can become negatively charged in contaminated process waters. In addition to the water quality, the PCC concentration also affects the surface charge [9]. The water used in all of the experiments was clean (tap-water quality) and was never recirculated.

Anionic, acrylic-acid based stabilizer was used to treat the PCC to provide PCC with a strong negative charge. In this case, the PCC negative charge serves to

maximize the electrostatic repulsion between the pigment and negatively charged fibers.

Cationic starch CATO 237 was used to treat the PCC pigment. The role of the cationic starch was similar to that of PEI, i.e. to render the pigment positively charged. The cationic starch was also passed through the already-formed wet sheet.

Polyethylenimine (PEI) under the commercial name of Polymin P was utilized for the PCC treatment and was also passed through the formed wet sheet.

8.5. Pilot paper machines

Pilot trials were performed on two experimental Fourdrinier machines: a slow machine (CSSP in Trois-Rivières, Quebec, Canada), running at $v_p = 0.67$ m/s, and a fast machine (GL&V, Watertown, NY), running at $v_p = 10$ m/s. On both machines, a secondary headbox was used and was located at the dryline with a slice opening of $s = 3$ mm. The widths of both machines were 68 cm, and the basis weights were in the range of 85-110 g/m². On the slow machine, $v_s = v_p$, whereas on the fast machine, $v_s = 0.5v_p$.

A schematic diagram of the setup for filling wet paper is shown in Fig. 8.2. A filler suspension (clay for the slow machine, PCC for the fast machine) was pumped from the mixing tank to the secondary headbox. On the slow machine, a constant flow rate was achieved by the means of an overflow, thus creating a constant pressure to drive the flow. On the fast machine, a secondary fan pump with a flow rate of 3 L/s pumped water to the secondary headbox, and the filler suspension was injected in this

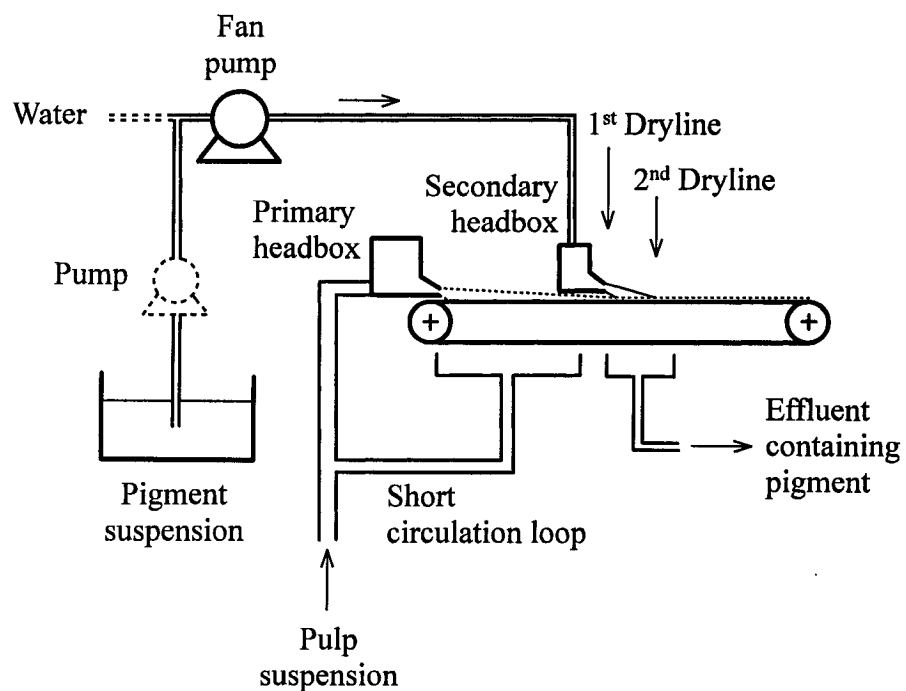


Fig. 8.2: Schematic drawing of filling wet paper on a Fourdrinier machine equipped with a secondary headbox. On the slow machine, the filler suspension was pumped directly to the headbox using the fan pump only. On the fast machine, the filler suspension was pumped (dashed pump) into a waterline (dashed) that fed the secondary headbox.

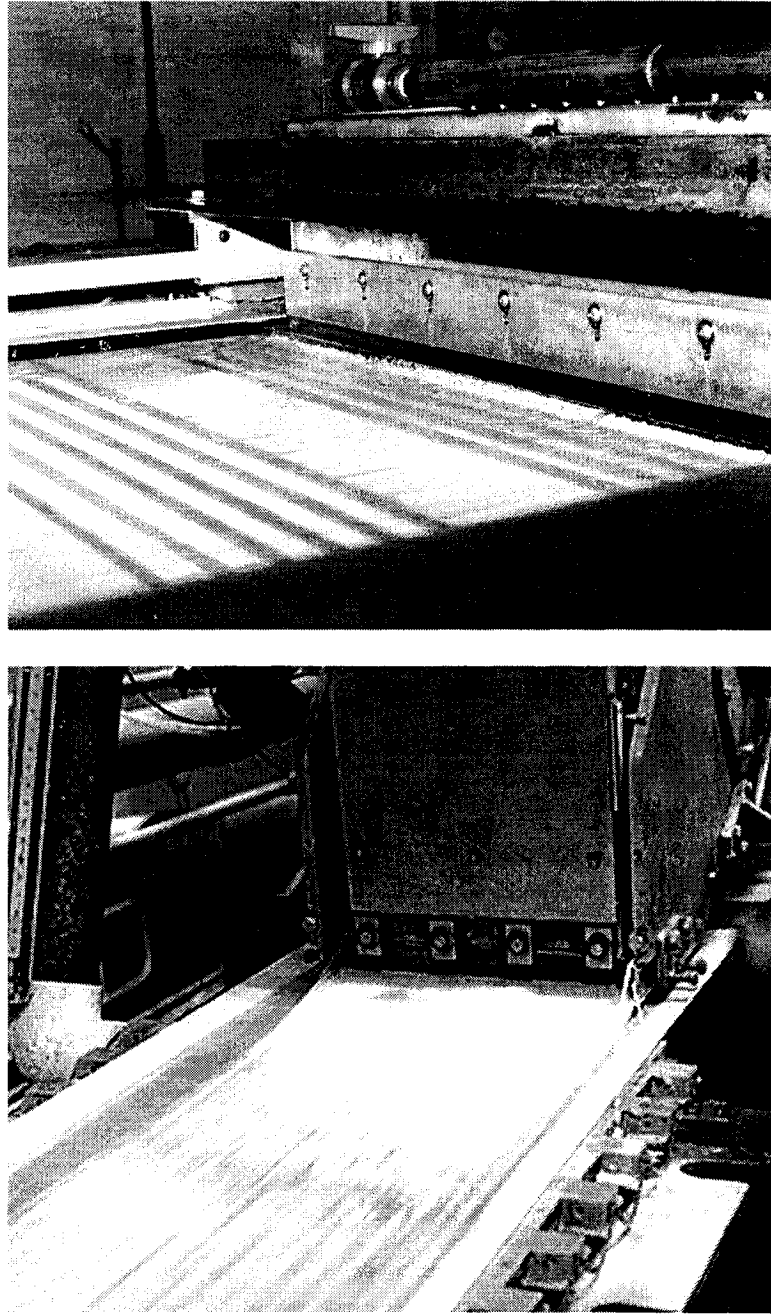


Fig. 8.3: Photographs of a filler suspension flowing out of the secondary headbox onto wet paper on a slow Fourdiner machine (top) and a fast Fourdiner machine (bottom). The locations of the two drylines are consistent with the predictions of Eq. 3.

flow line with a velocity of 0.75 L/s. On the slow machine, all of the paper was dried on the machine, whereas on the fast machine, wet paper after the press was collected for periods of a few seconds and was dried off-line. Photographs of the secondary headbox operating at both machines are shown in Fig. 8.3.

For the slow machine, Eq. 3 predicts that the distance between the slice and the dryline, l , is about 20 cm, assuming a drainage velocity of 1 cm/s, which is typical [10]. On the fast machine, assuming that the drainage is twice as fast, we expect the dryline to be at $l \approx 75$ cm. These values are close to the observed values, indicating that estimated drainage velocities are realistic (cf. Fig. 8.3).

Trials were first performed on the slow Fourdrinier, to establish the validity of the filler displacement concept. After successful results had been obtained, the concept was validated on a fast Fourdrinier pilot machine, which is more representative of a commercial paper machine.

On the slow Fourdrinier machine, clay suspensions of 1, 10, 100, and 200 g/L were applied to the wet paper from the secondary headbox. Some clay was treated with PEI (1 mg/g clay) to reduce the surface charge and promote fiber-clay interactions. In addition, a few PEI solutions at a concentration of 1 mg/g fiber were passed through the sheet to demonstrate that polymers can also be retained in this way. The clay that passed through the sheet was collected in a separate drain and was not mixed with the whitewater in the wire pit, which was used to dilute the pulp to the desired consistency.

On the fast machine, paper was made from unbleached kraft at 1% consistency, and no retention aids were used. It took about 100 s for the PCC pigment

to reach the slice of the secondary headbox after the valve from the feeding tank to the secondary fan pump had been turned on. A PCC pulse of about 1 min was applied. If mixing had been perfect, the maximum concentration of PCC applied from the secondary headbox would have been 160 g/L (in most cases). However, because of turbulence created by the fan pump, the 1-min pulse resulted in a varying secondary headbox concentration lasting for several minutes, with a maximum concentration reaching about one-half of the target concentration. Therefore, the secondary headbox concentrations could not be preset. Instead, samples were taken for each run, and the concentrations were determined by drying and weighing. They varied from 10 to 115 g/L. Samples of the corresponding paper after the press were collected and dried off-line. The PCC used in the experiments was untreated, treated with cationic starch (10 mg/g PCC), treated with PEI (1 mg/g PCC), or treated with an anionic stabilizer (5 mg/g PCC). Also, PEI and starch solutions at dosages of 1 and 10 mg/g fiber, respectively, were passed through the wet sheets. When required, the starch and PEI contents of the sheets were determined by an enzymatic reaction and the Kjeldahl method, respectively.

8.6. Results

8.6.1. Slow Fourdrinier machine

The addition of clay to paper resulted in the expected increase in basis weight. The results for untreated clay showed a linear increase of basis weight with clay content, from 85 to 110 g/m², with clay contents up to 25%.

Figure 8.4 shows how the ISO opacity and ISO brightness vary with clay content for papers containing either untreated or PEI-treated clay. No statistically significant differences were found between the brightness from the topside and the wire sides of the sheets. It can be seen that both brightness and opacity increase with increasing clay content. Furthermore, the optical properties of the sheets filled with treated and untreated clay seem to be identical.

Figure 8.5 shows the TEA (total energy absorption) as a measure of the strength of the sheets. The control is the paper sheet made from the primary headbox, with no water from the secondary headbox passing through it. Blanks (fibers only) for the fast machine (see Fig. 8.11 below) do fall on the same curves as filled sheets, implying that passing water through a sheet does not affect strength. It can be seen that, for low filling levels (about 2%), the strength of the sheet increases, whereas for high filler levels, the expected trend is found, namely, a decrease in strength with increasing clay content [11]. The increase in strength at low filling levels could be caused by the low probability that clay particles would deposit in locations where they would interfere with interfiber bonding during drying. Some of the clay particles could strengthen the sheet by forming a bridge between fibers that otherwise would not be linked. In this respect, clay particles can act similarly to bentonite, which is used, in combination with cationic polyacrylamide, as a retention aid system to increase the bond strength between particles [12]. Also included in Fig. 8.5 are the results for sheets to which PEI was added (without clay). It was found that PEI addition resulted in strengthening of the sheets. Attempts to measure the amount of PEI by the Kjeldahl method were not very accurate because of a significant nitrogen

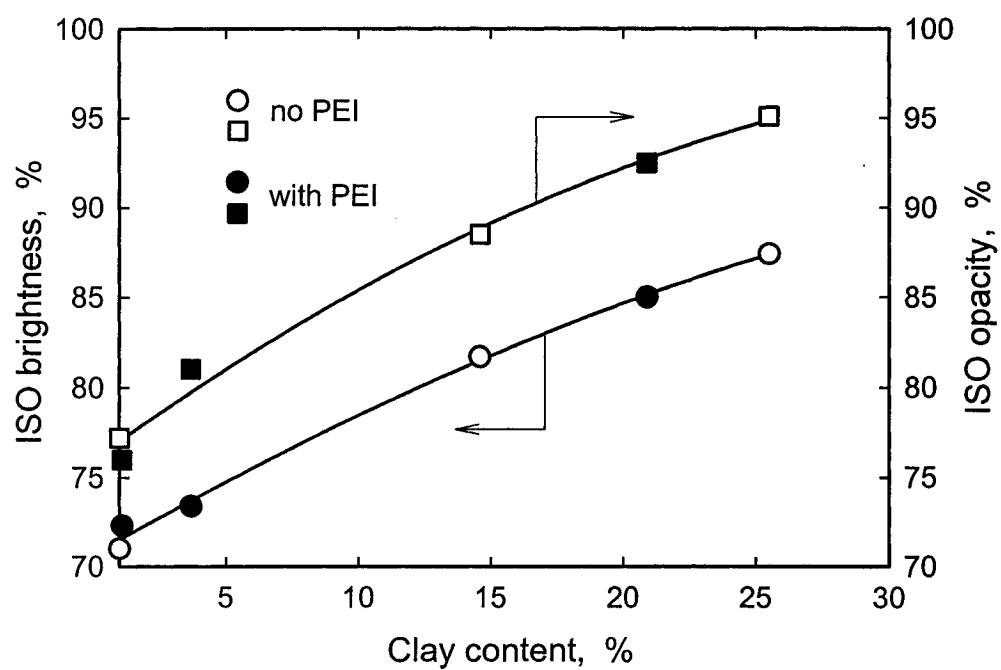


Fig. 8.4: ISO brightness and ISO opacity for papers filled with clay from the secondary headbox.

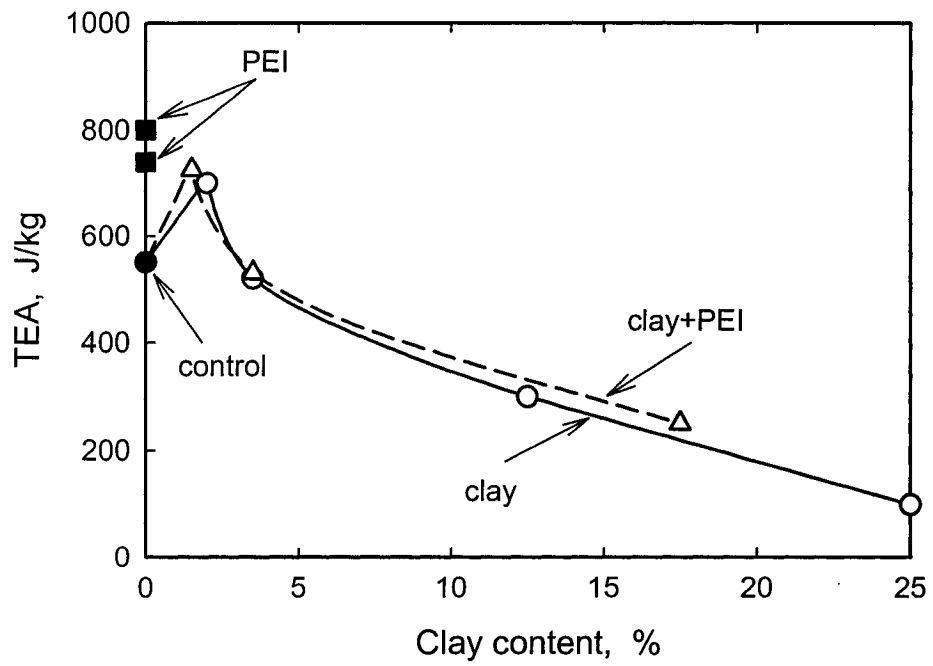


Fig. 8.5: Total energy absorption (TEA) of wet-filled sheets as a function of clay content.

background from the fibers themselves, but estimates suggest that close to monolayer coverage must have been present. This observation suggests that it might be advantageous to add strength agents to wet paper by this method.

SEM images of highly filled sheets show that clay fills the space between the fibers, but little or no deposition of clay on the fibers occurred. This is to be expected, as clay and fibers are both negatively charged. In treating clay with PEI, insufficient PEI was added to reverse the charge of the clay; instead, PEI induced clay flocculation. For highly filled sheets, the top side and wire side exhibit similar surface characteristics, whereas for lower filler levels, more clay was observed at the top side than at the wire side, similar to the filling of stationary sheets [7] and the filling on a fast Fourdrinier machine (see below).

8.6.2. Fast Fourdrinier machine

Large amounts of PCC could be retained in the sheet by filling wet paper. Figure 8.6 shows the retention for PCC's treated in various ways and for various PCC dosages. The highest loading obtained was more than 35%, which was found for the addition of nearly 45% PCC treated with cationic starch. Interestingly, untreated PCC can be successfully retained in the sheet without the use of retention aids. Also, the strongly negative PCC that was treated with the anionic stabilizer can be retained in the paper using this filling method. The reason is that the fillers remain in the water in the sheet after pressing and, during drying, they collapse onto the fibers. It is of interest to note that the added amounts are consistent with those required for full water displacement. Assuming a typical solid content of 10-15% at the dryline [10],

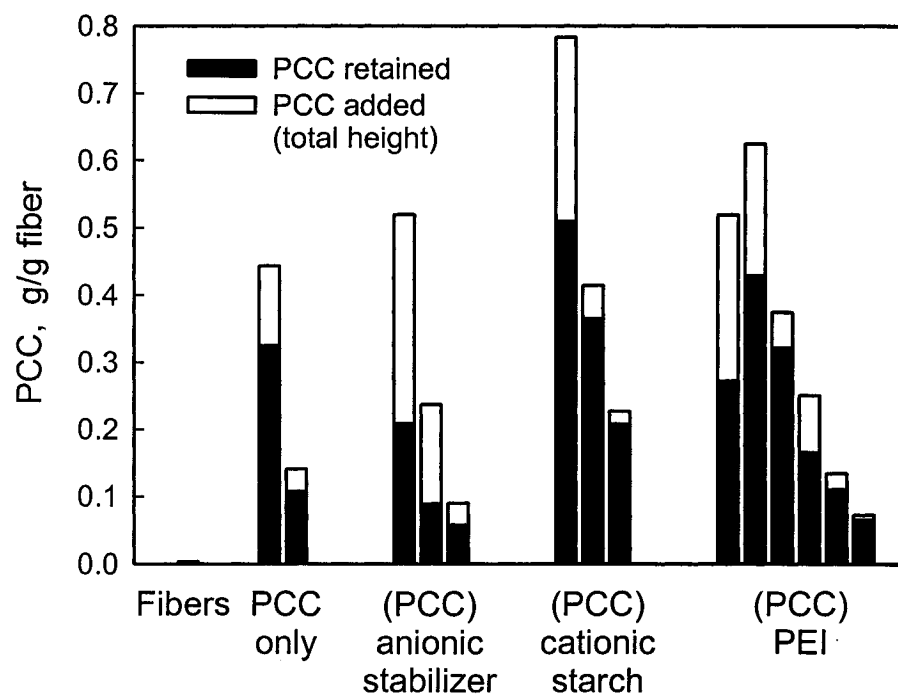


Fig. 8.6: Retention of PCC in paper (black bars). The total bar height corresponds to the amount of PCC added. The parentheses refer to PCC treatments with polymers. The different bars are for various runs with different secondary headbox concentrations (proportional to the addition levels shown in the figure).

then for 1 g fiber, 8.5-9 g water is present. However, about 1 g is associated with the fiber wall, and other 1.5-2 g water are inside the lumen, leaving about 6 g water in the interfiber space in the sheet. At the highest addition of 115 g/L PCC, a displacement of 6 cm³ water/g fiber results in a filling of about 0.7 g/g, which is close to filler addition (0.78 g/g). Because the flow rate from the secondary headbox was constant, the same water displacement occurred for all runs.

To better illustrate the retention of pigment in the paper, the amount of retained PCC was plotted against the amount of PCC added (see Fig. 8.7). The retentions of positive calcium carbonate fillers, whether untreated or treated with cationic polymers, followed the same pattern. It seems that, when PCC that had a positive surface charge, it could deposit onto fibers through electrostatic attraction. The origin of the positive charge seemed to have no effect on the deposition. This shows that PCC retention was mainly driven by the electrostatic attraction between positive fillers and negative fibers. In contrast, when negatively charged PCC was used, the retention was much lower, although filling levels of up to 18% were obtained. The filler that was not retained in the paper went through the wire to the suction boxes, and the rest was squeezed out in the press section of the machine.

The ISO brightness of the sheet increased with increasing filler content as expected. These results are presented in Fig. 8.8. The treatment of PCC with various polymers had little effect on the ISO brightness. The scatter in the data could be due to different degrees of filler flocculation in the sheet caused by the different surface treatments. To better appreciate the effects of surface treatment and also the degree of two-sidedness, the ISO brightness results for the various PCC's are plotted in Fig.

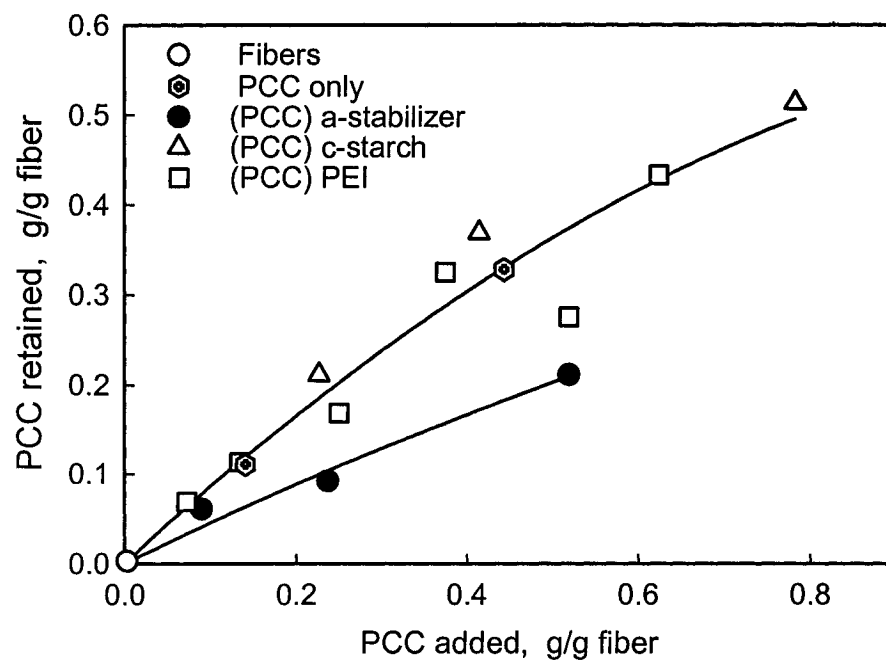


Fig. 8.7: Relation between retained and added PCC for positive and negative PCC's. The parentheses refer to PCC treatments with polymers; a-stabilizer and c-starch represent anionic stabilizer and cationic starch, respectively.

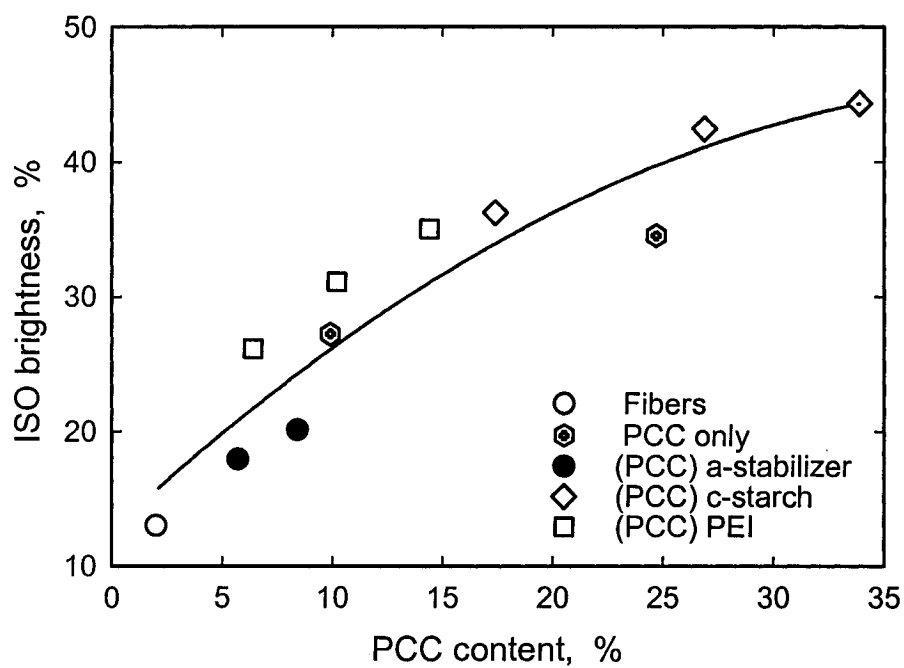


Fig. 8.8: ISO brightness of top sides of sheets as a function of PCC content. The parentheses refer to PCC treatments with polymers; a-stabilizer and c-starch represent anionic stabilizer and cationic starch, respectively.

8.9. It can be seen that all sheets (except the blank) exhibited two-sidedness. The largest two-sidedness was found for sheets with cationic PCC, but the two-sidedness diminished with increasing filler content. The two-sidedness of sheets filled with negative PCC was surprisingly low. One sample with 5.7% PCC exhibited negligible two-sidedness. The trend in two-sidedness agrees with the findings in stationary sheets [7]. The differences between cationic and anionic fillers are due to kinetic effects: the top side is exposed to fillers for a longer time, and more filler deposition on the fibers takes place. No such deposition occurs for negative fillers. Some filtration of the pigment on top of the sheet could also possibly occur.

The two-sidedness was further tested by peeling off individual layers of the sheet and determining their ash content at 550 °C. The results are presented in Fig. 8.10. Interestingly, the first layer did not exhibit the highest pigment content. Nevertheless, there was a gradual decrease in PCC concentration throughout the sheet, responsible for the two-sidedness in brightness. Layers 1 and 6 did not follow the downward trend, probably because of experimental error. Given that the top layers did not have excessive amounts of PCC, this is a good indication that retention of the pigment by filtration was not a factor.

The strength of the sheets was determined, both in the machine direction and in the cross direction. The strength is expressed in terms of breaking length, which follows trends similar to those exhibited by TEA. The results are shown in Fig. 8.11. For the same PCC content, the sheet was almost three times stronger in the machine direction than in the cross direction. The treatment of PCC with polyelectrolytes had no effect on paper strength. The treatment of fibers with PEI or cationic starch

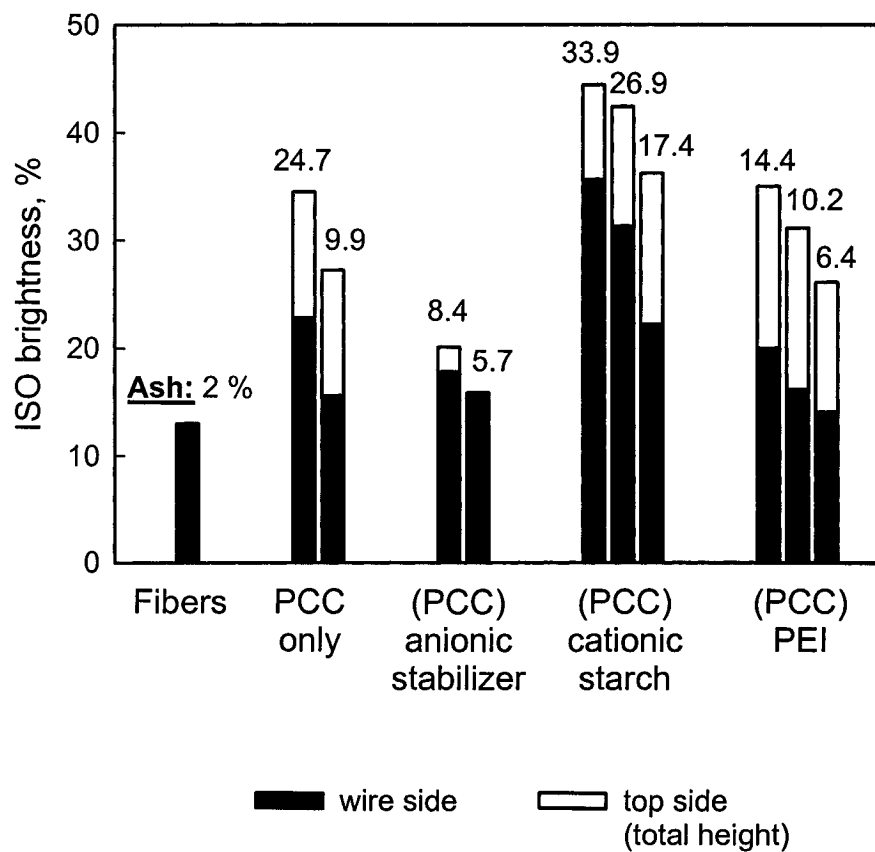


Fig. 8.9: Comparison of brightness on top and bottom sides of sheets filled with various amounts of PCC, treated in various ways. The parentheses refer to PCC treatments with polymers.

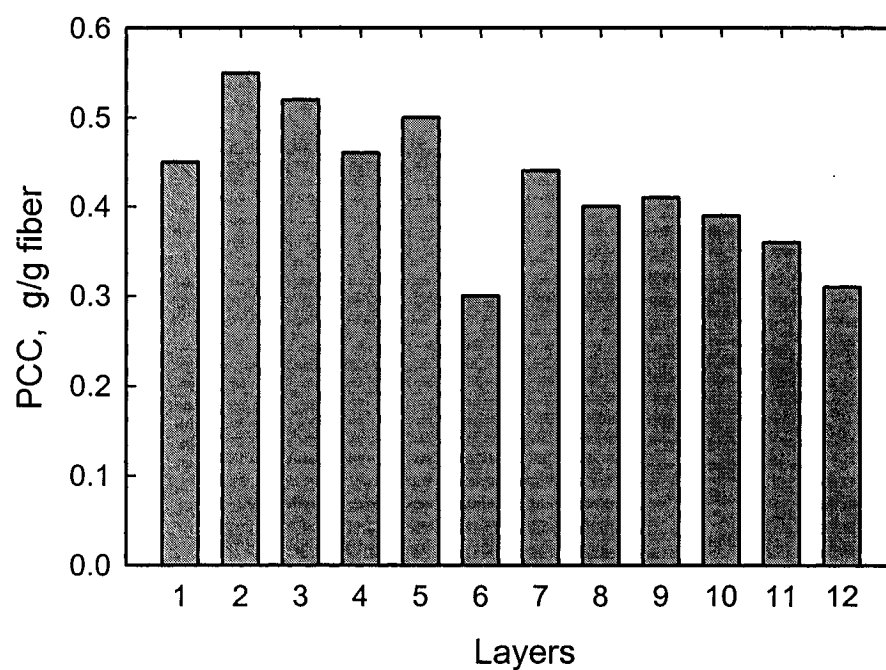


Fig. 8.10: Concentration of starch-treated PCC throughout the sheet. The sheet was divided in 12 layers by peeling. Layer 1 is the top layer; layer 12 is the bottom layer.

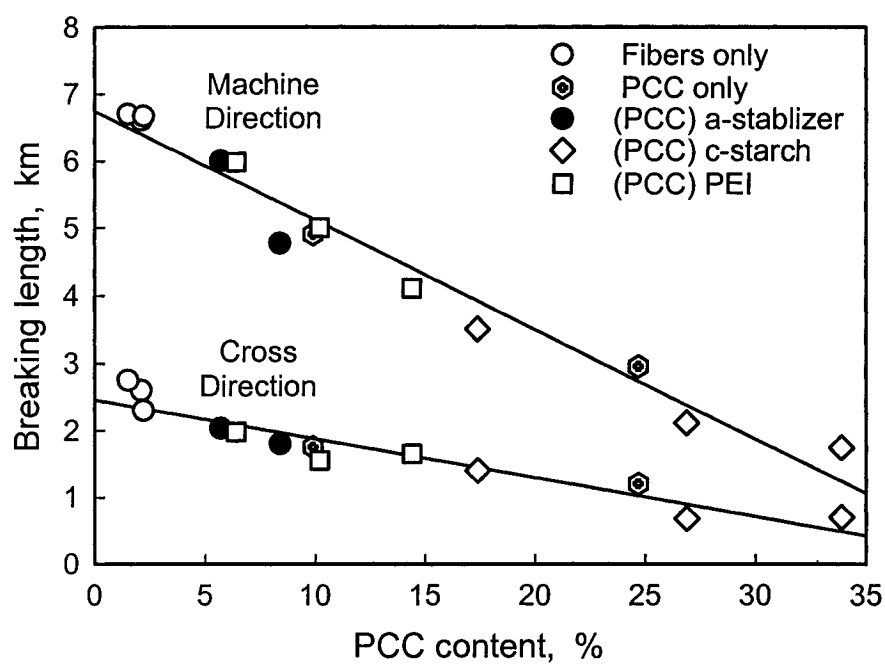


Fig. 8.11: Breaking length of PCC-filled sheets as function of PCC content, in both the machine and cross directions. The parentheses refer to PCC treatments with polymers; a-stabilizer and c-starch represent anionic stabilizer and cationic starch, respectively.

showed no increase in the strength, which is in contrast to what was seen on the slow Fourdrinier machine (cf. Fig. 8.5). Because the unbleached pulp was refined to 550 mL CSF, the tensile strength of the paper was much greater than for the slow Fourdrinier machine, where unbeaten pulp was used. The contribution of the PEI or cationic starch to the tensile strength of an already very strong sheet is therefore insignificant. Given that we do not have data for low degrees of loading (around 1%), because of the difficulty in presetting PCC concentrations in the secondary headbox (cf. section **8.5. Pilot Paper Machines**), we could not find an initial increase in strength for small loading levels. It is also possible that PCC acts differently than clay, because of their different shapes (round vs plate-like).

As mentioned earlier, determining the PEI concentration in the sheets was difficult, because of high background levels of nitrogen from nitrogen-rich compounds in the fibers. For sheets to which 10 mg/g of starch had been added, enzymatic starch determination showed that 70% of the starch was retained, which corresponds to about a monolayer of starch on the fibers [13]. These examples demonstrate again that polymers can be incorporated in wet sheets as well.

Finally, the sheets were examined by scanning electron microscopy (SEM). Figure 8.12 shows the top and bottom sides of a sheet containing PCC treated with anionic polymer. It can be seen that the two sides look very similar, which is in agreement with the low two-sidedness seen in brightness (cf. Fig. 8.9). Figure 8.13 shows SEM images of the top and bottom sides of paper highly filled with PEI-treated PCC. These papers show a two-sidedness that tends to diminish at higher filler content. Sheets filled with clay showed a trend in two-sidedness similar to that of

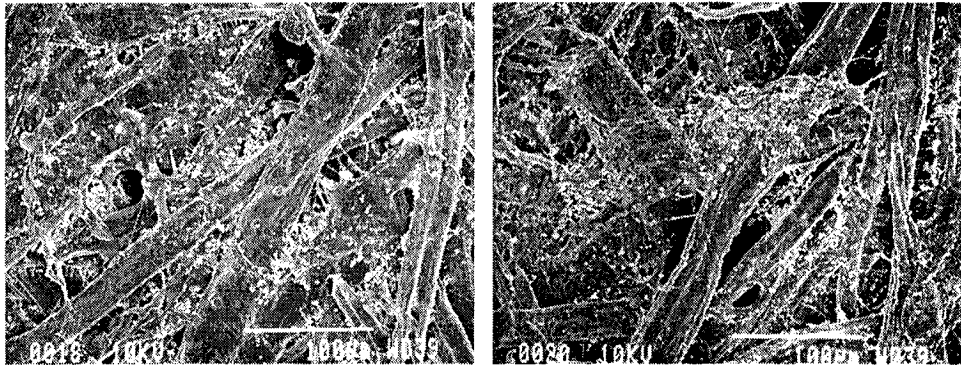


Fig. 8.12: SEM images of top and bottom sides (left and right images, respectively) of sheet filled with anionic PCC. The PCC content is 8.4%.

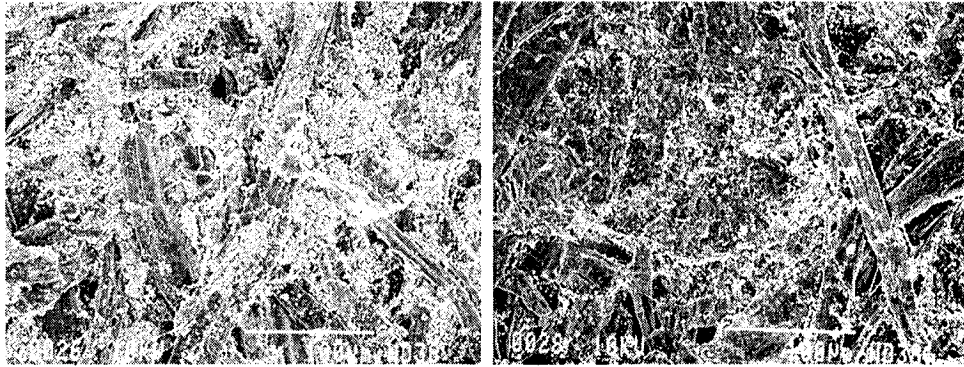


Fig. 8.13: SEM images of top and bottom sides (left and right images, respectively) of sheet filled with PEI-treated PCC. The PCC content is 14.4%.

sheets filled with PCC, indicating that the speed of the machine has little effect on the filler distribution in the sheet.

8.7. Concluding Remarks

The pilot trials described herein were a success in many ways. They demonstrated that paper can be filled with clay or PCC by applying a concentrated filler suspension to a sheet of paper, with the use of a secondary headbox placed near the dryline of a Fourdrinier paper machine. Filler contents of up to 35% were obtained. Both positive and negative fillers can be incorporated in the sheet, with or without a retention aid. Loading levels are higher for positive fillers, but at the cost of a greater two-sidedness. The two-sidedness decreases with increasing loading level. For negative fillers, two-sidedness is negligible. Also, polymers can be incorporated into paper this way as well.

The presence of pigment had a detrimental effect on the paper strength. Thus, the assumption that paper made in this way would be stronger than conventionally filled paper because of a reduced probability that fillers would enter spaces between fibers that are in a favorable positions to bond was found to be invalid.

8.8. Acknowledgment

The authors thank André Leger, Michel Farell, Dr. Bob Alince, Rick Collins, and Louis Godbout for their help in the pilot trials. The help of Jean Paradis (CSSP) and Marc Foulger (GL&V) and the donation of clay by ECC (now IMERYS) and PCC by Specialty Minerals are gratefully acknowledged.

8.9. References

1. Fougler, M.; Parisian, J.; Didwania, H. P.; Taylor, J., "New technology to apply starch and other additives". *Pulp Pap. Can.*, **100**(2), 24 (1999).
2. Bower, C. L., "Method of curtain coating". *U.S. Patent Application* 20010016231 (2001).
3. Gueggi, M.; Varli, S., "Method and apparatus for curtain coating". *PCT International Patent Application* WO 2003053597 (2003).
4. Ito, K.; Zama, Y.; Higuchi, A., "A study on pigment coated paper produced by high-speed curtain coating". *Kami Parupu Kenkyu Happyokai Koen Yoshishu*, **70**, 130 (2003).
5. Davies, B. R. F., "Starch spraying". *Pap. Technol. Ind.*, **18**(6), 186 (1977).
6. Procter, A. A., "Developments in starch spraying techniques in paper and board making". *Pap. Technol.*, **15**(10), 283 (1974).
7. Alince, B.; Vanerek, A.; van de Ven, T. G. M., "Clay Particle Deposition in a Fibre Web: An Alternative Way of Filling Paper?", *J. Pulp Pap. Sci.*, **28**(9), J315-J321 (2002).
8. Li, P.; Pelton, R., "Wood Pulp Washing. 2. Displacement Washing of Aqueous Lignin from Model Beds with Cationic Polymer". *Colloids Surf.*, **64**(3-4), 223 (1992).
9. Vanerek, A.; Alince, B.; van de Ven, T. G. M., "Colloidal Behaviour of Ground and Precipitated Calcium Carbonate Fillers: Effect of Cationic Polyelectrolytes and Water Quality". *J. Pulp Pap. Sci.*, **26**(4), 135 (2000).

10. van de Ven, T. G. M., "Theoretical Aspect of Drainage and Retention of Small Particles on the Fourdrinier". *Pulp Pap. Can.*, **85**(3), 157 (1984).
11. Alince, B., "Optimization of Pigment Performance in Paper". In *Fundamentals of Papermaking, Transactions of the 9th Fundamental Research Symposium, Cambridge, U.K.*; Baker, C. F., Punton, V. W., Eds.; Mech. Eng. Publ., Ltd.: London, Vol. 1, p 495 (1989).
12. Asselman, T.; Alince, B.; Garnier, G.; van de Ven, T. G. M., "Mechanism of Polyacrylamide-Bentonite Microparticulate Retention Aids". *Nord. Pulp Pap. Res. J.*, **15**(5), 515 (2000).
13. van de Ven, T. G. M., "A Model for the Adsorption of Polyelectrolytes on Pulp Fibers: Relation between Fiber Structure and Polyelectrolyte Properties". *Nord. Pulp Pap. Res. J.*, **15**(5), 51 (2001).

Chapter 9

CONCLUSIONS

9.1. Overview

This thesis focused on two important processes in wet-end of papermaking. Firstly, the colloidal behavior of a mineral pigment and its flocculation with pulp fibers using retention systems comprising cationic polyelectrolytes alone or in conjunction with mineral microparticles was thoroughly investigated. Secondly, the retention of colloidal particles and polyelectrolytes in a wet fiber web using unconventional methods was tested on pilot paper machines.

In Chapter 2, colloidal behavior of untreated ground and precipitated calcium carbonate fillers was found to be almost identical. The surface charge, i.e. positive or negative, of both fillers changed depending on the filler concentration. This was a direct result of impurities present in water as they adsorbed on the filler and reversed the positive charge at low filler concentrations. Highly charged cationic polyethylenimine stabilized both fillers due to increased electrostatic repulsion. Weakly charged cationic polyacrylamide, on the other hand, flocculated both by a bridging mechanism. Furthermore, low additions of the polyacrylamide caused flocculation of the fillers even in the presence of large excess of dissolved anionics such as sulfonated kraft lignin.

In Chapter 3, the effect of water quality on the surface charge of ground and precipitated carbonate fillers was further evaluated by deposition of the fillers on pulp fibers. Both fillers were positively charged in deionized water and deposited on negatively charged fibers. In tap water, the fillers became negative and electrostatic repulsion prevented the filler deposition on fibers. An appropriate amount of cationic polyethylenimine promoted deposition of the filler on fibers based on electrostatic

interaction. Cationic polyacrylamide caused flocculation of the pigment and its deposition on fibers regardless of the amount of cPAM added. However, the bridging mechanism alone was inadequate in explaining the overall behavior.

In Chapter 4, the formation of a polyelectrolyte complex between cationic polyacrylamides and an anionic sulfonated kraft lignin was investigated. The reaction between cationic polyacrylamides and anionic lignin was found to be nearly stoichiometric resulting in the formation of colloidal and coacervate complexes. The sum of both complexes was constant for a given cPAM charge, but the weight ratio between them varied depending on the molecular weight of cPAM used. Due to differences in characteristic times of lignin association with polyacrylamide, clustering of and reformation of polyacrylamide molecules, the formation of the coacervate complex increased with increasing molecular weight of polyacrylamide while low molecular weight polyacrylamide formed predominantly colloidal complexes with lignin.

In Chapter 5, the performance of kaolin clay and montmorillonite in the role of microparticles was evaluated and compared to conventional bentonite by observing deposition of a calcium carbonate pigment on kraft fibers suspended in water. Unlike bentonite, kaolin clay and montmorillonite were ineffective, but upon treatment with sodium-rich solutions, the montmorillonite delaminated and calcium carbonate deposition on fibers increased considerably. After treatment, the kaolin clay showed only a marginal degree of delamination and, as a consequence, calcium carbonate deposition increased only marginally. Commercial bentonite was treated with strong acid, which resulted in a larger particle size, but lower deposition of calcium

carbonate on fibers. The overall behavior indicates that the flocculation efficiency of microparticles is related to its ability to delaminate.

In Chapter 6, bentonite delamination induced by polymer-coated pulp fibers was investigated. The extent of bentonite delamination was monitored by deposition of a calcium carbonate filler. Experimental results seem to suggest complete bentonite delamination with a monolayer coverage of bentonite at an addition of 2.5 mg/g fiber. Addition of bentonite to a suspension consisting of fibers, calcium carbonate and cationic polyacrylamide showed that the maximum pigment deposition occurred at a bentonite addition of 10 mg/g fiber. Together, these two results seem to suggest that bentonite bridge between polymer-covered surfaces contained on average four platelets.

In Chapter 7, the feasibility of incorporating a mineral filler into paper by passing a clay suspension while at the same time displacing existing water through a wet fiber web was determined. The negative charge of either fibers or clay was modified by cationic polyethylenimine, which resulted in deposition due to electrostatic attraction. When both the fibers and the clay had a similar charge, negative or positive, the clay did not deposit on the fiber and was easily removed by washing. The clay particles uniformly covered the fibers, providing enough clay was available in the pigment suspensions.

In Chapter 8, pilot-scale trials on slow and fast Fourdrinier paper machines showed that by passing concentrated clay or calcium carbonate suspensions through a wet sheet of paper using a secondary headbox can result in highly filled papers. The flow from the secondary headbox, located on the dryline, proved not to damage the

wet sheet. An uneven distribution of filler in the sheet was observed in the z direction at low filler concentrations, but at high filler levels, the unevenness in filler distribution decreased. The strength of the paper seemed to decrease with increasing filler concentration, as is the case for conventionally filled paper. Besides mineral fillers, other chemicals, such as cationic polyethylenimine and cationic starch can be retained by this process as well.

9.2. Original contributions

1. Determination of the origin of the reversal of surface charge, from positive to negative, at low calcium carbonate pigment concentrations.
2. Demonstration of two different mechanisms by which cationic polyelectrolytes, employed as retention aids, can operate.
3. Elucidation of the behavior of cationic polyelectrolytes in the presence of dissolved anionic substances.
4. Characterization of polyelectrolyte complexes based on charge density and molecular weight of cationic polyacrylamide.
5. Proposal of a new mechanism by which cationic polyelectrolytes, employed as retention aids, operate in the presence of dissolved and anionic substances.
6. Demonstration of the effect of microparticle delamination on their performance in microparticle retention aid systems.
7. Quantification of the extent of bentonite delamination in pulp suspensions subjected to high shear.

8. Demonstration of the feasibility of incorporating mineral fillers in paper by passing concentrated filler suspensions through wet paper.
9. Demonstration of the feasibility of incorporating polymer in paper by passing concentrated polymer suspensions through wet paper.